ROLE OF TYPE-I INTERFERONS AND TOLL-LIKE RECEPTORS IN EXPERIMENTAL SYSTEMIC LUPUS ERYTHEMATOSUS

By

PUI YUEN LEE

A DISSERTATION PRESENTED TO THE GRADUATE SCHOOL
OF THE UNIVERSITY OF FLORIDA IN PARTIAL FULFILLMENT
OF THE REQUIREMENTS FOR THE DEGREE OF
DOCTOR OF PHILOSOPHY

UNIVERSITY OF FLORIDA

2008

To my mother, Kit Ying Ip; and my father, Tsun Kin Lee, for their unconditional love and support.

ACKNOWLEDGMENTS

It is with my deepest gratitude that I acknowledge the following individuals for their contributions to my development as a scientist and as a person. I am forever indebted for their assistance, guidance and support that have made this work possible.

First I would like to thank a number of faculty members for their invaluable contributions. I sincerely thank my mentor Dr. Westley Reeves for the years of guidance. His knowledge and insights have ignited my interest in immunology and his compassion in both research and clinical care has shown me how a physician-scientist should be. I am grateful to my co-mentor Dr. Mark Segal for introducing me to biomedical research during my undergraduate studies and serving as a role model ever since. The experience in his laboratory has been instrumental to my research endeavors and ultimately led to my decision to pursue the MD-PhD program. I would like to express my gratitude to my committee members Drs. Richard Moyer and Edward Chan for providing helpful advice and keeping me on track. I also thank Dr. Eric Sobel for his valuable insights on mouse models of lupus and Dr. Minoru Satoh for answering my countless questions regarding the pristane model and keeping me accompanied in the lab on weekends.

I am grateful for the friendship and collaboration of all members of the Reeves laboratory. In particular, I would like to thank Jason Weinstein for sharing his expertise in flow cytometry, which created many new possibilities for my project; Dina Nacionales for putting together study protocols and always being available to assist with animal studies; Edward Butfiloski for ordering supplies and for his help with i.v. injection for labeling studies; and Yi Li for managing the lab and sharing her humorous views of life. I also thank Tolga Barker, Philip Scumpia, and Matt Delano for their intellectual contribution on many projects.

I thank Dr. Richard Johnson for his encouragements and the Division of Nephrology for generously providing my NIH T32 training grant support. I also appreciate the help of Dr. Wei

Mu in the Johnson laboratory, and Dr. Yanpeng Diao, Elaine Beem, and Larysa Sautin in the Segal laboratory for their assistance with various aspects of my work.

A significant portion of this work could not be completed without the generosity of Professor Shizuo Akira in Osaka University. I am grateful to be provided the long list of knock-out strains not available elsewhere and given the opportunity to perform my experiments in Japan. I would like to thank Yutaro Kumagai, Drs. Osamu Takeuchi, Taro Kawai, and Masahiro Yamamoto of the Akira laboratory for their contributions that made it possible for me to complete my project there in a timely manner.

I would like to extend my appreciation to my middle school teacher Anita Amigo who tirelessly taught me the English language when I moved to the U.S. and high school teachers Karen Kissel and Nancy Kinard who helped me discover my interest in medical science. Further, I wish to acknowledge Manru Connie Xu, Frank Huang and many friends for their continuous support and helping me overcome obstacles. I also thank my grandparents for their confidence and trust in me. Finally, I would like to thank my parents for their love and guidance. Their hard work and sacrifice have given me the opportunity to succeed in life.

TABLE OF CONTENTS

LIST OF TABLES

LIST OF FIGURES

LIST OF ABBREVIATIONS

Ago2	argonaute-2
ANA	antinuclear antibodies
APC	allophycocyanin
BMDM	bone marrow-derived macrophages
Clo-lip	clodronate-containing liposomes
CLP	cecal ligation and puncture
DiD	1,1'-dioctadecyl-3,3,3',3'-tetramethylindodicarbocyanine perchlorate
DiD-lip	DiD-labeled liposomes
DNA	deoxyribonucleic acid
DTR	diphtheria toxin receptor
ELISA	enzyme-linked immunosorbent assay
FACS	fluorescence-activated cell sorting
FBS	fetal bovine serum
FcγR	Fc gamma receptor
FITC	fluorescein isothiocyanate
IFN	interferon
IFNAR	interferon alpha/beta receptor
Ig	immunoglobulin
IL	interleukin
iNOS	inducible nitric oxide synthase
i.p.	intraperitoneal
IPS-1	interferon-β promoter stimulator-1
IRF	interferon-regulated factor
ISG	interferon-stimulated genes

i.v.	intravenous
LPS	lipopolysaccharide
MΦ	macrophages
MCP-1	monocyte chemoattractant peptide-1
MDA-5	melanoma differentiation associated gene-5
MDC	myeloid dendritic cells
MHC	major histocompatibility complex
MO	mineral oil
Mx-1	myxoma resistance response gene-1
MyD88	myeloid differentiation factor-88
NZB/W	New Zealand Black / New Zealand White F1
PBMC	peripheral blood mononuclear cells
PCR	polymerase chain reaction
PDC	plasmacytoid dendritic cells
PDCA-1	plasmacytoid dendritic cell antigen-1
PE	phycoerythrin
PEC	peritoneal exudate cells RNA ribonucleic acid
Poly I:C	polyinosinic: polycytidylic acid
RIG-I	retinoic acid inducible gene-I
SLE	systemic lupus erythematosus
RT-PCR	real-time quantitative PCR
Sm	Smith antigen
snRNP	small nuclear ribonucleoproteins
TBK-1	TANK-binding kinase-1
TGF	transforming growth factor

TLR	Toll-like receptor
TMPD	2,6,10,14 tetramethylpentadecane
TNF	tumor necrosis factor
TRIF	TIR domain-containing adaptor inducing IFN-β
Yaa	Y-linked autoimmune acceleration

Abstract of Dissertation Presented to the Graduate School
of the University of Florida in Partial Fulfillment of the
Requirements for the Degree of Doctor of Philosophy

ROLE OF TYPE-I INTERFERONS AND TOLL-LIKE RECEPTORS IN EXPERIMENTAL SYSTEMIC LUPUS ERYTHEMATOSUS

By

Pui Yuen Lee

August 2008

Chair: Westley H. Reeves
Major: Medical Sciences – Immunology and Microbiology

Systemic lupus erythematosus (SLE) is a chronic autoimmune disorder affecting multiple organ systems. Although the etiology remains unclear, it is increasingly recognized that derangements of innate as well as adaptive immunity are important to the pathogenesis SLE. Recent evidence suggests that type-I interferons (IFN-I), a family of anti-viral cytokines, are integral to the pathogenesis of SLE. More than half of SLE patients display upregulation of a group of IFN-I-stimulated genes (ISGs). This "interferon signature" is clinically relevant as it correlates with active disease, presence of certain autoantibodies, and an increased incidence of renal involvement. The mechanism responsible for the dysregulation of IFN-I production and the source of these immunostimulatory cytokines are not clear.

Experimental lupus induced by tetramethylpentadecane (TMPD) displays key immunological and clinical features of human SLE. TMPD-induced lupus is at present the only model of SLE associated with excess IFN-I production and ISG expression. Therefore, investigated the mechanism and cell subset(s) responsible for the excess IFN-I production in this model. We demonstrate that TMPD treatment induces the accumulation of immature Ly6C^{hi} inflammatory monocytes, which are a major source of IFN-I in this lupus model distinct from IFN-producing dendritic cells. The expression of IFN-I and ISGs was rapidly abolished by

monocyte depletion whereas systemic ablation of dendritic cells had little effect. In addition, we found that IFN-I are required to maintain the chronic recruitment of Ly6C^{hi} monocytes by inducing the secretion of monocyte chemoattractants, thereby creating a vicious cycle of monocyte influx and IFN-I production.

We also show for the first time that TMPD elicits IFN-I production and autoantibody production exclusively through a Toll-like receptor 7 (TLR7)- and myeloid differentiation factor 88 (MyD88)-dependent pathway. The effects of TMPD were amplified by the Y-linked autoimmune acceleration (Yaa) cluster, which carries a duplication of the TLR7 gene. In contrast, other TLRs and cytoplasmic nucleic acid sensors were dispensable for IFN-I induction in this model. The deficiency of Fcγ receptors also did not impact the production of IFN-I, arguing against the conventional view that autoantibody immune complexes are responsible for the excess IFN-I in SLE. Taken together, these findings illustrate the importance of IFN-I and TLR7 in the pathogenesis of TMPD-induced lupus and provide novel insights into the "interferon signature" seen in patients with SLE.

CHAPTER 1
INTRODUCTION

This chapter discusses the epidemiology, clinical manifestations, and immunological abnormalities associated with systemic lupus erythematosus (SLE). The basic immunology of type-I interferons (IFN-I) and the interferon signaling pathway, as well as current evidence for the involvement these anti-viral cytokines in the pathogenesis of SLE will be presented. This introduction will also provide the rationale for studying the dysregulation of IFN-I using murine models of SLE.

Systemic Lupus Erythematosus

SLE is a chronic autoimmune disease that affects multiple organ systems including the joints, skin, kidneys, lungs, heart, and nervous system (1). In healthy individuals, the immune system functions to detect the presence pathogens such as bacteria and viruses by distinguishing self-antigens from foreign antigens. Upon encountering pathogen-associated molecular patterns (PAMPs) such as nucleic acids of microbial origin, the innate immune system initiates a non-specific inflammatory response via a number of highly conserved Toll-like receptors. The production of inflammatory cytokines and chemokines recruits antigen presenting cells such as monocytes and dendritic cells, which direct the adaptive immune response to produce antigen-specific T and B cell against the foreign antigen. Unlike PAMPs, self-antigens are typically either not recognized by the immune system, or are precluded from interaction with immune cells by anatomical barriers. The occasional generation of autoreactive lymphocytes is also guarded by a number of censoring mechanisms. For reasons not completely understood, such tolerance to self tissues is breached in SLE and the immune system actively responds to a wide-array of autoantigens by generating either autoreactive T cells or B cells. In SLE, the resulting immune cell activation leads to autoantibody production and a vicious cycle of chronic

inflammation and tissue destruction. While the clinical manifestations and severity of the disease vary widely, most lupus patients experience alternating periods of flares and remission. The etiology of SLE remains unclear, although both genetic and environmental factors are believed to play essential roles. Currently there is no cure for SLE and treatment is aimed at symptomatic relief.

Epidemiology

In the United States, the prevalence of SLE is estimated to be 15 to 50 cases per 100,000 and about 5 million individuals are affected world-wide (2). Although males are susceptible, 90% of lupus patients are females and most are of child-bearing age. SLE is more common in African-Americans and in Hispanic and Asian populations than in Caucasians. Hereditary factors contribute to the susceptibility for SLE as a concordance of 26% was found in monozygotic twins vs. 5% in dizygotic twins (3). Moreover, the familial prevalence is 10-12% for individuals having one or more first-degree relatives diagnosed with SLE (4). Significant familial aggregation with other autoimmune diseases including rheumatoid arthritis and Sjogren's syndrome has also been described (5).

Clinical Manifestations

The American College of Rheumatology (ACR) has defined 11 criteria for the classification of SLE (6, 7). The clinical criteria consist of malar rash, discoid rash, photosensitivity, oral ulcers, arthritis, serositis, renal involvement, neurologic disorders (seizure or psychosis) and hematologic abnormalities. Immunological criteria include the presence of antinuclear antibodies (ANA) and more specific autoantibodies such anti-double-stranded (ds)-DNA, anti-Sm, and anti-phospholipid. A diagnosis of SLE is made with 95% certainty if a patient meets any 4 of the 11 ACR criteria.

In most patients, the onset of autoantibodies precedes clinical manifestations (8). While almost all patients are positive for ANA, the presence of autoantibodies against dsDNA and the Sm antigen are highly specific to lupus. Symptoms of SLE can vary widely due to fluctuations in disease severity. The most common clinical findings include fatigue, arthralgia, arthritis, photosensitivity, anemia, and leucopenia. Malar rash with the characteristic "butterfly" distribution is found in about half of lupus patients and often reflects the presence of active disease. Lupus nephritis occurs in 30-50% of patients and represents a major cause of early mortality (9). Although less common, SLE patients can present with manifestations of cardiovascular, neurologic, gastrointestinal, pulmonary, or ocular origin.

Immunological Abnormalities

Although the cause of SLE is not known, it is widely accepted that a combination of genetic predisposition and environmental influence results in the loss of immunologic tolerance and induction of autoimmunity. The immune system plays a central role in this process by promoting the recognition of self-antigens and subsequent production of autoantibodies. Hyperactivation of lymphocytes, ineffective clearance of apoptotic cells and aberrant cytokine production are among the most studied immunological defects in SLE.

During a normal immune response to foreign antigens, antigen presenting cells (APCs) such as dendritic cells, macrophages and B lymphocytes present processed antigenic peptides to CD4+ helper T cells via class II major histocompatibility complex (MHC) molecules. Through direct cell contact and cytokine secretion, these helper T cells in turn stimulate B lymphocytes to initiate the production of antibodies. Although lymphopenia is often a manifestation of SLE, B and T cells from lupus patients often exhibit a hyperactive phenotype. B cells from SLE patients display enhanced proliferation, elevated antibody production and aberrant intracellular signaling upon B cell receptor activation (10, 11). Expansion of memory cells and plasma cells has also

been linked to the hypergammaglobulinemia associated with SLE (12). Similarly, T cells from lupus patients exhibit abnormal signal transduction upon activation (13). They also show elevated surface expression of costimulatory molecules such as CD40-ligand and the T-cell specific inducible costimulator (ICOS) (14), which help to promote B cell activation. Paradoxically, while lymphocytes from lupus patients are highly reactive to nuclear antigens (15, 16), they often respond weakly to foreign antigens such as tetanus toxoid (16). This discrepancy may be responsible for the increased susceptibility to infections and high failure rate of vaccination seen in SLE patients.

The abnormal activation of lymphocytes in SLE may be partly explained by dysregulated production of cytokines, a group of molecules critical to the function of innate and adaptive immunity. In line with the excess antibody production, elevated serum levels of the T helper 2 (T_h2) cytokines IL-6 (a required factor for the differentiation of B cells into antibody-secreting plasma cells) and IL-10 (a promoter of IgG production) are found in lupus patients (17, 18). Over-expression BAFF/Blys, which promotes the survival and proliferation of B cells, has also been recently described (19). While Th2 cytokines are essential for antibody production (20), activation of T cells and monocyte/macrophages by Th1 cytokine production are linked to tissue damage in SLE. Increased glomerular expression of IL-12 and IFN-γ is associated with lupus nephritis and ablation of these cytokines ameliorates glomerulonephritis in several models of SLE (21-24)). The cytokine imbalance in SLE is complex and likely involves a broad-spectrum of these immune modulators. More recently, research studies have shown a prominent role of the anti-viral IFN-I in the pathogenesis of SLE. The immunobiology of IFN-I and their role in both human lupus and murine models will be discussed in detail in the next section.

Another immunological abnormality seen in SLE is the impairment in phagocyte functions. Apoptosis or programmed cell death is a physiological process that controls cell proliferation and maintains tissue homeostasis. Despite the continuous turnover of aging or injured cells, apoptotic cell debris normally does not activate the immune system as they are rapidly taken up by surrounding cells or phagocytes such as macrophages (25). This clearance mechanism is impaired in lupus patients and the accumulation of dead or dying cells provides a source of a variety of intracellular antigens normally not exposed on the cell surface (26). In addition, endogenous nucleic acids such as DNA and RNA can also function as a danger signal to activate antigen presenting cells via TLRs (27, 28). This problem is compounded by the deficiency of complement and impaired activity of endogenous nucleases such as DNase I and II in the serum of SLE patients (29). This defective clearance mechanism also may be involved in the pathogenesis of photosensitivity, a common clinical manifestation of lupus patients. Exposure to sunlight is often sufficient to trigger a disease flare (2). It has been hypothesized that apoptosis of skin cells and the inability to clear the debris may be partially accountable for this effect.

Treatment

Currently there is no cure for SLE and drug treatment is directed by disease severity and organ involvement. In milder cases, non-steroidal anti-inflammatory drugs (NSAIDs) and anti-malarials are effective for the treatment of fatigue, skin rash, and arthritis (2). High dose corticosteroids are often used during a disease flare followed by low-dose maintenance therapy. For lupus nephritis, cytotoxic drugs such as cyclophosphamide and mofetil mycophenolate are effective in controlling renal damage (2). However, most current medications act by non-specifically suppressing the immune system and are associated with many side-effects. Many ongoing clinical trials are evaluating the efficacy of novel compounds that specifically inhibit

lymphocyte activation molecules (i.e. anti-CD40 and CTLA4-Ig) or cytokines such as IL-6 and IFN-I.

Involvement of IFN-I in the Pathogenesis of SLE

Originally discovered for their anti-viral properties, IFN-I exert a multitude of immunological functions and have been increasingly recognized as a key cytokine in the pathogenesis of autoimmune diseases. Increased serum IFN-I levels in lupus patients were first reported over twenty years ago (30). Recent studies have found that more than half of SLE patients display excess production of IFN-I and upregulation of a group of IFN-I-stimulated genes (ISGs), a feature associated with active disease (31-33). In addition, IFN-I also contributes to the pathology of several murine models of SLE. This section summarizes the biology of the IFN-I and current evidence of their involvement in human SLE as well as murine models of the disease.

Type-I Interferon Signaling Pathways

The fourteen subtypes of IFN-α, four IFN-α pseudogenes, and the single IFN-β, -κ, -ω, and -ε species together comprise the IFN-I cluster on human chromosome 9p22 within a genomic duplication (34, 35). In terms of immunity and autoimmunity, IFN-α and IFN-β are the main types of interest. All members of the IFN-I family bind to a ubiquitously expressed heterodimeric receptor complex composed of an α (IFNAR1) and a β (IFNAR2) chain. While IFNAR2 serves as the ligand-binding domain, both chains are required for effective signal transduction (36).

Ligand-induced dimerization of the receptor chains results in auto- and trans-phosphorylation of two receptor-associated Janus protein tyrosine kinases: Tyk2 on IFNAR1 and Jak1 on IFNAR2 (37). These events provide docking sites for the recruitment and

phosphorylation of STAT1 and STAT2. Phosphorylated STAT1/STAT2 heterodimers then translocate into the nucleus, associate with IFN regulatory factor 9 (IRF-9, also known as p48) and form the heterotrimeric complex IFN-stimulated gene factor 3 (ISGF3) (36, 38). Subsequently, ISGF3 initiates the transcription of hundreds of IFN-I inducible genes by binding to the upstream consensus IFN-stimulated response elements (ISRE) (39). Although not directly involved with Jak-STAT signaling, activation of p38 mitogen-activated protein kinase (MAPK) is required for effective formation of ISGF3 and transcription of ISRE-regulated genes (40-42). A schematic of the IFN-I signaling cascade is depicted in Figure 1-1A.

Immunomodulatory Effects of IFN-I

The IFN-I system is an essential component linking innate and adaptive immunity. Secreted in response to extracellular or intracellular pathogens, IFN-I enhance the expression of class I and class II major histocompatibility complex (MHC) molecules on antigen presenting cells and induce dendritic cell maturation (43). During the early phases of an infection, IFN-I signaling also activates the transcription of antimicrobial genes, linking innate and adaptive immunity and inhibits the proliferation of infected cells (44-46). In adaptive immunity, IFN-I regulate T cell functions by promoting the effects of T_H1 cytokines and augmenting the survival of activated T cells (47). IFN-I signaling is also crucial for effective B cell differentiation and memory B cell responses (48). Moreover, IFN-I have adjuvant effects, augmenting antigen-specific immunoglobulin production and isotype switching when administered along with soluble antigen (49). The broad effects of IFN-I further extend to the regulation of other cytokines. IFN-I can up-regulate IFN-γ production, enhance IL-6 signaling, and stimulate the proinflammatory activity of IL-10 (50). These diverse and potent immune-enhancing effects may underlie the involvement of IFN-I in autoimmune disorders.

Pathways of IFN-I Induction

The production of IFN-I in response to pathogens is mediated in part by the Toll-like receptors (TLRs), a highly conserved family of membrane receptors specialized in the recognition of pathogen-associated molecular patterns (51). While almost all TLRs are capable of triggering the production of inflammatory cytokines such as tumor necrosis factor α (TNFα) and IL-6 upon ligand binding, only TLR3, -4, -7, -8, and -9 trigger IFN-I production. TLR3 recognizes viral double-stranded RNA whereas TLR4 is the receptor for bacterial lipopolysaccharide and certain viral proteins. Induction of IFN-β through these two surface TLRs requires the adaptor molecule Toll/interleukin-1 receptor domain-containing adaptor-inducing IFNβ (TRIF) (52). In contrast to the endosomal location of TLR3, TLR4 is present on the cell surface, although recent evidence suggests that upon LPS binding TLR4 also enters the endosomal compartment prior to TRIF activation (53). TLR-7/-8, and -9 are also located in endosomes but signal IFNβ expression via the adaptor protein myeloid differentiation factor 88 (MyD88) (54). TLR7 and -8 bind viral single-stranded RNA while TLR9 recognizes unmethylated CpG DNA found in bacteria (55, 56). Activation of TRIF or MyD88 recruits IκB kinases (IkkB), which phosphorylate the downstream factors IRF-3, IRF-5, and IRF-7, culminating in the transcription of IFN-β. Once expressed and secreted, IFN-β binds to the IFNAR in an autocrine manner, resulting in the transcription of a group of IFN-I inducible genes. Subsequent expression of IFN-α and IRF-7, an essential transcription factor for IFN-I, establishes a positive-feedback loop for signal amplification (57, 58). The TLR signaling pathways leading to IFN-I production are illustrated in Figure 1-1B.

Recently, several viruses have been shown to induce IFN-I production independent of TLRs, uncovering novel mechanisms of detecting intracellular viral RNA via the cytoplasmic

helicase proteins retinoic-acid-inducible protein I (RIG-I) and melanoma-differentiation-associated gene 5 (MDA-5) (59, 60). These sensors mediate IFN-I production through the adaptor IPS-1 (IFN-β promoter stimulator protein-1; also known as MAVS, VISA, or Cardif) (61). Finally, research on intracellular infection by Listeria *monocytogenes* have unveiled a pathway to trigger IFN-I production by intracellular DNA (62). Although the molecule responsible for DNA interaction remains unclear, this pathway requires the activation of TANK-binding kinase-1 (TBK-1) and IRF-3 (63). These pathways are also depicted in Figure 1-1B.

Interferon-Producing Cells

Although almost all nucleated cells are capable of producing IFN-I, a small population of "natural IFN-producing cells" in the circulation, now known as plasmacytoid dendritic cells (PDC) are the most potent (64, 65). Human PDCs are lineage negative cells generally characterized by the surface expression of CD4, CD123, CD83, and class II MHC. Two other markers, blood dendritic cell antigen 2 (BDCA-2) and BDCA-4, are also commonly used for detecting and isolating human PDCs (66). These natural IFN-I producers can synthesize up to 1000-fold more IFN-α/β than other cells and production can be enhanced further upon activation of endosomal TLR7 and TLR9. A high constitutive expression of IRF-7 in these cells may be partly responsible for their high IFN-I production (67). Upon activation, PDCs migrate to lymph nodes in response to chemokines.

Myeloid dendritic cells (MDC) are also strong IFN-I producers during viral infections, but whether they are as potent as PDCs is controversial (65, 68). Although monocytes/macrophages are weak producers of IFN-I in response to TLR ligands, activation of the cytoplasmic nucleic acid sensors can trigger high levels of IFN-β production in these cells (62). In fact, it was recently shown that macrophages in the lungs function are the primary IFN-I producers during viral infection and PDCs assumes the role in the absence of macrophages (69).

Dysregulated IFN-I Production in Human SLE

Given the pleiotropic effects of IFN-I on DC maturation, T cell survival, and antibody production, it is conceivable that excess IFN-I or aberrant regulation of IFN-I signaling could contribute to autoimmunity. Consistent with that possibility, IFNα treatment in hepatitis C infection, malignant carcinoid syndrome, or chronic myelogenous leukemia is associated a wide array of autoimmune manifestations. A positive fluorescent ANA test can be found in as many as 22% of patients treated with IFN-α (70). The onset of SLE, autoimmune (Hashimoto) thyroiditis, autoimmune hemolytic anemia, rheumatoid arthritis, vasculitis, and psoriasis all have been reported following IFNα therapy (71-73).

High levels of IFNα in the sera of SLE patients were first described by Hooks et al. in 1979 (30). The significance of this observation remained unclear for decades until it was shown that serum from lupus patients, especially those with active disease, promotes the differentiation of blood monocytes into dendritic cells (74). The capacity to induce dendritic cell differentiation correlates with IFN-I levels and neutralization of IFN-I completely abrogates this effect.

Recent studies further demonstrated that the dysregulation of IFN-I in SLE is also evident in gene expression profiles of lupus peripheral blood mononuclear cells (PBMCs). Since all IFN-I subtypes signal through the same receptor complex, levels of IFN-I can be quantified by measuring interferon stimulated gene (ISG) expression using gene microarray and real-time polymerase chain reaction (PCR) (31, 32, 75). IFN-I inducible genes over-expressed in SLE include anti-viral proteins [e.g. myxoma-response protein-1 (Mx-1)], apoptosis regulators (phospholipids scramblase, TRAIL), MHC molecules (class I and II), Toll-like receptors (TLR-3 and -7), Fcγ receptors (CD32a and CD64) and several interferon-inducible chemokines (CCL2/MCP-1, CXCL10/IP-10). PBMC expression of ISGs, therefore, provides a robust

surrogate read-out of systemic IFN-I levels. Approximately half of SLE patients display abnormally high ISG expression (defined as > 2 standard deviations above the mean ISG expression in healthy controls). This "interferon signature" is associated with disease severity, renal involvement, and the presence of autoantibodies against dsDNA and RNA-associated nuclear antigens such as Sm/nRNP, SSA/Ro, and SSB/La (33, 76).

In healthy individuals, the production of IFN-I and expression of ISGs are elevated transiently during viral infection. However, why this "interferon signature" is consistently detected in many SLE patients is poorly understood. While evidence linking the abnormal IFN-I production to a common exogenous trigger (i.e. viruses) has not been convincing, a number of endogenous mechanisms for IFN-I induction have been identified. An early study described a serum interferon-inducing factor (IIF) suggestive of DNA-antibody immune complexes in SLE patients (77). Supporting these findings, immune complexes consisting of plasmid DNA and anti-dsDNA autoantibodies stimulate IFN-I in normal PBMC (28), while mammalian DNA alone has little effect (78). The identification of TLRs strengthened the notion that self-DNA may trigger IFN-I production in SLE. In the presence FcγRIIa (CD32), internalized DNA-containing immune complexes activate dendritic cells via TLR-9, the receptor for unmethylated CpG DNA found in bacteria (and plasmid DNA) (79).

Several groups have recently reported that endogenous RNA also may induce IFN-I by binding to TLRs (27, 80, 81). Originally described to recognize viral G/U-rich single-stranded RNAs (55), TLR7 is capable of binding certain mammalian RNA sequences resulting in the activation of PDCs (80, 81). Consistent with these reports, human U1 RNA (associated with snRNP particles) and Y RNAs (associated with Ro60 protein) also potently induce IFN-I production through an endosomal MyD88-dependent pathway involving TLR7 (80, 82).

Based on these findings, many researchers believe that the endogenous stimulatory DNA and RNA molecules may originate from apoptotic or necrotic cells in the circulation (83). Unlike healthy individuals, the mechanism for apoptotic cell clearance is impaired in SLE patients, providing a source of endogenous nucleic acids. It is believed that the presence of DNA or RNA is not sufficient to initiate an inflammatory response because the TLRs recognizing these ligands are located in the endosomes (78). In the presence of autoantibodies (i.e. anti-dsDNA, anti-Sm/RNP), however, the formation of immune complexes may then enhance the internalization the endogenous nucleic acids present in apoptotic bodies into endosomes (Figure 2)**.** Thus, interaction of the endogenous ligands with corresponding endosomal TLRs is hypothesized to be responsible for the "interferon signature" in SLE, though this remains to be verified experimentally and whether immune complex or FcγRs are absolute requirements is controversial (27, 84).

Most studies to date have attributed the elevated IFN-I production in SLE to PDCs, a view supported by the ability of DNA and RNA immune complexes to induce IFN-I production by PDCs *in vitro* (28, 80). The TLRs implicated in binding endogenous nucleic acids, specifically TLR7, 8 and 9 are highly expressed on human PDCs and B cells but not myeloid dendritic cells (MDCs), monocytes, or macrophages (85). However, the number of circulating PDCs in SLE patients is unexpectedly low. A profound reduction in the number of PDCs and MDCs is characteristic of SLE patients, especially those with renal involvement (33). Similar findings have been reported by other groups and most believe that the depletion of PDCs reflect migration of these cells to tissues and lymphoid organs following activation (64). Consistent with this view, increased numbers of PDCs and elevated IFN-I secretion have been found in lupus skin lesions and lymph node biopsies from SLE patients (86). Nevertheless, direct

evidence showing PDCs are the primary source of excess IFN-I in SLE is lacking. Depletion of PDCs *in vitro* reduced IFN-I production by only ~40%, suggesting that other cell types may also be involved (74).

Evidence of IFN-I involvement in Murine Models of SLE

The involvement of IFN-I in the pathogenesis of SLE has also been studied in many experimental models of the disease. While both New Zealand Black (NZB) and New Zealand White (NZW) strains are autoimmune-prone, the F1 generation bred from these strains (NZB/W F1) spontaneously develop a lupus-like disease characterized by immune-complex glomerulonephritis and autoantibodies to dsDNA (87). The NZB/W model is most valuable for studying the role of genetics in SLE as multiple susceptibility loci are required for disease manifestations. A recent study illustrated that the development of glomerulonephritis, ANA and anti-dsDNA antibodies is accelerated by exogenous IFN-α (88), whereas deletion of IFN-α/β receptor (IFNAR) in NZB mice slows the progression of autoimmune hemolytic anemia and enhances survival (89). In line with these findings, the development of ANA and renal disease in B6.Nba2 congenic mice (C57/BL6 mice with a susceptibility loci derived from the NZB strain) is also dependent on IFN-I signaling (90).

Unexpectedly, the role of IFN-I seems to be reversed in the $MRL^{lpr/lpr}$ model. The combination of the autoimmune-prone MRL background and the lpr mutation (disruption of the pro-apoptotic regulator fas) results in a lymphoproliferative disorder with features of SLE including glomerulonephritis, arthritis, and autoantibodies to Sm and anti-dsDNA (91). In contrast to NZB/W F1 mice, disease amelioration has been reported in $MRL^{lpr/lpr}$ mice treated with exogenous IFN-I while IFNAR deficiency reduced survival (92). Whether these findings reflect the role of IFN-I in human SLE remains to be determined as intrinsic upregulation of

IFN-I and ISG expression (in the absence of exogenous IFN-I) seen in lupus patients has not been reported in these mouse models.

The only reported murine model that recapitulates the "interferon signature" seen in human SLE is experimental lupus induced by the hydrocarbon 2,6,10,14-tetramethylpentadecane (TMPD), also known as pristane (93). For decades, TMPD has been utilized to induce plasmacytoma and enhance antibody production by hybridoma (94, 95). In 1994, Satoh et. al. reported that a single peritoneal injection of TMPD in non-autoimmune prone strains (e.g. BALB/c) was sufficient to induce many key immunological and clinical features of human SLE, including the production of autoantibodies against dsDNA and Sm/nRNP, and the development of immune complex-mediated glomerulonephritis as well as late-onset arthritis (96, 97). In addition to the chronic inflammatory response in the peritoneal cavity, mice treated with TMPD display upregulated expression of ISGs such as Mx-1 and IRF7 in the peripheral blood. Importantly, renal disease and the generation of anti-dsDNA and anti-Sm/nRNP autoantibodies are highly dependent on IFN-I as these features of SLE are abolished in IFNAR-deficient mice (93). Consistent with the ability to elicit IFN-I production, TMPD-treatment of NZB/W F1 mice accelerates disease progression and induces the development of anti-Sm/nRNP autoantibodies, which are normally absent in this strain (98).

The presence of the "interferon signature" and the dependency of disease features on IFN-I signaling offer the unique opportunity to dissect the role of IFN-I in experimental lupus. The mechanism responsible for TMPD-induced IFN-I production and the subsequent lupus manifestations is largely unknown. Whether PDCs and/or other cell subsets are the main producers of IFN-I in this model is of great interest since the source of IFN-I in human SLE is also unclear. Finally, whether chronic inflammation induced by the hydrocarbon contributes to

the production of IFN-I and the onset of autoimmunity also warrants attention. The subsequent chapters will address these questions in detail. Results from these studies may shed light on the same questions regarding human SLE.

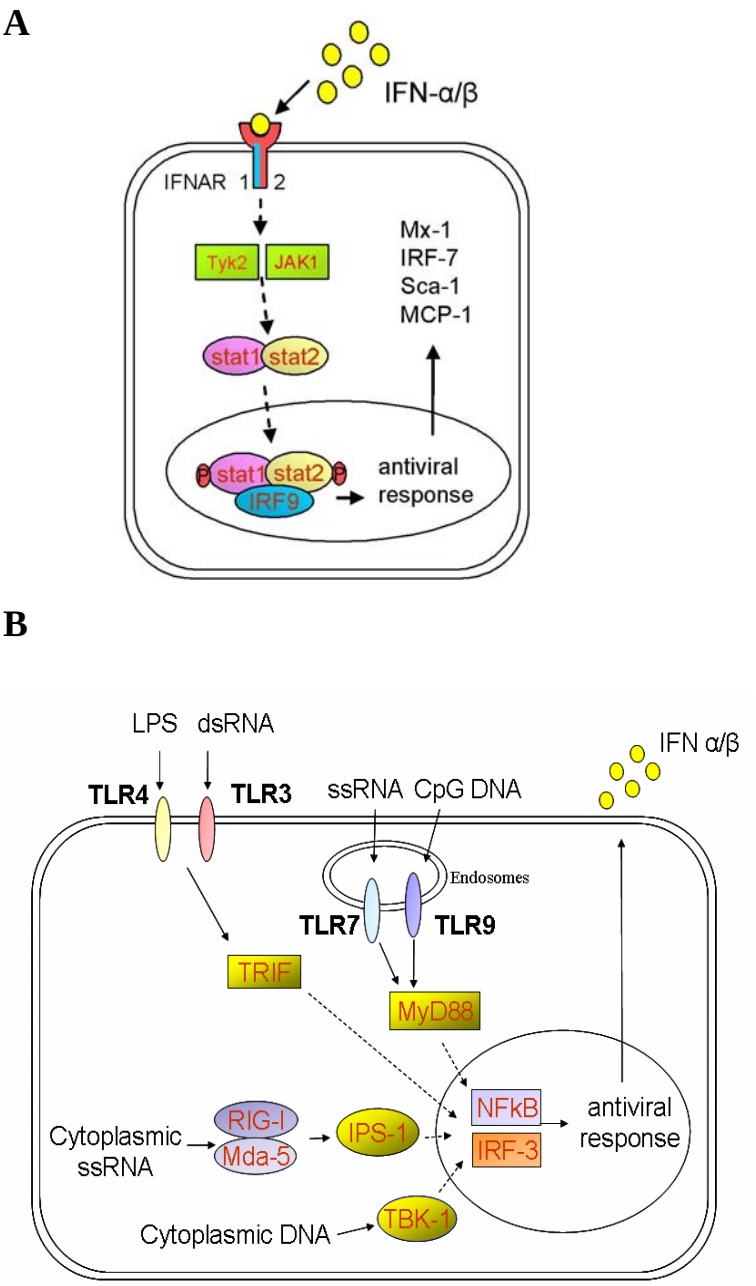

Figure 1-1. Schematic of IFN-I signaling pathways. A) All subtypes of IFN-I bind to the IFNAR complex and initiate phosphorylation of the kinases JAK1 and Tyk2. Subsequent phosphorylation and translocation of STAT1 and STAT2 triggers the transcription of interferon-stimulated genes such as Mx-1, IRF7, Sca-1 and MCP-1. B) IFN-I induction by pathogen-associated molecular patterns such as viral RNA and DNA is mediated by TLRs and cytoplasmic nucleic acid sensors.

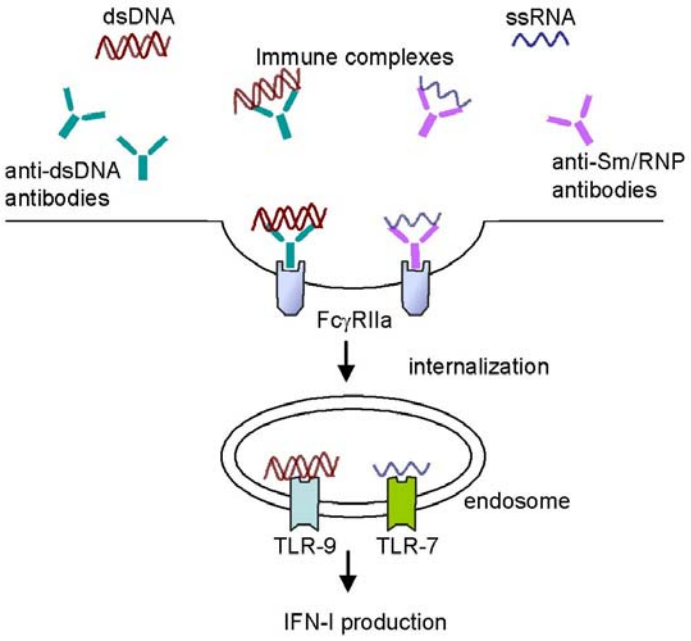

Figure 1-2. Schematic of IFN-I induction by endogenous nucleic acids. Mammalian nucleic acids are normally non-stimulatory because they do not enter endosomes, where TLR7 and TLR9 are present. Immune complexes formed by lupus autoantibodies and endogenous nucleic acids are internalized via FcγRIIa and allows the interaction between the nucleic acids and TLRs, leading to the production of IFN-I.

CHAPTER 2
METHODS AND MATERIALS

Mouse Strains

These studies were approved by the Institutional Animal Care and Use Committees at the University of Florida (Gainesville, FL) and Osaka University (Osaka, Japan). C57BL/6 wild type, B6.IL-1R$^{-/-}$, B6.IL6$^{-/-}$, B6.CCR2$^{-/-}$, BXSB.Yaa males and BXSB female controls, wild-type BALB/cJ and BALB/c.IFNγ-/- mice were purchased from Jackson Laboratories (Bar Harbor, ME). B6.FVB-Tg$^{Itgax\text{-}DTR/EGFP.57}$Lan/J backcrossed to a BALB/c background, referred to as CD11c-DTR (diphtheria toxin receptor) mice (99, 100), were a gift from L.Moldawer (UF). CD11c-DTR mice were maintained as heterozygote crosses and littermates not expressing the transgene were used as controls. BXSB X B6 F1 mice were generated by breeding BXSB males with C57BL/6 females. FcγRI/III$^{-/-}$ mice were purchased from Taconic (Hudson, NY). 129Sv/Ev Type I interferon receptor α-chain deficient (IFNAR$^{-/-}$) mice and wild type controls (129Sv/Ev) were purchased from B&K Universal Limited (Grimston, Aldbrough, England). These mice were all housed in a specific pathogen-free (SPF) facility at Malcolm Randall VA Medical Center (Gainesville, FL).

MyD88$^{-/-}$, TRIF$^{-/-}$, TLR7$^{-/-}$, TLR9$^{-/-}$, IFNAR$^{-/-}$ mice (backcrossed >7 generations to the C57BL/6 background) and IPS-1$^{-/-}$, TNF$^{-/-}$, TNF$^{-/-}$TBK1$^{-/-}$ (on a mixed 129Sv/ B6 background) have all been described previously (52, 54, 56, 69, 101, 102) and were bred and maintained in a SPF facility in the Research Institute for Microbial Diseases, Osaka University. Wild-type C57BL/6 and heterozygous littermates were used as controls. BALB/c.TLR7$^{-/-}$ and TLR9$^{-/-}$ mice (backcrossed >8 generations to the BALB/c background) and wild-type BALB/c mice used for long-terms studies of autoantibody production from acquired from Oriental Bioservices (Kyoto, Japan) and housed in an SPF facility at Osaka University.

Treatment and Tissue Harvest

Eight to sixteen week-old mice received a single intraperitoneal (i.p.) injection of 0.5 ml TMPD (Sigma-Aldrich, St. Louis, MO), mineral oil (Harris Teeter, Mathews, NC), 4% thioglycollate (BD Bioscience, San Jose, CA), squalene (Sigma), n-hexadecane (Sigma), or PBS. For short-term experiments, blood samples were obtained before, and weekly after TMPD treatment by tail-vein bleed. Peritoneal cells were collected by lavage using 5 ml of DMEM supplemented with 10% fetal calf serum, 10 mM HEPES, glutamine, and penicillin/streptomycin (complete DMEM) and isolated for RNA extraction or flow cytometry analysis and lavage fluid was stored at -80°C for ELISA. Spleen cells were collected by meshing the spleen against a 45μM plastic strainer followed by red blood cell lysis before resuspension in complete DMEM. For long-term experiments, serum was collected monthly after treatment for 6-8 months. Kidneys were harvested and frozen immediate in OCT compound (TissueTek, Torrance, CA) for tissue section. Cecal ligation and puncture were performed as described (100, 103).

Flow Cytometry and Cell Sorting

The following conjugated antibodies were used: CD11b-phycoerythrin (PE), anti-CD11b-allophycocyanin (APC), anti-CD4-APC, anti-CD8-PE, anti-CD11c-PE, anti-CD11c- fluorescein isothiocyanate (FITC), anti-B220-APC Cy7, anti-CD80-PE, anti-CD86-FITC, anti-I-A/I-E-PE, anti-Mac-3-FITC, anti-Ly6G-PE, anti-Sca-1-PE, anti-NK1.1-PE (all from BD Bioscience, San Jose, CA), anti-Ly6C-FITC, anti-Ly6C-biotin, avidin-APC (eBioscience, San Diego, CA), anti-F4/80-FITC, anti-Moma2-FITC (Serotec, Raleigh, NC), and anti-CD11b-Pacific blue (Caltag Laboratories, Burlingame, CA). Prior to surface staining, 10^5 peritoneal or ficoll gradient-isolated peripheral blood cells were incubated with anti-mouse CD16/32 (BD Bioscience) for 10 min. Cells were then stained with optimized amount of primary antibody or the appropriate isotype control for 10 min at room temperature before washing and resuspending in PBS

supplemented with 0.1% NaN_3 and 1% bovine serum albumin. For intracellular staining, cells were permeabilized with Perm/Fix buffer (BD Bioscience) and incubated with antibodies against Mac-3 and Moma-2 in Perm/Wash buffer (BD Bioscience). Fifty thousand cells per sample were acquired by a CYAN cytometer (Dako, Fort Collins, CO) and analyzed with FCS Express 3 (De Novo Software, Ontario, Canada).

For cell sorting, peritoneal cells from TMPD-treated mice (10^7) were stained with anti-Ly6G-PE, washed, and incubated with magnetic bead-conjugated anti-PE (Miltenyi Biotec, Auburn, CA). Granulocytes (>99% purity) were positively selected using MS columns while the negative fraction was stained with anti-CD11b-APC, washed, and incubated with magnetic bead-conjugated anti-APC (Miltenyi Biotec). Positive selection using MS columns yielded >85% $Ly6C^{hi}$ monocytes. The negative fraction consisted of lymphocytes and dendritic cells (DCs). Cell sorting using a FACS DIVA flow cytometer (BD Bioscience) yielded similar results with a higher purity of $Ly6C^{hi}$ monocytes (>95%). For morphological analysis, 3 X 10^4 sorted cells were cytospun onto glass slides and stained using the Hema3 kit (modified Wright stain; Fisher Scientific, Pittsburg, PA)

Conventional and Real-Time Quantitative PCR

Total RNA was extracted from 10^6 cells using Trizol reagent (Invitrogen, Carlsbad, CA) and cDNA was synthesized using Superscript II First-Strand Synthesis Kit (Invitrogen). Real-time PCR was performed using the SYBR Green Core Reagent Kit (Applied Biosystems, Foster City, CA) with an Opticon II thermocycler (MJ Research, Waltham, MA). Amplification conditions were: 95°C for 10 min, followed by 45 cycles of 94°C for 15 s, 60°C for 25 s, and 72°C for 25 s. After the final extension (72°C for 10 min), a melting-curve analysis was performed to ensure specificity of the products. IFN-I genes were amplified by conventional

PCR using a PTC-100 programmable thermal controller (MJ Research). Amplification conditions were: 95°C for 5 min, followed by 40 cycles of 94°C for 30 s, 60°C for 1 min, and 72°C for 1 min. After a final extension (72°C for 10 min), PCR products were analyzed by agarose gel electrophoresis. Sequences of all real-time and conventional PCR primers are provided in Table 2-1.

Cytokine ELISA

ELISAs for IL-6, IL-12, MCP-1, TNF-α and IFN-β in peritoneal lavage fluid and cell culture media were performed as using monoclonal antibody pairs (BD Bioscience). After incubation with biotinylated cytokine-specific antibodies, 100 μl/well of 1:1000 streptavidin-alkaline phosphatase was added and the reaction was developed with p-nitrophenyl phosphate substrate (Sigma). Standard curves were generated using recombinant cytokines and cytokine concentrations were calculated using a four-parameter logistic equation (Softmax Pro 3.0).

Monocyte and Dendritic Cell Depletion

Depletion of peritoneal monocytes was performed by injecting 200 μL of clodronate-containing liposomes (clo-lip) a gift from Roche Pharmaceuticals) i.p. in wild-type BALB/c mice treated with TMPD two weeks earlier. To trace monocyte subsets *in vivo*, PBS-containing liposomes were labeled with the fluorescent dye 1,1'-dioctadecyl-3,3,3',3'-tetramethylindodicarbocyanine perchlorate (DiD) as described (12, 13). To label Ly6C$^-$ monocytes, 150 μL of DiD-liposomes were injected i.v. into TMPD-treated mice. Clo-lip (200 μl) was delivered i.v. 24 hr prior to the injection of DiD-liposomes for the labeling of Ly6C^{hi} monocytes. Analysis was performed 24 hr after labeling. DC ablation was performed in TMPD-treated CD11c-DTR mice by injecting 4 ng/g body weight of diphtheria toxin (DT; Sigma) i.p. Mice were sacrificed for analysis 48 hr after clo-lip or DT administration.

Autoantibody Measurement

Antinuclear antibodies were measured by indirect immunofluorescence using HEp-2 cells (INOVA, San Diego, CA). Sera were diluted 1:40 and titers were determined using an Image Titer titration emulation system (Rhigene, Inc., Des Plaines, IL).

Anti-nRNP/Sm antigen capture ELISA was performed by coating microtiter plates (Nunc) overnight with 50 µ1 of human anti-nRNP IgG (20 pg/ml). Half of the wells were incubated for 1 h with 50 µ1 of K562 cell lysate and the other half with NET/NP40 alone. After washing, 100 µ1 of diluted mouse serum (l:250) were added to wells coated with either K562 cell lysate or buffer alone, incubated for 1 h, washed three times, followed by 1 h incubation with alkaline phosphatase-conjugated goat anti-mouse IgG antibodies (Southern Biotechnology). OD reading at 405 nm was converted to units based on a standard curve generated by known concentrations of anti-RNP antibodies (clone 2.73). Specific binding was determined by subtracting the value of the control wells (coated with antibodies but no antigen) from the value of the antigen-coated wells.

To measure anti-dsDNA autoantibodies, ELISA plates were coated with calf thymus DNA (60µg) resuspended in Reacti-bind DNA binding buffer (Pierce). Anti-ssDNA autoantibodies were measured similarly except calf thymus DNA was denatured (95 Cº x 5 min) and incubated on ice for 5 min prior to resuspension in Reacti-bind buffer. After overnight incubation, plates were blocked with NET/NP40 + 0.5% BSA for 1 h, followed by the addition of 100 µ1 of diluted mouse serum (l:250) to each well. Subsequent steps were performed as described above for Anti-nRNP/Sm ELISA.

In Vitro Stimulation

Whole PECs or sorted populations were resuspended in complete DMEM (containing 10% FCS, 10 mmol/L HEPES, glutamine, and penicillin/streptomycin plus 10 U/ml heparin) were

seeded on 96 well cell-culture plates (5 X 10^4 cells/well). Cells were stimulated with the indicated doses of peptidoglycan, poly I:C, R848, CpG ODN2395 (Invivogen, San Diego, CA), or LPS (from *Salmonella typhimurium*; Sigma) and incubated at 37°C in a 5% CO_2 atmosphere for 24 h before collecting the supernatant.

Cell Culture with TMPD

One mL of TMPD, mineral oil, or squalene was added to 9 mL of fetal bovine serum in a 15 mL polypropylene tube and rotated for 48 h at 4°C. The surface layer of unincorporated hydrocarbon oil was removed by aspiration at the end of the incubation. The amount of TMPD incorporated using this method was approximately 1 μg/mL as determined by gas chromatography / mass spectroscopy (not shown; Analytical Toxicology Core, University of Florida). J774 cells or BMDM were seeded on 24-well plates (5 X 10^5 cells/well) and cultured overnight in complete DMEM containing 10% FCS with or without hydrocarbon oils. For subsequent stimulation, cells were washed with PBS and fresh complete medium was added prior to the addition of TLR ligands. Incorporation of TMPD in DMSO and β-cyclodextrin (Sigma) has been described previously (104). TMPD (10% v/v) also was added to ethanol or mannide monooleate (Sigma; 5% in PBS). Solvent alone was used as a control and a range of TMPD concentrations (3 – 300 μM) was tested.

Endocytosis and Phagocytosis Assays

Endocytosis was quantified by uptake of FITC-dextran (5 μg/mL; Sigma) and phagocytosis by internalization of FITC-labeled microbeads (10:1 beads:cells ratio; Invitrogen) or DiD-labeled apoptotic BW5147 cells (10:1 apoptotic cell : target cell ratio) following overnight incubation of J774 cells in complete medium with or without TMPD. Apoptosis of BW5147 cells was induced by heat-shock at 45 ºC for 10 min. Following 4 h incubation at 37

ºC, apoptotic cells (>80% annexin V positive) were labeled with the fluorescent dye DiD (tetramethylindodicarbocyanine perchlorate; Invitrogen). J774 Cells were washed and incubated (in PBS + 0.5% BSA) with the fluorescent substrates for 30 min at 37º C, washed 3 times, and analyzed by flow cytometry.

Statistical Analysis

For quantitative variables, differences between groups were analyzed by the unpaired Student's t-test. Survival curves were analyzed using the log-rank test. ANA titers and autoantibody levels were compared using Mann-Whitney U test. Data are presented as mean ± s.d. All tests were two-sided and a p-value less than 0.05 was considered significant. Statistical analyses were performed using Prism 4.0 (GraphPad Software, San Diego, CA).

Table 2-1. Conventional and real-time PCR primers

Gene	Forward	Reverse
Mx-1	GATCCGACTTCACTTCCAGATGG	CATCTCAGTGGTAGTCAACCC
CCL2	AGGTCCCTGTCATGCTTCTG	GGATCATCTTGCTGGTGAAT
IP-10	CCTGCAGGATGATGGTCAAG	GAATTCTTGCTTCGGCAGTT
IFN-α*	ATGGCTAGRCTCTGTGCTTTCCT	AGGGCTCTCCAGAYTTCTGCTCTG
IFN-α5*	TGTGACCTTCTTCAGACTC	CTCCTCCTTGCTCAATC
IFN-β*	AGCTCCAAGAAAGGACGAACAT	ATTCTTGCTTCGGCAGTTAC
iNOS	ATCGACCCGTCCACAGTATG	GATGGACCCCAAGCAAGACT
IL-12p40	GAGTGGACTGGACTCCCGA	CAAGTTCTTGGGCGGGTCTG
β-actin	CCCACACTGTGCCCATCTAC	CGCTCGGTCAGGATCTTCAT
IRF-7	TGCTGTTTGGAGACTGGCTAT	TCCAAGCTCCCGGCTAAGT
CCR2	CTGCCTGCAAAGACCAGAAG	TATGCCGTGGATGAACTGAG
TLR3	TCCGCCCTCTTCGTAACT TG	TTGGCGGCTGGTAATCTTCT
TLR4	GAGGCAGCAGGTGGAATT GT	TGCTCAGGATTCGAGGCTTT
TLR7	GGCTGAACCATCTGGAAGAA	TAAGCTGGATGGCAGATCCT
TLR9	TGCTTTGGCCTTTCACTCTT	AACTGCGCTCTGTGCCTTAT
CCL7	GATCTCTGCCACGCTTCTGT	ATAGCCTCCTCGACCCACTT
CCL12	GTCCTCAGGTATTGGCTGGA	CACTGGCTGCTTGTGATTCT
CX3CL1	CGCGTTCTTCCATTTGTGTA	AGCTGATAGCGGATGAGCAA
CXCL1	GCTGGGATTCACCTCAAGAA	TCTCCGTTACTTGGGGACAC
CXCL5	CCCCTTCCTCAGTCATAGCC	TGCATTCCGCTTAGCTTTCT
Arg-1	GCACTGAGGAAAGCTGGTCT	GACCGTGGGTTCTTCACAAT
18S RNA	CGGCTACCACATCCAAGGAA	GCTGGAATTACCGCGGCT

* primers designed for conventional PCR.

CHAPTER 3
NOVEL TYPE-I INTERFEREON-PRODUCING CELLS IN TMPD-INDUCED LUPUS

Introduction

Systemic lupus erythematosus (SLE) is a chronic autoimmune disorder affecting multiple organs including the skin, joints, kidneys, lungs, heart and the nervous system (1). Antinuclear antibodies against small ribonucleoproteins (snRNPs) and double-stranded (ds) DNA are pathognomonic of the disease (1). Recent evidence suggests that type-I interferons (IFN-I), a family of anti-viral cytokines, are integral to the pathogenesis of SLE. More than half of SLE patients display upregulation of a group of IFN-I-stimulated genes (ISGs) (31-33). This "interferon signature" is clinically relevant as it correlates with active disease, presence of certain autoantibodies, and an increased incidence of renal involvement (33, 76). Supporting a causal role of IFN-I, therapeutic use of recombinant IFN-α is linked to a wide array of autoimmune manifestations and there are reports of SLE following treatment (72). Although an association between elevated IFN-I levels and SLE is well established, its origin is unclear.

Experimental lupus induced by 2, 6, 10, 14-tetramethylpentadecane (TMPD) displays key immunological and clinical features of human SLE, including the production of autoantibodies against dsDNA and snRNPs, and the development of immune complex-mediated glomerulonephritis and arthritis (96). We recently reported that TMPD-induced lupus is associated with excess IFN-I production and upregulation of ISGs (103). This is at present the only murine model reported to have the "interferon signature". IFN-I signaling is critically required in this model as shown by the absence of lupus autoantibodies and kidney disease in IFN-I receptor deficient mice (93). The source of the excess IFN-I, however, has not been examined. In this study, we aimed to identify and characterize the cell population(s) responsible for increased IFN-I production in TMPD-induced lupus.

Materials and Methods

Mice

Wild-type BALB/cJ, and B6.FVB-Tg*(Itgax-DTR/EGFP.57)*Lan/J backcrossed to a BALB/c background, referred to as CD11c-DTR (diphtheria toxin receptor) mice (99, 100), were purchased from Jackson Laboratories (Bar Harbor, ME) and housed in a conventional facility. CD11c-DTR mice were maintained as heterozygote crosses and littermates not expressing the transgene were used as controls. 129Sv/Ev Type I interferon receptor α-chain deficient mice ($IFNAR^{-/-}$) and wild type controls (129Sv/Ev; $IFNAR^{+/+}$) were purchased from B&K Universal Limited (Grimston, Aldbrough, England). Eight-week-old mice received a single intraperitoneal (i.p.) injection of 0.5 ml TMPD (Sigma-Aldrich, St. Louis, MO), mineral oil (Harris Teeter, Mathews, NC), 4% thioglycollate (BD Bioscience, San Jose, CA), squalene (Sigma), n-hexadecane (Sigma), or PBS. Peritoneal cell isolation, and cecal ligation and puncture were performed as described (100, 103).

Quantitative Real-Time PCR

Real-time PCR (RT-PCR) and conventional PCR were performed as described (103). Briefly, total RNA was extracted from 10^6 peritoneal cells using Trizol reagent (Invitrogen, Carlsbad, CA) and cDNA was synthesized using Superscript II First-Strand Synthesis Kit (Invitrogen). RT-PCR was performed using the SYBR Green Core Reagent Kit (Applied Biosystems, Foster City, CA) with an Opticon II thermocycler (MJ Research, Waltham, MA). Amplification conditions were: 95°C for 10 min, followed by 45 cycles of 94°C for 15 s, 60°C for 25 s, and 72°C for 25 s. After the final extension (72°C for 10 min), a melting-curve analysis was performed to ensure specificity of the products. IFN-I genes were amplified by conventional PCR using a PTC-100 programmable thermal controller (MJ Research). Amplification conditions were: 95°C for 5 min, followed by 40 cycles of 94°C for 30 s, 60°C for

1 min, and 72°C for 1 min. After a final extension (72°C for 10 min), PCR products were analyzed by agarose gel electrophoresis.

Flow Cytometry

All antibodies were purchased from BD Bioscience with the exceptions of anti-Ly6C-FITC, anti-Ly6C-biotin, avidin-APC (eBioscience, San Diego, CA), anti-F4/80-FITC, anti-Moma2-FITC (Serotec, Raleigh, NC), and anti-CD11b-Pacific blue (Caltag Laboratories, Burlingame, CA). Cell staining was performed as described (103). Propidium iodide (Invitrogen) staining was performed following manufacturer's protocol. Fifty thousand events per sample were acquired by a CYAN ADP flow cytometer (Dako, Fort Collins, CO) and analyzed with FCS Express 3 (De Novo Software, Ontario, Canada).

Cell Sorting

Peritoneal cells from TMPD-treated mice (10^7) were stained with anti-Ly6G-PE, washed, and incubated with magnetic bead-conjugated anti-PE (Miltenyi Biotec, Auburn, CA). Granulocytes (>99% purity) were positively selected using MS columns while the negative fraction was stained with anti-CD11b-APC, washed, and incubated with magnetic bead-conjugated anti-APC (Miltenyi Biotec). Positive selection using MS columns yielded >85% $Ly6C^{hi}$ monocytes. The negative fraction consisted of lymphocytes and dendritic cells (DCs). Cell sorting using a FACS DIVA flow cytometer (BD Bioscience) yielded similar results with a higher purity of $Ly6C^{hi}$ monocytes (>95%). For morphological analysis, 3 X 10^4 sorted cells were cytospun onto glass slides and stained using the Hema3 kit (modified Wright stain; Fisher Scientific, Pittsburg, PA).

Monocyte Labeling and Depletion

Clodronate (a gift from Roche Diagnostics) liposomes (Clo-lip) and 1,1'-dioctadecyl-3,3,3',3'-tetramethylindodicarbocyanine perchlorate (DiD)-liposomes were produced as

described (105, 106). To label Ly6C^{-} monocytes, 150 μL of DiD-liposomes were injected i.v. into TMPD-treated mice. Clo-lip (200 μl) was delivered i.v. 24 hr prior to the injection of DiD-liposomes for the labeling of Ly6C^{hi} monocytes. Analysis was performed 24 hr after labeling. To deplete peritoneal monocytes, 200 μL of clodronate-containing liposomes were injected i.p. in wild-type BALB/c mice treated with TMPD two weeks earlier.

Dendritic Cell Depletion

DC ablation was performed in TMPD-treated CD11c-DTR mice by injecting 4 ng/g body weight of diphtheria toxin (DT; Sigma) i.p. Mice were sacrificed for analysis 48 hr after clo-lip or DT administration.

Statistical Analysis

For quantitative variables, differences between groups were analyzed by the Student's unpaired t-test. Bivariate correlations were assessed using Spearman's correlation coefficient. Data were presented as mean ± s.d. All tests were two-sided and a p-value less than 0.05 was considered statistically significant. Statistical analyses were performed using GraphPad Prism 4.0 (GraphPad Software, San Diego, CA).

Results

The "Interferon Signature" Precedes Lupus Disease Onset

Although the link between SLE and IFN-I is firmly established, it remains unclear whether the "interferon signature" precedes disease manifestations. In the TMPD model of SLE, production of lupus autoantibodies (anti-Sm, -nRNP and -dsDNA) and development of immune-complex-mediated glomerulonephritis occur approximately four to six months after peritoneal exposure to the hydrocarbon oil (96). Upregulation of IFN-α and IFN-β, on the other hand, was observed in peritoneal exudate cells (PECs) within two weeks of TMPD treatment (Figure 3-1A).

Although consensus PCR primers can amplify most IFN-α subtypes, quantification of ISG expression allows assessment of total IFN-I proteins, since all IFN-I subtypes bind to single receptor complex to activate ISG expression. Accordingly, a panel of ISGs including myxoma resistance protein-1 (Mx-1), macrophage chemoattractant protein-1 (MCP-1/CCL2), and IP-10/CXCL10 were also highly upregulated (Figure 3-1B) two weeks after TMPD treatment. In contrast, ISG expression was only modestly increased in mice treated with mineral oil, a control hydrocarbon oil that triggers chronic inflammation without features of lupus. Supporting the gene expression data, elevated levels of IFN-β and MCP-1 protein along with the inflammatory cytokines tumor necrosis factor-α (TNF-α) and interleukin (IL)-12 were demonstrated in peritoneal lavage fluid of TMPD-treated mice (not shown). Thus, the "interferon signature" induced by TMPD was established within 2 weeks of treatment, long before the appearance of lupus autoantibodies and kidney pathology.

Accumulation of Ly6C^{hi} Monocytes Induced by TMPD Treatment

To identify the source of IFN-I production, we analyzed different cell populations in the peritoneal exudate two weeks following TMPD treatment. More than 80% of the cells in the inflammatory exudate were CD11b^{+} (not shown). Since CD11b is expressed by monocytes/macrophages, granulocytes and peritoneal B1 cells, we utilized the marker Ly6C to distinguish these populations (107, 108). In untreated or PBS-treated animals, resting peritoneal cells predominantly consisted of macrophages (CD11b^{hi} Ly6C^{-}) and B1 cells (CD11b^{mid} Ly6C^{-}; Figure 3-1C). As described previously (107), peritoneal macrophages expressed the F4/80 antigen while B1 cells were positive for the B cell markers B220 and CD5 (not shown). Interestingly, both resting cell types were depleted two weeks following TMPD treatment while two distinct populations emerged: CD11b^{+} Ly6C^{hi} cells (R1), consistent with the phenotype of immature monocytes (108), and CD11b^{+} Ly6C^{mid} cells (R2) characteristic of granulocytes

(Figure 3-1C, D). The latter (R2) also expressed the neutrophil marker Ly6G (not shown). These populations each represented ~ 30% of cells in the peritoneal inflammatory infiltrate. Morphology of the monocyte and granulocyte populations was consistent with their surface marker profile (Figure 3-1E). These findings were consistent in other wild-type strains (C57/BL6 and BALB/c), except that these strains showed a greater influx of granulocytes (not shown).

Treatment with mineral oil, which does not induce the interferon signature, resulted in similar accumulation of granulocytes, but few Ly6C^{hi} monocytes were present (Figure 3-1C, D). Instead, mature monocytes resembling resting peritoneal macrophages were found (R3, Figure 3-1C, D). Compared to the Ly6C^{hi} monocytes, these cells were larger, more vacuolated, and displayed rounded nuclei, suggestive of a more differentiated phenotype (Figure 3-1E). The accumulation of Ly6C^{hi} monocytes was specific to TMPD treatment as this pattern was not seen in sterile peritonitis induced by thioglycollate or septic peritonitis induced by cecal ligation and puncture (CLP; Figure 3-1C).

Flow cytometry analysis of Ly6C^{hi} monocytes from TMPD-treated animals demonstrated intense expression of the myeloid markers Mac-3 and Moma-2 (Figure 3-1F).

Supporting their immature phenotype, only a small fraction of Ly6C^{hi} monocytes expressed the macrophage marker F4/80, major histocompatibility complex (MHC) class II (I-A), and the costimulatory molecules CD80 and CD86 (Figure 3-1F). This was in sharp contrast to mature peritoneal macrophages, which expressed these markers at high levels (not shown). Ly6C^{hi} monocytes also lacked markers of dendritic cells (CD11c and CD205), B cells (B220 and CD19), T cells (CD3), granulocytes (Ly6G) or NK cells (Pan-NK; Figure 3-1F and not shown). The absence of B220 and CD11c expression distinguishes these cells from the previously described natural interferon-producing cells, which also express Ly6C, albeit at much lower

levels compared to Ly6C^{hi} monocytes (64, 109). Curiously, these monocytes exhibited strong expression of Sca-1 (Ly6A/E; Figure 3-1F), a marker normally found on hematopoietic stem cells and certain T-cell subsets (110).

While the accumulation of Ly6C^{hi} monocytes was evident after two weeks, these cells appeared in the peritoneal cavity as early as one day after TMPD treatment (Figure 3-1G). However, this observation was not limited to TMPD as a similar pattern of acute peritoneal inflammation was elicited by mineral oil (Figure 3-1G). But the appearance of Ly6C^{hi} monocytes in response to mineral oil was transient compared to TMPD. Only a small population of Ly6C^{hi} monocytes was found in the peritoneal cavity two weeks after mineral oil treatment whereas the response was maintained for several months with TMPD treatment (Figure 3-1C and not shown).

To investigate the source of the accumulating Ly6C^{hi} monocytes, we first performed a cell cycle analysis to determine whether these cells were proliferating in the peritoneal cavity. Propidium iodide staining revealed that virtually all Ly6C^{hi} monocytes in the peritoneal exudate elicited by TMPD were in G1 phase (Figure 3-2A), indicating that extramedullary myelopoiesis at the site of inflammation is not a likely explanation for the monocyte accumulation.

Recent studies have demonstrated that Ly6C^{hi} monocytes egress from the bone marrow and that expression of Ly6C diminishes as they mature in the circulation (105). We therefore examined whether TMPD treatment alters the maturation profile of peripheral blood monocytes. In untreated animals, mature circulating monocytes (Ly6C^{-}) outnumbered their immature Ly6C^{hi} counterparts by about 2:1 (Figure 3-2B). Two weeks after TMPD treatment, the frequency of Ly6C^{hi} monocytes in the peripheral blood doubled while the Ly6C^{-} subset remained constant (Figure 3-2B).

To demonstrate the migration of Ly6C^{hi} monocytes into the peritoneal cavity following TMPD injection, we selectively labeled monocyte subsets *in vivo*. As described previously (105), intravenous injection of liposomes containing the fluorescent dye DiD labeled strictly Ly6C^{-} monocytes in the circulation (Figure 3-2C left). Consistent with the paucity of Ly6C^{-} monocytes in the response to TMPD, DiD^{+} cells were not recovered from the peritoneal cavity. Using clodronate-containing liposomes first to deplete mature monocytes (105), circulating Ly6C^{hi} monocytes were specifically labeled by the subsequent administration of DiD-liposomes (Figure 3-2C right). After 24 hours, more than one-third of Ly6C^{hi} monocytes in the peritoneal cavity were DiD^{+}, indicating that TMPD treatment induces rapid and specific recruitment of this monocyte subset. Taken together, the data suggest that TMPD treatment results in the export of Ly6C^{hi} monocytes from the bone marrow into the circulation and followed by their specific recruitment and accumulation in the peritoneal cavity.

Immature Ly6C^{hi} Monocytes are a Major Source of IFN-I Production

Using magnetic bead sorting, we separated PECs from TMPD-treated mice into Ly6C^{hi} monocytes, Ly6G^{+} granulocytes, and a negative fraction consisting of lymphocytes and dendritic cells. Although the Ly6C^{hi} monocyte fraction contained a small percentage of contaminating Ly6G^{+} granulocytes, DCs were found only in the negative fraction (not shown). PCR analysis revealed that Ly6C^{hi} monocytes were the predominant source of IFN-α and IFN-β expression (Figure 3-3A). IFN-I transcripts also were detected in other populations, albeit at significantly lower levels (Figure 3-3A). Ly6C^{hi} monocytes expressed high levels of the interferon-stimulated chemokine MCP-1 and moderate levels of TNF-α and IL-12 (Figure 3-3B) as well. Granulocytes accounted for the remaining TNF-α transcripts and the majority of inducible nitric oxide synthase (iNOS) expression. Not surprisingly, IL-12 transcripts were found predominantly in cells of the negative fraction as this cytokine was most likely derived from DCs (Figure 3-3B).

Similar results were obtained when this experiment was repeated using flow cytometric cell sorting to increase the purity of sorted populations (not shown).

To confirm that Ly6C^{hi} monocytes were major producers of IFN-I, we asked whether their depletion abolishes the interferon signature. Treatment with clodronate-containing liposomes (clo-lip) effectively eliminates monocytes *in vivo* (106). Indeed, a single dose of clo-lip i.p. was sufficient to eliminate about 80% of peritoneal Ly6C^{hi} monocytes in mice pretreated with TMPD (Figure 3-3C). There were also slight reductions in the number of DCs and lymphocytes (not shown) whereas the number of CD11b^{+} Ly6C^{mid} Ly6G^{+} granulocytes was unaffected by clo-lip treatment.

Concomitant with the depletion of Ly6C^{hi} monocytes, the expression of IFN-α, IFN-β, and ISGs was drastically reduced (Figure 3-3D, E). Similarly, the expression of TNF-α, which was highly expressed by Ly6C^{hi} monocytes, also diminished upon their depletion. The expression of IL-12, which was expressed mainly by the negative cell fraction comprised of lymphocytes and DCs, did not change significantly after clo-lip treatment (Figure 3-3E). The effect of clo-lip was transient as the number of Ly6C^{hi} monocytes and the expression of ISGs returned to pre-treatment levels after four days (not shown).

Induction of IFN-I by TMPD is not Dependent on DCs

Plasmacytoid DCs are capable of secreting large amounts of IFN-I during viral infection and are thought to be primary interferon producers in SLE (64, 84). In the peritoneal cavity of TMPD-treated animals, CD11c^{+} I-A^{+} DCs comprised of ~ 2% of the infiltrating inflammatory cells. Most peritoneal DCs expressed CD11b but not B220 (Figure 3-4A), consistent with the phenotype of myeloid DCs. However, PDCs may home to other secondary lymphoid tissue following activation (64, 109). To elucidate the extent to which DCs contribute to IFN-I

production in the TMPD model, we utilized transgenic mice carrying the simian diphtheria toxin receptor under the control of the CD11c promoter (CD11c-DTR)(99). Injection of diphtheria toxin (DT) rapidly ablates both PDCs and MDCs systemically in CD11c-DTR mice whereas wild-type mice are unaffected by the toxin (99).

Two days following DT injection, TMPD-treated CD11c-DTR mice showed >85% depletion of $CD11c^+$ $I\text{-}A^+$ DCs in the peritoneal exudate compared to wild-type controls (Figure 3-4B,C). In line with previous reports (100, 111), DC depletion was systemic as splenic MDCs and PDCs were also depleted by 70-80% (Figure 3-4B,C). In contrast, there was no significant difference in the peritoneal accumulation of $Ly6C^{hi}$ monocytes, granulocytes, and lymphocytes (Figure 3-4C and not shown). Both $CD11c^{hi}CD11b^+I\text{-}A^+$ MDCs and $CD11c^+B220^+PDCA\text{-}1^+$ PDCs were depleted to a similar degree in the spleen (Figure 3-4D) and lymph nodes (not shown). Systemic depletion of DCs did not affect TMPD-induced IFN-I production as the expression of IFN-I and ISGs were unaffected in CD11c-DTR animals (Figure 3-4E,F). The expression of TNF-α and iNOS was also unchanged (not shown). In contrast, IL-12 expression was drastically reduced in the absence of DCs (Figure 3-4F), consistent with the cell sorting experiment (Figure 3-3E). Taken together, the data indicate that DCs were the primary source of IL-12 but not IFN-I.

We also tried to deplete PDCs using the recently described PDC-specific antibody 120G8 (112). Treatment with 120G8 i.p. resulted in ~70% depletion of splenic PDCs after 24 hr, comparable to the levels seen in CD11c-DTR mice. However, peritoneal $Ly6C^{hi}$ monocytes and T lymphocytes were also reduced by >50% (not shown). While the antigen bound by 120G8 and PDCA-1 is normally expressed on PDCs, its expression can be induced by IFN-I in other cell types (112, 113). Indeed, elevated IFN-I production in TMPD mice is associated with the

expression of this PDC antigen on Ly6C^{hi} monocytes, granulocytes and T lymphocytes (not shown), making selective antibody-mediated depletion of PDCs unfeasible in this model.

Accumulation of Ly6C^{hi} Monocytes is Associated with Autoantibody Production

Expression of ISGs is associated with autoantibodies against Sm/RNP in SLE patients (33, 76). In the TMPD model, 60-70% of treated BALB/c mice exhibit anti-Sm/RNP antibodies after 4-6 months vs. 0% of IFN-I receptor deficient mice (93). These autoantibodies either appear less frequently or are completely absent in mice treated with other adjuvant oils such as n-hexadecane, squalene, or mineral oil (114). Interestingly, treatment with n-hexadecane (which induces anti-Sm/RNP in about 25% of treated animals) elicited the accumulation of Ly6C^{hi} monocytes, albeit the response was milder than with TMPD, whereas squalene (which induces a weak anti-Sm/RNP response in <10% of treated animals) recruited mostly mature monocytes/macrophages and few Ly6C^{hi} monocytes, resembling the pattern seen with MO (Figure 3-5A). Since Ly6C^{hi} monocytes were the major source of IFN-I in TMPD-treated mice, we examined whether the frequency of anti-Sm/RNP autoantibodies correlates with the number of these cells. Indeed, the adjuvant oils' ability to elicit anti-Sm/RNP antibodies was highly correlated (r^2=0.98) with the accumulation of Ly6C^{hi} monocytes (Figure 3-5B, upper panel). Numbers of Ly6C^{hi} monocytes also correlated with ISG expression (Figure 3-5B, lower panel), supporting our finding that these cells are major IFN-I producers. In contrast, the recruitment of granulocytes was similar among all treatment groups and more DCs were present in the PECs following MO or squalene treatment than TMPD (not shown).

Surface Expression of Ly6C on Monocytes is not IFN-I-Dependent

Since Ly6C is an interferon-inducible gene (115), it is possible that IFN-I production triggered by TMPD treatment contributes to the Ly6C^{hi} monocyte phenotype. To address this issue, we analyzed monocyte subsets in IFN-I receptor-deficient (IFNAR$^{-/-}$) mice. Compared to

wild type controls, untreated IFNAR$^{-/-}$ mice showed similar levels of Ly6C^{hi} and Ly6C^{-} monocytes in the circulation, accounting for approximately 2 and 5% of PBMC, respectively (not shown). Two weeks following TMPD treatment, IFNAR$^{-/-}$ mice also displayed increased numbers of circulating Ly6C^{hi} monocytes, albeit the response was milder than that of wild type controls (Figure 3-6). Importantly, Ly6C^{hi} and Ly6C^{-} monocytes, as well as the Ly6C^{mid} granulocyte populations in the peripheral blood were clearly discernible even in the absence of IFN-I signaling. The number of bone marrow precursors of Ly6C^{hi} monocytes was also comparable between wild-type and IFNAR$^{-/-}$ mice (Figure 3-6). These data suggest that although IFN-I have been shown to induce Ly6C expression (115), the Ly6C^{hi} phenotype of the immature monocyte population in naïve or TMPD-treated mice was not dependent on IFN-I signaling.

Discussion

Elevated serum IFN-I was first associated with SLE over two decades ago (30). Recent studies using microarrays and RT-PCR further defined a panel of ISGs over-expressed in the peripheral blood of SLE patients (31-33). While this interferon signature has been linked to disease activity, kidney involvement, and autoantibody levels, the source of IFN-I responsible for the interferon signature remains a matter of speculation. This issue has been difficult to address using animal models as most of them do not exhibit upregulation of IFN-I.

We recently reported that murine lupus induced by TMPD is associated with elevated IFN-I production and ISG expression (103). Disruption of IFN-I signaling completely abrogates the development of kidney disease and the onset of autoantibody production (93). In this study, we show that Ly6C^{hi} monocytes are a major source of IFN-I in the TMPD model of lupus. Upregulation of IFN-I and ISGs occurred long before the clinical manifestations of lupus and coincided with an accumulation of Ly6C^{hi} monocytes. These immature monocytes expressed

large amounts of IFN-I and the "interferon signature" was rapidly abolished upon depletion of these cells by clo-lip. Moreover, the abundance of Ly6C^{hi} monocytes was highly associated with the ability of various adjuvant oils to induce anti-Sm/RNP antibodies. In contrast, systemic depletion of DCs did not alter IFN-I production triggered by TMPD.

While Ly6C^{hi} monocytes were found in the inflammatory infiltrate one day after thioglycollate (105, 106) or mineral oil administration , the response was transient as the number of these cells was drastically reduced after 72 hours. The recruitment and accumulation of Ly6C^{hi} monocytes seen in TMPD-treated animals, on the other hand, persisted for as long as 4 months after treatment. A recent study shows that the egression of Ly6C^{hi} monocytes from the bone marrow in response to *Listeria monocytogenes* infection is dependent on the interaction between the monocyte attractant CCL2/MCP-1 and its receptor CCR2 (116). Interestingly, as confirmed here, MCP-1 is an ISG that is induced by TMPD treatment, raising the possibility that the production of interferon-inducible chemokines may drive the recruitment of Ly6C^{hi} monocytes. This is relevant to human SLE as elevated serum levels of MCP-1 have been associated with the interferon signature (32). How TMPD-treatment maintains the infiltrating monocytes in an immature state is unknown, but a defect intrinsic to the cells is unlikely as Ly6C^{hi} monocytes spontaneously acquired a mature macrophage-like phenotype (Ly6C^{-} F4/80^{+} I-A^{+}) *in vitro* (not shown). The immaturity of Ly6C^{hi} monocytes may be important to their ability to produce IFN-I as their mature counterparts elicited by mineral oil displayed significantly lower levels. Analogously, PDCs also are better equipped to secrete large amounts of IFN-I when immature (117).

Prolonged elevation of IFN-I may promote DC maturation (74), T cell survival (47), isotype class-switching (49), and B cell maturation into plasma cells (48), culminating in the loss

of tolerance and autoantibody production. It is noteworthy that while IFN-I is essential to TMPD-induced lupus (93), other factors such as IL-12 and IFN-γ play important roles since autoantibody production and kidney disease development are reduced in deficient mice (23, 24).

Our findings challenge the conventional view that PDCs are solely responsible for the elevated IFN-I in SLE. In TMPD-treated mice, the vast majority of the increased IFN-I production is derived from the 20-30% of peritoneal cells that are $Ly6C^{hi}$ $CD11b^{+}$ $B220^{-}$ $CD11c^{-}$ monocytes. Although, PDCs can synthesize up to 1000-fold more IFN-α than most other cell types (65), the number of circulating PDCs is drastically reduced in SLE patients (33, 118). While it is plausible that PDCs home to tissues following activation, a view supported by the presence of these cells in lupus skin lesions (86), there is little direct evidence connecting tissue PDCs to the excess serum IFN-I seen in SLE patients. Indeed, as tissue (e.g. spleen) PDCs were greatly reduced by DT treatment of CD11c-DTR mice, despite little effect on ISG expression, it is unlikely that PDCs were the main source of IFN-I in TMPD-induced lupus. Also, the elevation of IFN-I in this model occurs within two weeks of treatment, long before the appearance of autoantibodies against dsDNA and snRNP and formation of immune complexes. The proposed mechanism of IFN-I induction in PDCs by endogenous nucleic acids present in immune complexes, therefore, is not a likely explanation of our findings (84). Nevertheless, PDCs may function to amplify IFN-I production once autoantibodies and immune complexes develop. MDCs also play a role in TMPD-induced lupus as they are the major source of IL-12, a cytokine critical for the development of kidney disease in this model (24). The role of DCs in human SLE is more difficult to assess as targeted DC therapy is not yet available.–

It is noteworthy that $Ly6C^{hi}$ monocytes also have been recently reported to play a role in atherosclerosis (119). Therefore, these monocyte-like interferon producing cells could play a role

in the premature atherosclerosis seen in SLE patients. A $CD14^{hi}CD16^{-}$ monocyte subset (also called “classical monocytes”) is the equivalent of murine $Ly6C^{hi}$ monocytes in terms of migratory properties (108). Whether this or other monocyte subsets produce IFN-I in human SLE warrants detailed investigation.

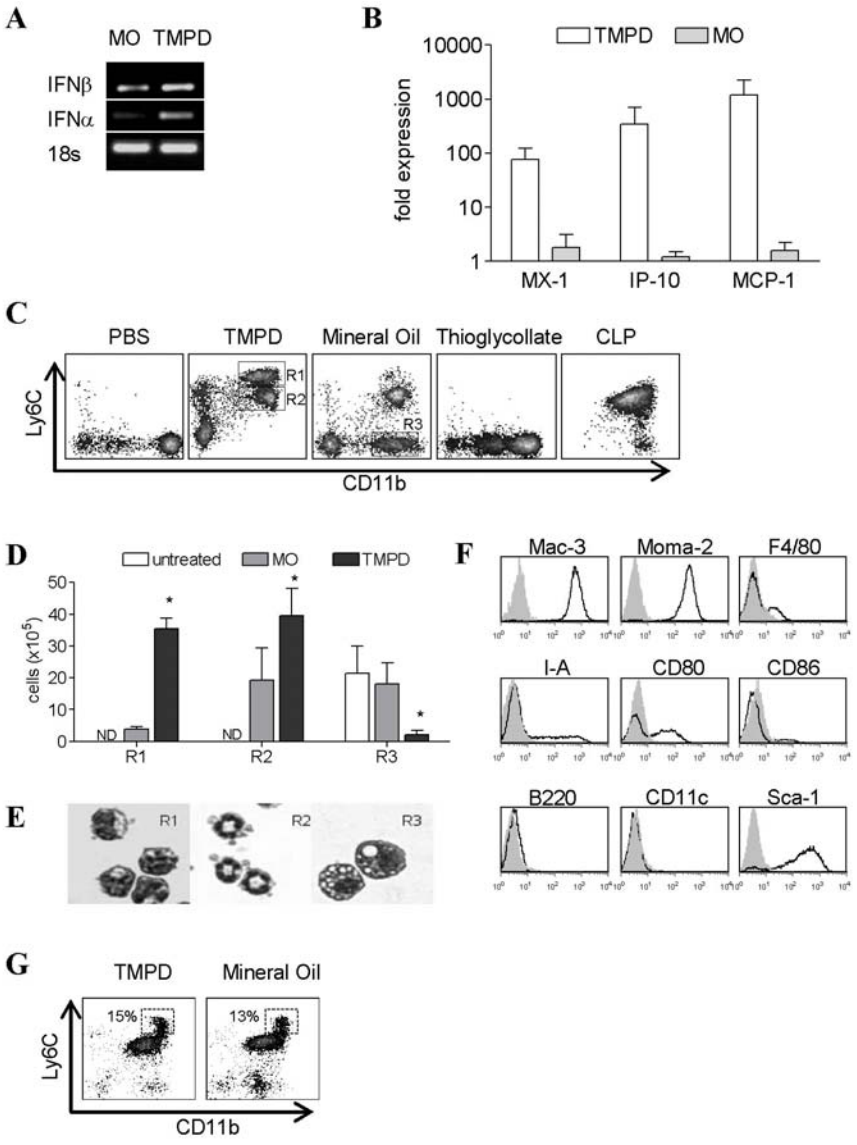

Figure 3-1. Elevated expression of IFN-I and accumulation of Ly6C^{hi} monocytes after TMPD treatment. Comparisons of A) IFN-I expression (conventional PCR) and B) ISG expression (RT-PCR) in peritoneal cells two weeks after TMPD or MO treatment. C) Flow cytometry of peritoneal cells in wild-type 129Sv mice treated with PBS, TMPD (2 weeks), mineral oil (2 weeks), thioglycollate (3 days), and cecal-puncture ligation (3 days). Boxes indicate Ly6C^{hi} immature monocytes (R1), CD11b^{+} Ly6C^{mid} granulocytes (R2), and Ly6C^{-} mature monocytes/macrophages (R3). D) Quantification and E) morphologic analysis of peritoneal cell populations. F) Flow cytometry of surface makers on Ly6C^{hi} immature monocytes. G) Flow cytometry of peritoneal cells from wild-type 129Sv mice treated with TMPD or mineral oil for 1 day. Shaded region (panel F) represents isotype control staining and boxes indicate Ly6C^{hi} immature monocytes. Each bar (panels B and D) represents the mean of 4 animals and error bars indicate standard deviation (s.d.). * $p < 0.05$ (Student's t-test).

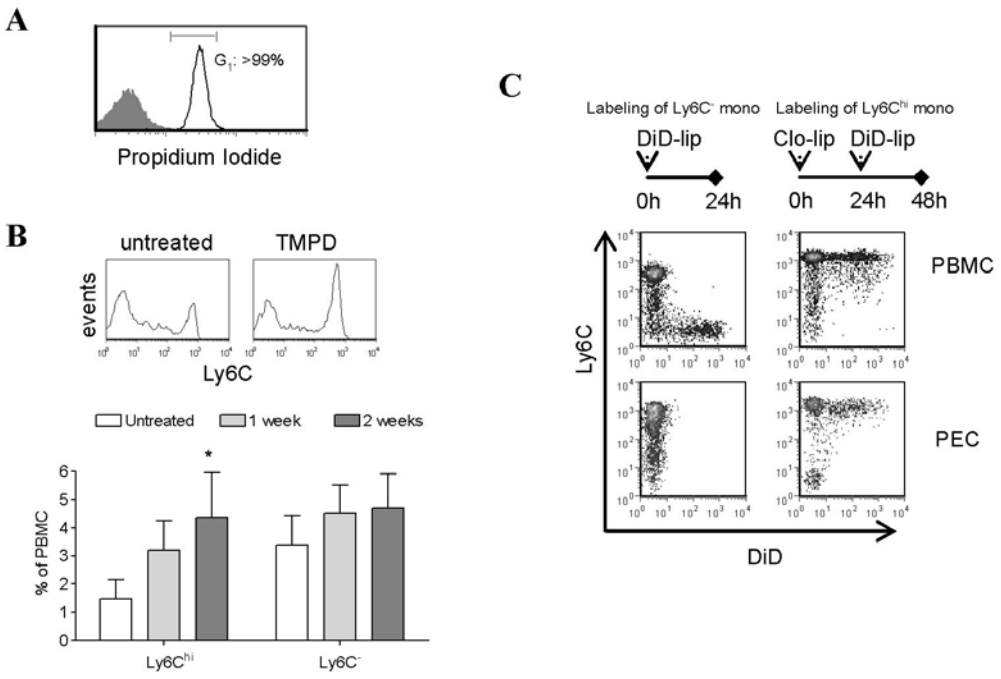

Figure 3-2. Direct recruitment of circulating Ly6C^{hi} monocytes after TMPD treatment. A) Propidium idodide cell cycle analysis of peritoneal cells two weeks after TMPD treatment. B) Flow cytometry of Ly6C expression on peripheral blood monocytes (gated on CD11b^{+}Ly6G^{-} cells) and quantification of peripheral blood Ly6C^{hi} and Ly6C^{-} monocytes following TMPD treatment (n = 4 per group). C) Flow cytometry of peripheral blood and peritoneal monocytes (gated on CD11b^{+}Ly6G^{-} cells) in TMPD-treated mice 24 hr after administration of DID-liposomes. Data are representative of 3 independent experiments.

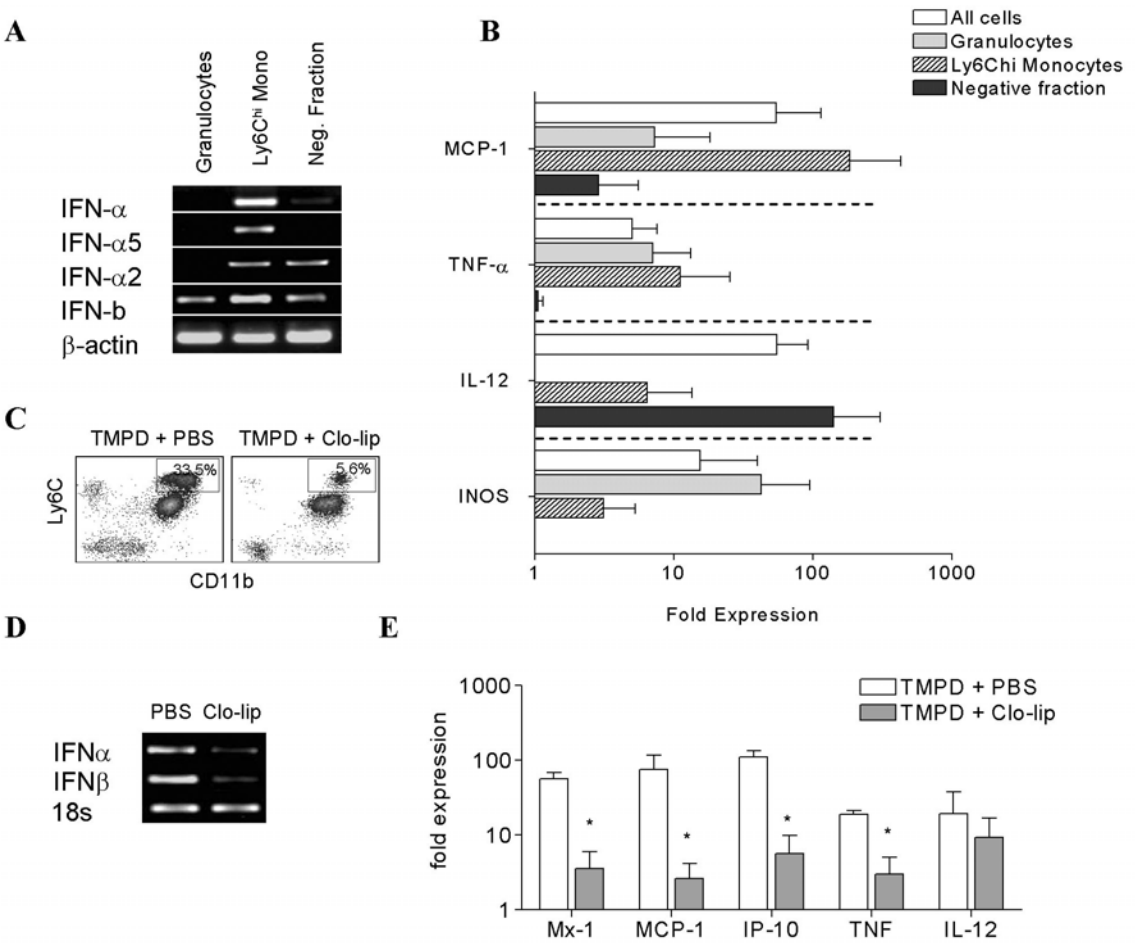

Figure 3-3. Immature Ly6C^{hi} monocytes are major producers of IFN-I. Analysis of A) IFN-I expression (conventional PCR) and B) ISG expression (RT-PCR) in magnetic bead-sorted peritoneal Ly6C^{hi} monocytes, granulocytes and the negative fraction (lymphocytes and DCs) from wild-type 129sv mice treated with TMPD (2 weeks). C) Flow cytometry of TMPD-elicited peritoneal cells 2 days following treatment with clodronate-containing liposomes (clo-lip). Box indicates Ly6C^{hi} monocytes. D) IFN-I expression (conventional PCR) and E) ISG expression (RT-PCR) in peritoneal cells after clodronate-liposome or PBS treatment. Each bar represents the mean of 5 animals and error bars indicate s.d. * $p < 0.05$ (Student's t-test).

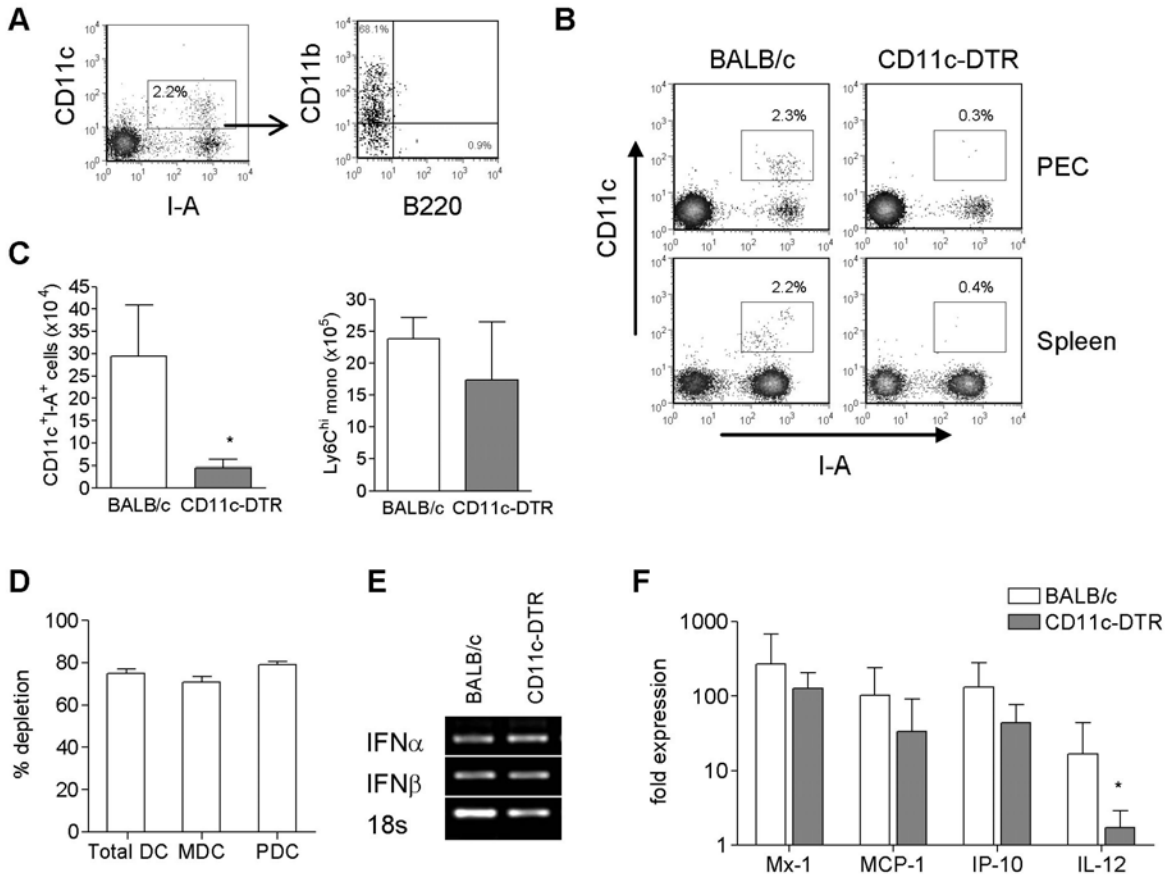

Figure 3-4. Dendritic cells are not required for IFN-I production induced by TMPD. A) Flow cytometry of peritoneal DCs two weeks after TMPD treatment. Box indicate $CD11c^+$ $I\text{-}A^+$ DCs. B) Depletion in CD11c-DTR mice 2 days after diphtheria toxin (DT) injection. Box indicates $CD11c^+$ $I\text{-}A^+$ DCs. C) Quantification of peritoneal dendritic cells and $Ly6C^{hi}$ monocytes. D) Quantification of splenic DC depletion. MDCs were defined as $CD11c^{hi}$ $I\text{-}A^+$ $CD11b^+$ cells and PDCs were defined as $CD11c^+$ $B220^+$ $PDCA\text{-}1^+$. E) IFN-I expression (conventional PCR) and F) ISG expression (RT-PCR) in peritoneal exudates cells. Each bar represents the mean of 6 animals and error bars indicate s.d. * $p < 0.05$ (Student's t-test).

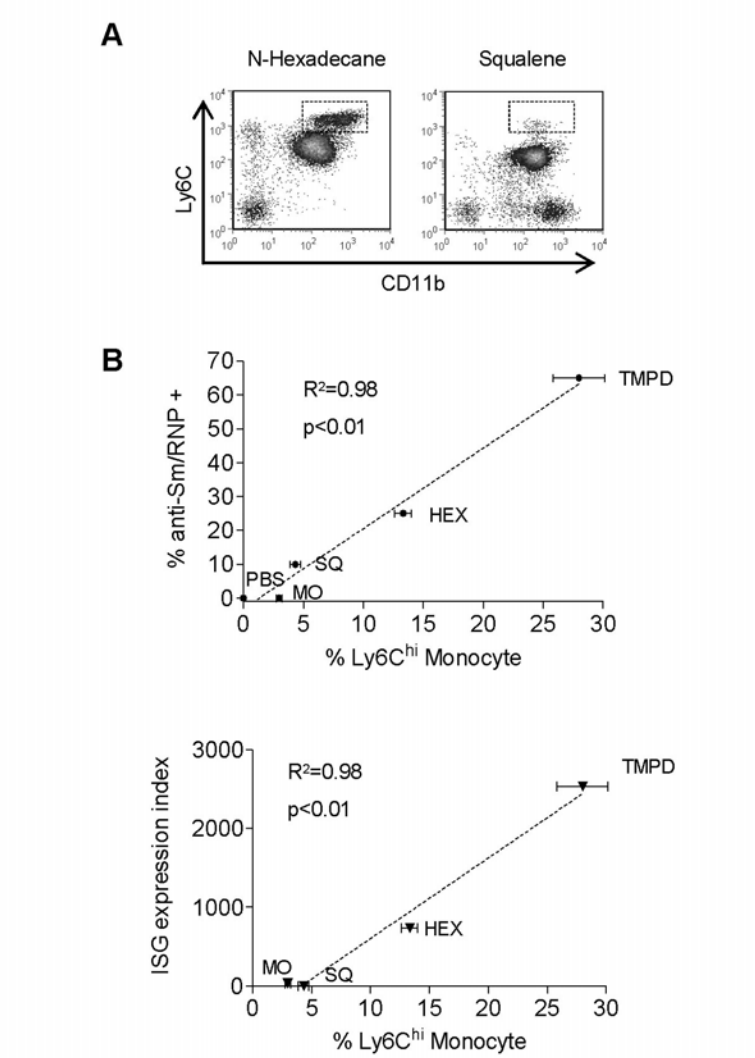

Figure 3-5. Accumulation of Ly6C^{hi} monocytes is correlated with the frequency of anti-Sm/RNP autoantibodies and upregulation of ISG expression. A) Flow cytometry of peritoneal cells in wild-type 129Sv mice treated with n-hexadecane (2 weeks) or squalene (2 weeks). Boxes indicate Ly6C^{hi} immature monocytes. Correlation of the levels of Ly6C^{hi} monocyte accumulation with B) the frequency of anti-Sm/RNP autoantibodies (6 months) and ISG expression (2 weeks) induced by TMPD, n-hexadecane (HEX), squalene (SQ), and mineral oil (MO) and PBS. Autoantibody frequencies represent the mean of >10 mice per group from previous studies. Percentage of Ly6C^{hi} monocytes and ISG expression index represent the mean of 4 mice. Error bars indicate s.d. ISG expression index was calculated as follows: mean relative expression of (Mx-1 + MCP + IP-10)/3.

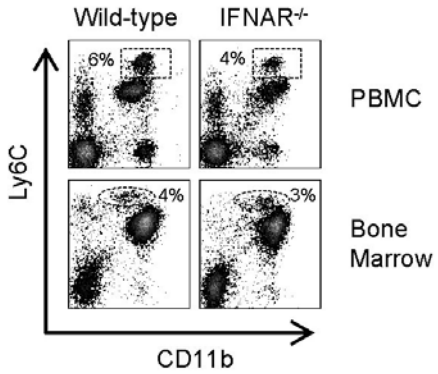

Figure 3-6. Expression of Ly6C on immature monocytes is not dependent on IFN-I signaling. Flow cytometry analysis of monocyte subsets in the peripheral blood (upper) and bone marrow (lower) of wild-type 129sv and IFN-I receptor-deficient mice two weeks after TMPD-treatment. Boxes and ovals indicate peripheral blood $Ly6C^{hi}$ monocytes and bone marrow $Ly6C^{hi}$ monocyte precursors, respectively.

CHAPTER 4
TOLL-LIKE RECEPTOR 7-DEPENDENT AND FCγR-INDEPENDENT PRODUCTION OF TYPE-I INTERFERON IN TMPD-INDUCED LUPUS

Introduction

SLE is a chronic autoimmune disease characterized by the production of autoantibodies against double stranded (ds)-DNA and small nuclear ribonucleoproteins (snRNPs), including the Sm/RNP antigens, Ro/SS-A, and other antigens (1). Recent evidence strongly suggests that type-I interferons (IFN-I), a family of antiviral cytokines, are integral to the pathogenesis of SLE. Elevated serum levels of IFN-I and over-expression of interferon-stimulated genes (ISGs) in the peripheral blood of SLE patients have been demonstrated by several groups (31, 32, 76). This "interferon signature" is associated with active disease and autoantibodies against dsDNA and the Sm/RNP and Ro/SS-A antigens (33, 75).

The etiology of excess IFN-I in SLE is incompletely understood. Research on innate immunity has led to the identification of several pathways mediating IFN-I production in mammalian cells. Toll-like receptor (TLR)3, a sensor for viral dsRNA, and TLR4, the receptor for lipopolysaccharide (LPS) both stimulate IFN-I secretion through TIR domain-containing adaptor inducing IFN-β (TRIF) (52). In contrast, TLR7/8 and TLR9 mediate IFN-I production via myeloid differentiation factor-88 (MyD88) in response to single-stranded(ss)-RNA and unmethylated CpG DNA, respectively (54, 55, 120). In addition, cytoplasmic receptors that recognize intracellular nucleic acids and induce IFN-I have been described recently. Retinoic acid inducible gene-I (RIG-I) and melanoma differentiation associated gene-5 (MDA-5) recognize cytoplasmic RNA and trigger IFN-I by activating interferon-β promoter stimulator-1 (IPS-1, also known as MAVS, VISA and CARDIF) and IRF-3 (60, 61, 121). Cytoplasmic DNA binds to a cytoplasmic sensor and triggers IFN-I production via a pathway requiring TANK-binding kinase-1 (TBK-1) and IRF-3 (62, 122).

Nucleic acids from dying cells may act as ligands for TLR7/8 and TLR9 to trigger IFN-I production in SLE. In plasmacytoid dendritic cells, immune complexes formed by autoantibodies to DNA and snRNPs help transport these "endogenous ligands" to endosomes containing TLR7, 8 and 9, resulting in IFN-I production (84). This hypothesis is supported by *in vitro* studies (77, 80). However, therapeutic administration of IFN-α can directly trigger the production of anti-dsDNA antibodies (72) and in several murine lupus models, IFN-I production is required for the induction of autoantibodies (89, 90, 93), suggesting that IFN-I dysregulation may occur upstream of autoantibody development. Therefore, it remains controversial whether nucleic acid-containing immune complexes in SLE initiate IFN-I production or act to perpetuate a positive feedback loop of IFN-production initiated by another factor, such as a viral infection.

Experimental lupus induced by TMPD (pristane) displays many key immunological and clinical features of human SLE, including the presence of the "interferon signature" and lupus autoantibodies such as anti-dsDNA, anti-Sm, and anti-RNP (96, 97, 103). Importantly, IFN-I play an essential role in this model as glomerulonephritis and autoantibody production (anti-Sm/RNP, -dsDNA, and -Su) are abolished in IFN-I receptor-deficient ($IFNAR^{-/-}$) mice (93). Unexpectedly, a population of $Ly6C^{hi}$ immature monocytes that accumulates in the peritoneal cavity after TMPD treatment, rather than dendritic cells, is the major source of IFN-I in this model (see chapter 3). The persistent influx of $Ly6C^{hi}$ monocytes and production of IFN-I occur within two weeks of TMPD treatment, long before the appearance of autoantibodies against snRNPs and dsDNA (3-5 months), suggesting that the initial wave of IFN-I production is independent of RNA-containing immune complexes. In this study, we aimed to elucidate the mechanism of IFN-I production in TMPD-induced lupus.

Materials and Methods

Mice

MyD88$^{-/-}$, TRIF$^{-/-}$, TLR7$^{-/-}$, TLR9$^{-/-}$, IFNAR$^{-/-}$ mice (backcrossed >7 generations to the C57BL/6 background) and IPS-1$^{-/-}$, TNF$^{-/-}$, TNF$^{-/-}$TBK1$^{-/-}$ (on a mixed 129Sv/ B6 background) have all been described previously (52, 54, 56, 69, 101, 102). Wild-type C57BL/6 and heterozygous littermates were used as controls. BALB/c.TLR7$^{-/-}$ (backcrossed >8 generations to the BALB/c background) and wild-type BALB/c mice were used for long-terms studies of autoantibody production. Animals were bred and maintained in a specific pathogen-free facility of the Research Institute for Microbial Diseases, Osaka University. C57BL/6 wild type and FcγRI/III$^{-/-}$ mice (Taconic, Hudson, NY) and BXSB mice (Jackson Laboratories, Bar Harbor, ME) were maintained in a specific pathogen-free facility at the University of Florida. BXSB X B6 F1 mice were generated by breeding BXSB males with C57BL/6 females. The mixed background of several strains used in this study did not alter the response to TMPD as measured by the expression of ISGs and peritoneal cell influx (data not shown). Twelve to sixteen-week old animals received a single intraperitoneal (i.p.) injection of 0.5 mL TMPD (Sigma-Aldrich, St. Louis, MO). Blood samples were obtained before, and weekly after TMPD treatment. Peritoneal cells, spleen, and blood were harvested two weeks after treatment. Monocyte depletion was performed by i.p. injection of clodronate-containing liposomes (200 μL) as described (106). These studies were approved by the Institutional Animal Care and Use Committee.

Real-Time Quantitative PCR

RT-PCR was performed as described (103). Briefly, total RNA was extracted from 10^6 peritoneal cells using Trizol reagent (Invitrogen, Carlsbad, CA) and cDNA was synthesized using Superscript II First-Strand Synthesis Kit (Invitrogen) following the manufacturer's

protocol. SYBR green RT-PCR analysis was performed using an Opticon II thermocycler (MJ Research, Waltham, MA). Amplification conditions were: 95°C for 10 min, followed by 45 cycles of 94°C for 15 s, 60°C for 25 s, and 72°C for 25 s. After the final extension (72°C for 10 min), a melting-curve analysis was performed to ensure specificity of the products. Primers used in this study are listed in Table 2-1. The expression of *Mx1*, *IRF7*, *18s* rRNA also were analyzed using Taqman primers and probes purchased from Applied Biosystems and the results were consistent with the SYBR green method (data not shown). Cytokine/chemokine PCR array (Superarray, Frederick, MD) analysis was performed using an ABI 7700 Sequence Detector (Applied Biosystems) following the manufacturer's protocols.

Flow Cytometry and Cell Sorting

The following conjugated antibodies were used: anti-CD11b-phycoerythrin (PE), anti-CD8-allophycocyanin (APC), anti-CD4- fluorescein isothiocyanate (FITC), anti-CD11c-PE, anti-B220-PerCPCy5.5, anti-Sca-1-PE, anti-CD64-PE, anti-CD32/16-PE(all from BD Bioscience), anti-Ly6C-FITC, anti-Ly6C-biotin, and avidin-APC (eBioscience, San Diego, CA). Prior to surface staining, peritoneal or peripheral blood cells were incubated with anti-mouse CD16/32 ("Fc block"; BD Bioscience) for 10 min. Cells were then stained with an optimized amount of primary antibody or the appropriate isotype control for 10 min at room temperature before washing and resuspending in PBS supplemented with 0.1% bovine serum albumin. Intracellular staining for TLR7 was performed as described (123) using rabbit anti-mouse TLR7 or rabbit IgG isotype control (EBioscience) and goat anti-rabbit IgG-FITC (Southern Biotechnology). Fifty thousand events per sample were acquired using a FacsCalibur (BD Bioscience) and analyzed with FCS Express 3 Software (De Novo Software, Ontario, Canada). Cell sorting was performed using a FACS DIVA flow cytometer (BD Bioscience). Peritoneal,

splenic, and bone marrow Ly6C^{hi} monocytes (CD11b^{+}Ly6C^{hi}), peritoneal dendritic cells (CD11c^{+}) and granulocytes (CD11b^{+}Ly6G^{+}) were sorted to >90% purity for cell culture or RNA isolation.

In Vitro Stimulation

Sorted cells resuspended in complete DMEM (containing 10% FCS, 10 mmol/L HEPES, glutamine, and penicillin/streptomycin plus 10 U/ml heparin) were seeded on 96 well cell-culture plates (5 X 10^4 cells/well). Cells were stimulated with the indicated doses of peptidoglycan, poly I:C, R848, CpG ODN2395 (Invivogen, San Diego, CA), or LPS (from *Salmonella typhimurium*; Sigma) and incubated at 37 ° C in a 5% CO_2 atmosphere for 24 h before collecting the supernatant. MCP-1 and IL-6 ELISAs (BD Biosciences) were performed following manufacturer's instructions. Optical density was converted to concentration using standard curves based on recombinant cytokines analyzed by a four-parameter logistic equation (Softmax Pro 3.1 software).

Autoantibody Analysis

Serum antinuclear antibodies in BALB/c.TLR7$^{-/-}$ and wild-type BALB/c mice were determined 12 and 24 wks after TMPD by indirect immunofluorescence using HEp-2 cells (INOVA, San Diego, CA). Sera were diluted 1:40 and titers were determined using an Image Titer titration emulation system (Rhigene, Inc., Des Plaines, IL). Immunoprecipitation and antigen-capture ELISA to detect serum autoantibodies against nRNP/Sm were performed as described (96, 124). Determination of anti-Su/ago2 by ELISA also has been described (125).

Statistical Analysis

For quantitative variables, differences between groups were analyzed by the unpaired Student's t-test. Survival curves were analyzed using the log-rank test. ANA titers and autoantibody levels were compared using Mann-Whitney U test. Data are presented as mean ±

s.d. All tests were two-sided and a p-value less than 0.05 was considered significant. Statistical analyses were performed using Prism 4.0 (GraphPad Software, San Diego, CA).

Results

Induction of IFN-I by TMPD Requires MyD88

To identify the mechanism of IFN-I induction by TMPD, we first analyzed the effect of TMPD on mice with deficiency of the adaptor molecules TRIF or MyD88. TRIF is required to trigger IFN-I production by TLR3 and TLR4 (52), whereas MyD88 mediates TLR7/8 and TLR9 signaling (54, 55, 120). Previously we have shown that within two weeks of TMPD treatment, an accumulation of IFN-I-producing $CD11b^{+}Ly6C^{hi}$ monocytes can be detected in the peritoneal cavity in wild-type mice concurrent with increased IFN-I production and ISG expression (see Chapter 3). Compared with wild-type mice, the total number of peritoneal exudate cells (PECs) was significantly reduced in $MyD88^{-/-}$ mice after TMPD treatment (Figure 4-1A). Both $Ly6C^{hi}$ monocytes and granulocytes (defined as $CD11b^{+}Ly6G^{+}Ly6C^{mid}$) were decreased by >90% (Figure 4-1A,B). Importantly, IFN-I induction by TMPD was completely dependent on MyD88 as elevated expression of the ISGs myxoma response protein-1 (*Mx1*) and interferon regulatory factor-7 (*IRF7*) in PECs was abolished in $MyD88^{-/-}$ mice as also seen in IFNAR-deficient mice (Figure 4-1C). The levels of the interferon-inducible chemokine monocyte chemoattractant protein-1 (MCP-1/CCL2) in the peritoneal lavage fluid were also reduced in the absence of MyD88 (Figure 4-1D). In contrast, TRIF deficiency did not impact the accumulation of PEC populations or the increased expression of ISGs (Figure 4-1A-D). Although we were unable to detect significant changes in serum IFN-α/β levels by ELISA, IFN-I secretion was required for the response to TMPD as the upregulation of ISGs and recruitment of $Ly6C^{hi}$ monocytes were

abolished in IFNAR$^{-/-}$ mice (Figure 4-1A-D). The absence of IFN-I signaling, however, did not affect the influx of granulocytes (Figure 4-1A,B).

The increase in IFN-I following TMPD treatment is not limited to the peritoneal cavity as the "interferon signature" is also detectable in the peripheral blood (93). We found that surface expression of the interferon-inducible gene Sca-1 (Ly6A/E) on B cells was dramatically up-regulated in wild-type mice treated with TMPD (Figure 4-1E). Although Sca-1 is naturally expressed by certain lymphocyte subsets and hematopoietic stem cells (110), TMPD induced Sca-1 expression in virtually all B cells in wild-type, but not IFNAR$^{-/-}$ mice (Figure 4-1E). Increased Sca-1 expression was also evident on CD8^{+} and CD4^{+} T cells (not shown). Similar to the pattern of ISG expression in PECs, upregulation of Sca-1 was reduced in MyD88$^{-/-}$, but not TRIF$^{-/-}$ mice (Figure 4-1E), further supporting an essential role of MyD88 in IFN-I production.

To address whether cytoplasmic nucleic acid sensors also contribute to TMPD-induced IFN-I production, we tested the effect of TMPD on IPS-1$^{-/-}$ and TNF$^{-/-}$TBK1$^{-/-}$ mice [TBK-1$^{-/-}$ is embryonically lethal unless crossed onto a TNFα-/- background (69)]. IPS-1 is a required adaptor for intracellular viral RNA detection via RIG-I and MDA-5 (61), whereas TBK-1 is required for cytoplasmic DNA-induced IFN-I secretion (126). Expression of *Mx1* and *IRF7* in PECs was comparable in wild-type, IPS-1$^{-/-}$, TNF$^{-/-}$TBK-1$^{-/-}$, and TNF$^{-/-}$ mice (Figure 4-2), suggesting that the intracellular nucleic acid-sensing pathways were not required for IFN-I production. The patterns of peritoneal cell influx and Sca-1 expression on peripheral blood lymphocytes were also similar among these strains (not shown). Taken together, our data indicate that TMPD-elicited IFN-I production was strictly MyD88-dependent.

Induction of IFN-I by TMPD is TLR7-Dependent, Immune Complex-Independent

Since MyD88 mediates IFN-I induction by TLR7 and TLR9, we next investigated which of these innate receptors is responsible for the effect of TMPD. Two weeks after TMPD

treatment, the number of PECs in TLR9$^{-/-}$ mice was reduced by about 20% compared to TLR7$^{-/-}$ and wild-type controls. The numbers of Ly6C^{hi} monocytes and granulocytes also were reduced in the absence of TLR9, although the pattern of the cellular influx remained similar to wild-type animals (Figure 4-3A, B).

Interestingly, TLR7$^{-/-}$ mice exhibited a specific reduction of Ly6C^{hi} monocytes in the peritoneal cavity (Figure 4-3A). Despite the decrease in these immature monocytes, total PEC counts in TLR7$^{-/-}$ mice were comparable to wild-type controls due to a significant increase in the number of granulocytes (Figure 4-3A, B). An accumulation of CD11b^{+}Ly6C^{-} residential macrophages also was evident in the absence of TLR7 (Figure 4-3B). These patterns are strikingly similar to those observed in IFNAR$^{-/-}$ mice (Figure 4-1A-D). Indeed, the increased *Mx1* and *IRF7* expression and MCP-1 production were abrogated in TLR7$^{-/-}$ mice (Figure 4-3C). Upregulation of Sca-1 expression on B cells also was reduced in these mice after TMPD treatment (Figure 4-3D), recapitulating the findings in MyD88$^{-/-}$ and IFNAR$^{-/-}$ mice. On the contrary, ISG expression in PECs and surface expression of Sca-1 were similar in TLR9$^{-/-}$ mice compared with wild-type controls. These findings suggest that although TLR9 may contribute to the inflammatory response, IFN-I induction by TMPD was mediated primarily by TLR7.

To further define the role of TLR7 in the inflammatory response to TMPD, we compared the expression of various cytokines and chemokines in wild-type and TLR7$^{-/-}$ animals using a PCR array. Following TMPD treatment, peritoneal cells from wild-type mice displayed dramatically higher expression of several interferon-stimulated chemokines including *CCL2*, *CCL12*, *CCL7*, and *CXCL10* in comparison with TLR7$^{-/-}$ mice (Table 4-1). This pattern of chemoattractant production is similar to the chemokine signature recently described in SLE patients (127). These observations support the role of TLR7 as the primary mediator of IFN-I

production in the TMPD lupus model. Interestingly, consistent with the increased number of peritoneal granulocytes in TMPD-treated TLR7$^{-/-}$ mice (Figure 4-3A), the neutrophil chemoattractant *CXCL5* was upregulated in the absence of TLR7 whereas the expression of other inflammatory mediators was comparable between the groups (Table 4-1).

Several studies have demonstrated that self-RNA present in immune complexes may act as an endogenous TLR7 ligand causing the production of IFN-I (77, 80). Fcγ-receptors (FcγR) have been reported to play an essential role in this process by enhancing the internalization of immune complexes, allowing RNA to interact with TLR7 in endosomes (128). Deficiency of either TLR7 or FcγR γ-chain, an integral component of FcγRI and FcγRIII, renders murine DCs unable to produce IFN-I in response to lupus immune complexes (129). Since TMPD induces IFN-I production long before the onset of lupus autoantibodies and immune complexes (see Chapter 3), we examined the potential role of FcγR in the IFN-I response to TMPD. Surface expression of FcγRI (CD64) and FcγRII/III (CD32/CD16) in TMPD-induced PECs was prominent on Ly6C^{hi} monocytes (Figure 4-4A). FcγRs were also expressed by a fraction of granulocytes, whereas lymphocytes and DCs in the peritoneal cavity displayed little surface expression of these receptors (Figure 4-4A).

We next analyzed the effects of TMPD on FcγR γ-chain-deficient mice (FcγR$^{-/-}$). The accumulation of Ly6C^{hi} monocytes and upregulation of ISG expression were comparable in FcγR$^{-/-}$ and wild-type mice (Figure 4-4B,C). Elevated surface expression of Sca-1 on peripheral blood lymphocytes was also similar between the groups (not shown). Taken together, these findings suggest that TMPD elicits IFN-I production through a TLR7-dependent, but FcγR-independent pathway.

Immature Ly6C^{hi} Monocytes Express High Levels of TLR7

Next we examined the distribution of TLR7 expression in the inflammatory infiltrate induced by TMPD. PECs from mice treated with TMPD two weeks earlier were sorted into four distinct populations based on surface marker phenotype: Ly6C^{hi} monocytes (CD11b^{+}Ly6C^{hi}; ~30% of PECs), granulocytes (CD11b^{+}Ly6G^{+}; ~30%), DCs (CD11c^{+}; ~2%), and a negative fraction containing mainly B and T lymphocytes. As reported previously (see Chapter 3), the DC fraction consisted of >80% CD11b^{+} myeloid DCs and few PDCs (CD11c^{+}CD11b^{-}B220^{+}) were present.

Quantitative PCR revealed that Ly6C^{hi} monocytes expressed higher levels of *TLR7* than other peritoneal cell subsets (Figure 4-5A). Prominent expression of the chemokine receptor CCR2 is consistent with their immature monocytic phenotype as reported previously (108). In striking contrast, elevated expression of *TLR7* was not a feature of Ly6C^{hi} monocytes in the spleen or bone marrow. While *TLR7* expression also was found on other PEC subsets, DCs displayed greater expression of *TLR3* and *TLR9* whereas *TLR4* transcripts were predominantly found in granulocytes (Figure 4-5A).

In line with these findings, when peritoneal Ly6C^{hi} monocytes were depleted by i.p. injection of clodronate-containing liposomes (clo-lip), the expression of *TLR7* by PECs was greatly reduced whereas the levels of *TLR9* transcripts remained unaffected (Figure 4-5B). We further analyzed the response of Ly6C^{hi} monocytes to various TLR ligands *in vitro*. Sorted Ly6C^{hi} monocytes secreted large amounts of MCP-1 and IL-6 when co-cultured with the synthetic TLR7 ligand R848 (Figure 4-5C). They also responded to the TLR4 ligand LPS, albeit less strongly even at the highest dose of LPS tested (10 μg/mL). Consistent with their low levels of TLR3 and TLR9 expression, Ly6C^{hi} monocytes exhibited weak responses to poly I:C and CpG DNA (Figure 4-5C). In contrast, isolated granulocytes did not produce measurable

amounts of MCP-1 or IL-6 in response to any TLR ligands used in this study (not shown). Hence, Ly6C^{hi} monocytes recruited to the peritoneal cavity after TMPD treatment expressed high levels of *TLR7* and actively responded to TLR7 ligands.

The Y-linked Autoimmune Accelerating (Yaa) Locus Amplifies the Effects of TMPD

The Yaa locus is essential for spontaneous development of autoantibodies and glomerulonephritis in the BXSB model of murine lupus (130). Yaa also accelerates disease onset in other lupus-prone strains (131, 132). *TLR7* is among the 17 genes found in the Yaa locus (133, 134). Because *TLR7* is normally located on the X chromosome, males possess one copy of the gene while a similar gene dosage is achieved females through X-inactivation. Male Yaa mice, however, have two functional copies of the gene (133, 134). A recent study showed that the *TLR7* gene duplication alone was responsible for the autoimmune features associated with the Yaa mutation (135).

Since TMPD induces IFN-I production via TLR7, we asked whether the effects of the adjuvant oil are more pronounced in the presence of the Yaa locus. Compared to female controls (designated TLR7$^{+/+}$), BXSB X B6 male mice carrying the Yaa mutation (TLR7$^{+/Yaa}$) exhibited greater accumulation of Ly6C^{hi} monocytes in the peritoneal cavity two weeks after TMPD treatment (Figure 4-6A). Importantly, increasing the gene dosage of TLR7 was associated with significantly higher production of IFN-I, assessed by measuring ISG expression (Figure 4-6B). In contrast, the IFN-I response to TMPD was similar between males and females in wild-type strains including C57BL/6, BALB/c, and 129Sv (not shown).

We further examined the long term effect of TMPD treatment in the BXSB model. Consistent with previous studies (130), BXSB males died prematurely beginning at 5 months of age (Figure 4-6C). Mortality was significantly accelerated when a single dose of TMPD was administered i.p. at 8-10 weeks of age. Sixty percent of TMPD-treated animals succumbed by 5

months of age, vs. 20% in the control group. Whereas 5/10 PBS-treated animals survived until 7 months, only 1/10 in the TMPD-treated group remained. Thus, not only was the induction of IFN-I accentuated by the Yaa mutation, TMPD treatment also hastened disease progression in the BXSB mice.

Essential Role of TLR7 in the Development of Autoantibodies

In MRL-*lpr* mice, TLR7 is required for the development of anti-Sm antibodies (136). To assess whether TLR7 also is involved in autoantibody production in the TMPD-lupus, we compared the long-term response to TMPD in wild-type BALB/c and BALB/c.TLR7$^{-/-}$ mice. No mortality was found in either group and only mild proteinuria was detected by 24 wks-post treatment (not shown). Comparable to previous observations (137), BALB/c mice displayed significant hypergammaglobulinemia 24 wks after TMPD treatment (Figure 4-7A). The increase in serum IgG was reduced by 50% in TLR7$^{-/-}$ mice while IgM levels were similar between groups. Consistent with the role of IFN-I in IgG2a isotype switching (48), IgG2a was profoundly reduced in TLR7$^{-/-}$ mice (Figure 4-7B). IgG1 and IgG2b levels also were reduced mildly in the absence of TLR7 whereas IgG3 increased slightly.

As early as 12 wks after TMPD treatment, 8/12 wild-type mice developed serum antinuclear antibodies (ANA) and anti-nRNP/Sm autoantibodies (Figure 4-7C, D). In contrast, only one TLR7$^{-/-}$ mouse showed a low titer ANA and none developed autoantibodies to nRNP/Sm (Figure 4-7C, D). Similar to IFNAR-deficient animals (93), most TLR7$^{-/-}$ mice exhibited low levels of ANA of unknown specificity by 24 wks post-treatment but the titers were lower than BALB/c controls (Figure 4-7C). A single TLR7$^{-/-}$ animal with high titer ANA (1:1280) produced autoantibodies against DNA/chromatin (not shown). In contrast, autoantibodies against nRNP/Sm remained undetectable in all TLR7$^{-/-}$ mice (Figure 4-7D). We further confirmed the autoantibody profile by immunoprecipitation using nuclear extracts from

^{35}S-labeled K562 cells. Consistent with the ELISA data, autoantibodies against various components of nRNP/Sm (A-G) were found in wild-type, but not TLR7$^{-/-}$ mice (Figure 4-7E).

Immunoprecipitation studies also revealed that autoantibodies against the Su antigen, which develops in ~20 % of lupus patients (138) and ~50% of TMPD-treated BALB/c mice (138), were not induced in TLR7$^{-/-}$ mice (Figure 4-8A). Su antigen is an RNA-binding protein, also known as argonaute 2 (ago2), involved in the microRNA pathway (125, 139). ELISA using recombinant ago2 confirmed that the development of autoantibodies against Su/ago2 required TLR7 (Figure 4-8B), suggesting that the autoimmune response to microRNA-associated antigens also is mediated by TLR7. Thus, in addition to its role in mediating IFN-I production, TLR7 is essential for the generation autoantibodies against RNA-associated antigens (nRNP/Sm and Su/ago2) in TMPD-induced lupus.

Discussion

Recent studies strongly suggest a link between elevated IFN-I production and the pathogenesis of SLE. More than half of SLE patients display increased expression of ISGs, often in association with active disease and autoantibodies against snRNPs and DNA, as well as renal involvement and endothelial dysfunction (31-33, 75, 76, 140). However, the exact cause of IFN-I dysregulation in lupus remains controversial and it is unclear whether IFN-I overproduction promotes autoantibody production or vice versa.

TMPD-induced lupus recapitulates many features of human SLE including glomerulonephritis, arthritis, and autoantibodies against dsDNA and snRNPs (96, 97). Like SLE, TMPD-lupus is more severe in females than males (141). We recently found that TMPD-treated mice exhibit the interferon signature and that their lupus is dependent on IFN-I signaling (93). Here, we show that TMPD triggers IFN-I production via the TLR7/MyD88 pathway. Our data also exclude a major role of other pathways of IFN-I production, including TLR9,

TLR3/TLR4/TRIF, RIG-I/Mda5/IPS-1, and DAI/TBK1. Although there was a strict requirement for TLR7 and MyD88, expression of ISGs and recruitment of $Ly6C^{hi}$ monocytes in response to TMPD was unexpectedly independent of FcγRs, suggesting that uptake of immune complexes is not required for IFN-I production in this model.

The innate sensors TLR7 and TLR9 have been implicated in SLE due to their ability to recognize endogenous nucleic acids and trigger IFN-I production (83). Mammalian nucleic acids are generally weak TLR ligands due in part to their inability to reach the endosomal compartment where TLR7 and TLR9 are localized. When they form ICs with lupus autoantibodies (anti-Sm/RNP or anti-dsDNA), endogenous nucleic acids may be delivered more efficiently to endosomes due to uptake by FcγRs, stimulating IFN-I production by PDCs (83, 84). This model for IFN-I induction in human SLE is supported by numerous *in vitro* studies (80, 82, 128). Whereas FcγRIIa mediates the activation of human PDCs, ICs trigger IFN-I production by murine PDCs in a TLR7- and FcγRI/III-dependent manner (129).

However, it is not known whether the development of anti-ribonucleoprotein autoantibodies is a cause of IFN-I dysregulation or a consequence of it. Therapeutic use of IFN-α can induce many features of SLE including anti-dsDNA antibodies, suggesting that IFN-I dysregulation occurs upstream of IC formation. Consistent with that view, IFN-I upregulation in the TMPD model occurs within the first two weeks of treatment, more than two months before the onset of lupus autoantibodies (see Chapter 3). FcγRI and FcγRIII were not required for the IFN-I response to TMPD, since it was unaffected in γ-chain-deficient mice. Moreover, a previous study showed that the absence of FcγRI/III or FcγRIIb does not affect anti-Sm/RNP autoantibody production in TMPD-treated mice (142). Although IC formation and FcγRs are not

required to initiate IFN-I production, we cannot exclude the possibility that they amplify IFN-I secretion and accelerate disease progression subsequent to the development of autoantibodies.

A pathogenic role of TLR7 has been described in several murine lupus models. The *lpr* mutation (which leads to aberrant apoptosis due to the deficiency of *fas*) drastically accelerates autoantibody production and kidney disease in the autoimmune prone MRL background (91). In MRL-*lpr* mice, TLR7 ligands accelerate the onset of glomerulonephritis whereas deletion of TLR7 abrogates the development of anti-Sm autoantibodies and reduces the severity of nephritis (123, 136). Lupus in MRL-*lpr* mice is ameliorated, not exacerbated by IFN-I (92), and the *lpr* defect prevents induction of TMPD-lupus (143).

Dual engagement of TLR7 and the B-cell receptor can directly activate autoreactive B cells in the AM14 model, which spontaneously produce rheumatoid factors derived from MRL-*lpr* mice (144). TLR7 also is required for the spontaneous production of autoantibodies against ssRNA in 564Igi transgenic mice, in which the heavy and light chain genes encoding an anti-RNA immunoglobulin have been inserted into the heavy and light chain loci of the non-autoimmune C57BL/6 background (145). The connection between TLR7 and the generation of RNA-associated autoantibodies is further illustrated by the recent demonstration of a duplication of the TLR7 gene in Yaa mice. The presence of the Yaa cluster was sufficient to induce RNA-associated autoantibodies in C57BL/6 FcγIIB$^{-/-}$ mice and C57BL6.Sle1 mice, two autoimmune strains that normally lack these antibody specificities (133, 134). TLR7, and not the other 16 genes affected by the Yaa mutation, is responsible for the autoimmune pathology (135). Increased IFN-I production has not been reported in these models, however. Our findings indicate that TLR7 also plays an essential role in TMPD lupus. Similar to MRL-*lpr* (136), TLR7 is required to generate anti-nRNP/Sm autoantibodies in TMPD-lupus. The interferon signature

in TMPD-treated mice, which is established within 2 weeks of treatment (long before the appearance of anti-nRNP autoantibodies), was abolished in the absence of TLR7. In contrast, the effects of TMPD were amplified in the presence of Yaa. Therefore, TLR7 is likely to be involved directly in the induction of IFN-I, even in the absence of autoantibodies and ICs.

We have shown previously that Ly6C^{hi} monocytes are a major source of IFN-I in the TMPD model. Depletion of monocytes, but not DCs, reduced IFN-I production and ISG expression. Here we found that Ly6C^{hi} monocytes express higher levels of TLR7 and display a greater response *in vitro* to R848 than to other TLR ligands. While TLR7 normally is found on monocytes and macrophages, its expression on peritoneal Ly6C^{hi} monocytes in TMPD-treated mice was several-fold higher than on splenic or bone marrow monocytes. In contrast, DCs in the peritoneal exudate displayed lower levels of TLR7 and more prominent TLR3 and TLR9 expression. The high expression of TLR7 by Ly6C^{hi} monocytes may be of critical importance in the pathogenesis of TMPD lupus, as increased TLR7 gene dosage is sufficient to trigger anti-RNA antibodies and glomerulonephritis in C57BL/6 mice (135). Interestingly, the recruitment of Ly6C^{hi} monocytes to the peritoneum seems partially dependent on IFN-I, as seen in TLR7$^{-/-}$, MyD88$^{-/-}$, and IFNAR$^{-/-}$ mice. TLR7 signaling also induces the expression of several interferon-stimulated chemokines (*CCL2*, *CCL7*, and *CCL12*), suggesting that the mechanism may involve enhanced production of monocyte chemoattractants, creating an amplification loop of Ly6C^{hi} monocyte recruitment and IFN-I production. The recruitment of DCs and granulocytes, on the other hand, was not dependent on IFN-I or TLR7.

The exact mechanism linking TMPD to the activation of TLR7 on Ly6C^{hi} monocytes and/or other cell subsets remains uncertain. While it is possible that the TMPD acts as a TLR7 ligand, its hydrocarbon structure is distinct from known TLR7 ligands including ssRNA, R848,

loxoribine, and other guanosine analogues. However, the structure of hydrocarbon oils is related to their ability to stimulate IFN-I production. Hexadecane, which differs from TMPD by the addition of one carbon and the absence of four methyl groups, elicits less ISG expression and a lower incidence of anti-RNP autoantibodies (see Chapter 3). Other adjuvant oils such as medicinal mineral oil lack the ability to induce lupus autoantibodies and IFN-I production (146). Alternatively, TMPD may function indirectly by modifying or stabilizing endogenous TLR7 ligands such as the U1 RNA component of the Sm/RNP antigen, which is released from dying cells (27, 81, 147). Incorporation of TMPD into the plasma membrane also could affect the function and/or stability of TLRs (148). Further studies are needed to define the mechanism of TLR7 activation by TMPD, although *in vitro* investigations on the proinflammatory properties of the adjuvant oil are significantly limited by the immiscible nature of TMPD in aqueous solutions. It is noteworthy that besides activating IFN-I production via TLR7, TMPD also induced granulocyte recruitment via a MyD88-dependent, but TLR7-independent pathway. The number of peritoneal granulocytes actually increased in the absence of IFN-I production, as seen in $TLR7^{-/-}$ and $IFNAR^{-/-}$ mice. MyD88 is employed in the signaling pathways of other cytokines (IL-1 and IL-18) and TLRs (except TLR3), which are potential mediators of granulocyte recruitment in this model.

Finally, our findings may shed light on other pathology induced by TMPD. The development of plasmacytomas following i.p. injection of TMPD in BALB/cAnPt mice was first described over three decades ago (94). Subsequently TMPD was used to enhance monoclonal antibody production by hybridomas (95). How TMPD elicits these effects is incompletely understood, although IL-6 has been implicated. Interestingly, while TLR7 can trigger B cell activation and antibody production (144), IFN-I plays an important role in antibody class-

switching and promotes plasma cell differentiation in the presence of IL-6 (149). Whether TLR7 activation and IFN-I production are involved in the pathogenesis of plasmacytomas and enhancement of antibody production by hybridomas warrants further investigation.

Table 4-1. Cytokine and chemokine PCR array analysis in TLR7$^{-/-}$ mice.

Ref Seq	Gene	Description	Fold Difference*
NM_011331	Ccl12	Chemokine (C-C motif) ligand 12	-33.9362
NM_013654	Ccl7	Chemokine (C-C motif) ligand 7	-28.4818
NM_011333	Ccl2	Chemokine (C-C motif) ligand 2	-24.7422
NM_021274	Cxcl10	Chemokine (C-X-C motif) ligand 10	-16.2245
NM_008599	Cxcl9	Chemokine (C-X-C motif) ligand 9	-6.08813
NM_013653	Ccl5	Chemokine (C-C motif) ligand 5	-5.58203
NM_011329	Ccl1	Chemokine (C-C motif) ligand 1	-5.45568
NM_008337	Ifng	Interferon gamma	-5.01697
NM_013652	Ccl4	Chemokine (C-C motif) ligand 4	-1.53374
NM_021443	Ccl8	Chemokine (C-C motif) ligand 8	-1.40583
NM_010735	Lta	Lymphotoxin A	-1.05032
NM_007768	Crp	C-reactive protein, pentraxin-related	-0.98869
NM_019932	Cxcl4	Chemokine (C-X-C motif) ligand 4	-0.62988
NM_021704	Cxcl12	Chemokine (C-X-C motif) ligand 12	-0.3878
NM_019494	Cxcl11	Chemokine (C-X-C motif) ligand 11	-0.38105
NM_011337	Ccl3	Chemokine (C-C motif) ligand 3	-0.3689
NM_011332	Ccl17	Chemokine (C-C motif) ligand 17	-0.18197
NM_010554	Il1a	Interleukin 1 alpha	-0.13888
NM_010798	Mif	Macrophage migration inhibitory factor	-0.07331
NM_011330	Ccl11	Small chemokine (C-C motif) ligand 11	-0.0577
NM_009142	Cx3cl1	Chemokine (C-X3-C motif) ligand 1	-0.04255
NM_011338	Ccl9	Chemokine (C-C motif) ligand 9	0.209733
NM_011577	Tgfb1	Transforming growth factor, beta 1	0.255246
NM_021283	Il4	Interleukin 4	0.375313
NM_009139	Ccl6	Chemokine (C-C motif) ligand 6	0.376835
NM_010548	Il10	Interleukin 10	0.385754
NM_011888	Ccl19	Chemokine (C-C motif) ligand 19	0.770252
NM_018866	Cxcl13	Chemokine (C-X-C motif) ligand 13	1.524727
NM_008518	Ltb	Lymphotoxin B	2.057481
NM_013693	Tnf	Tumor necrosis factor	2.238394
NM_008176	Cxcl1	Chemokine (C-X-C motif) ligand 1	2.893923
NM_016960	Ccl20	Chemokine (C-C motif) ligand 20	3.457557
NM_008361	Il1b	Interleukin 1 beta	3.74199
NM_019577	Ccl24	Chemokine (C-C motif) ligand 24	4.259322
NM_009138	Ccl25	Chemokine (C-C motif) ligand 25	8.293495
NM_009141	Cxcl5	Chemokine (C-X-C motif) ligand 5	15.13422

* fold difference indicates the average expression difference between TLR7$^{-/-}$ and wild-type mice (n = 2 per group). Positive values indicate increased expression in wild-type mice, negative values represent increased expression in TLR7$^{-/-}$ mice, and zero indicates identical expression levels.

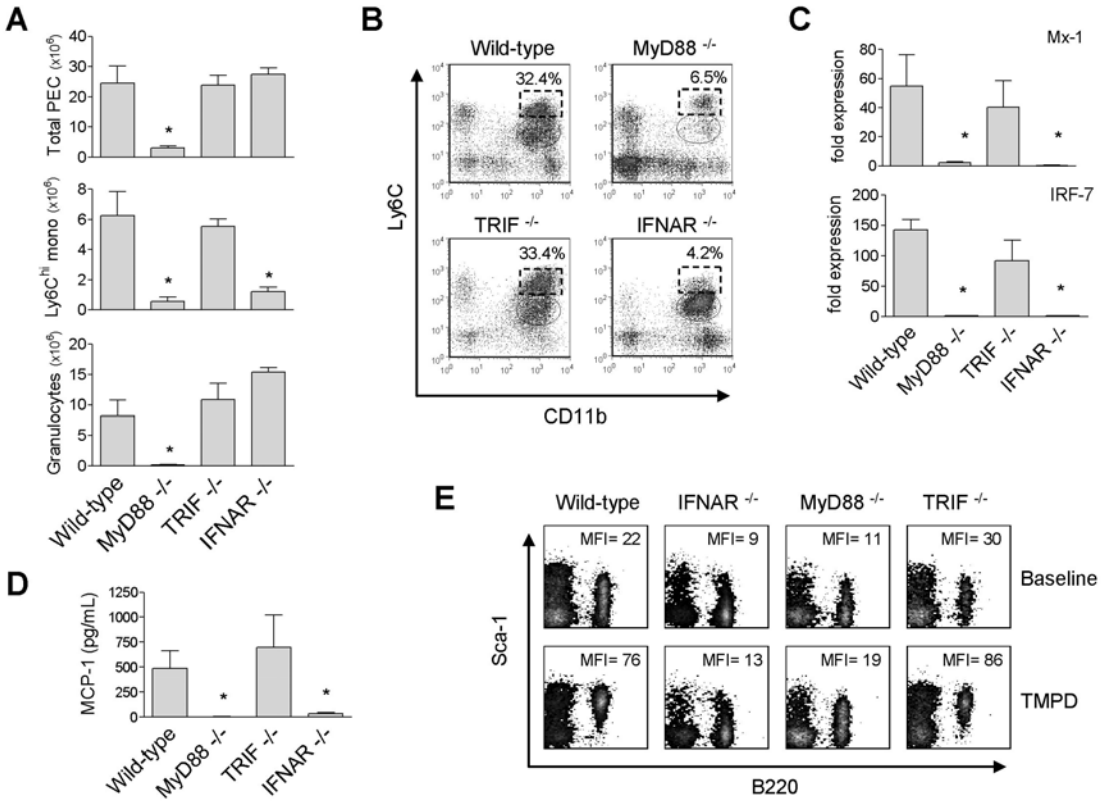

Figure 4-1. Induction of IFN-I by TMPD requires MyD88. A) Comparison of the number of total PEC, Ly6C^{hi} monocytes, and granulocytes two weeks after TMPD treatment in wild-type (n = 5), MyD88$^{-/-}$ (n = 6), TRIF$^{-/-}$ (n = 4) and IFNAR$^{-/-}$ mice (n = 4). B) Flow cytometry of peritoneal cells (box indicates Ly6C^{hi} monocytes and oval indicates granulocytes). C) RT-PCR analysis of *Mx1* and *IRF7* expression in PECs (normalized to peritoneal cells from an untreated wild-type mouse). D) ELISA quantification of MCP-1 in the peritoneal lavage fluid of TMPD treated mice. E) Flow cytometry analysis of Sca-1 expression on peripheral blood mononuclear cells (MFI denotes mean fluorescence intensity of Sca-1 on B220^{+} cells). Each bar (panels A, C, D) represents the mean and error bars indicate standard error (SE). * $p < 0.05$ (Student's t-test).

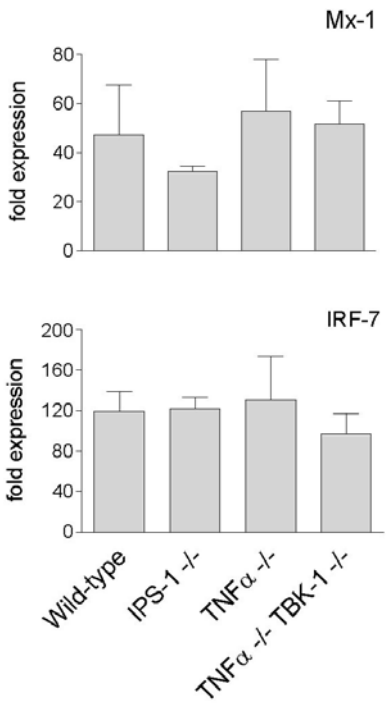

Figure 4-2. Cytoplasmic nucleic acid sensors do not contribute to IFN-I production. RT-PCR analysis of Mx1 and IRF7 expression in PECs from wild-type (n = 5), IPS-$1^{-/-}$ (n = 5), $TNF^{-/-}$ (n = 2), and $TNF^{-/-}$TBK-$1^{-/-}$ (n = 4) animals (normalized to peritoneal cells from an untreated wild-type animal) two weeks after TMPD treatment. Each bar represents the mean and error bars indicate SE.

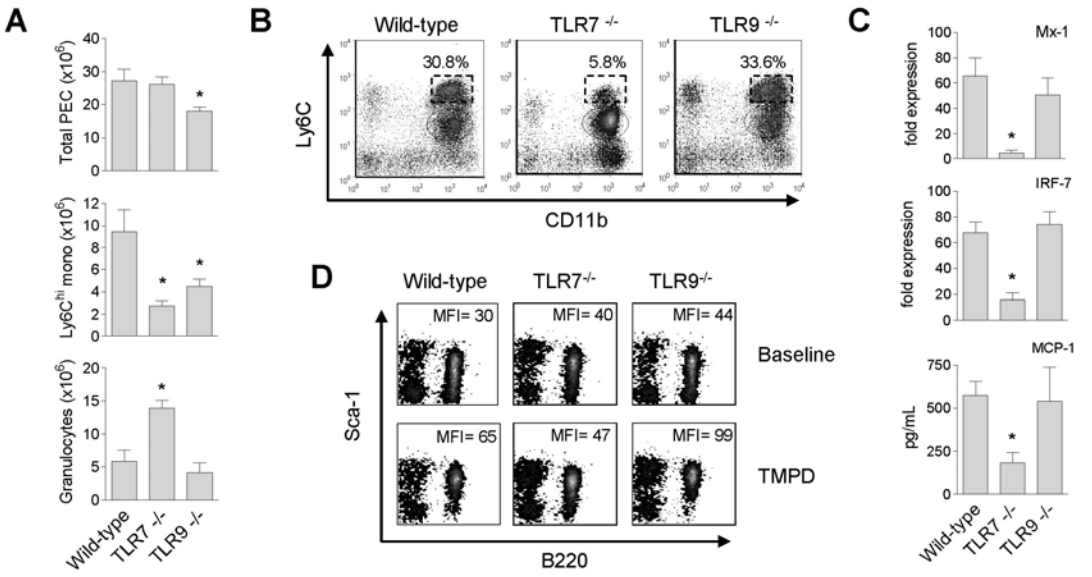

Figure 4-3. Induction of IFN-I by TMPD is TLR7-dependent. A) Comparison of the number of total PEC, Ly6C^{hi} monocytes, and granulocytes two weeks after TMPD treatment in wild-type (n = 5), TLR7$^{-/-}$ (n = 5), TLR9$^{-/-}$ (n = 5) mice. B) Flow cytometry analysis of peritoneal cells (box indicates Ly6C^{hi} monocytes). C) RT-PCR analysis of *Mx1* and *IRF7* expression in PECs (normalized to peritoneal cells from an untreated wild-type animal) and ELISA quantification of MCP-1 in the peritoneal lavage fluid. D) Flow cytometry of Sca-1 surface expression on peripheral blood mononuclear cells (MFI denotes mean fluorescence intensity of Sca-1 on B220^{+} cells). Each bar (panels A, C, D) represents the mean and error bars indicate SE. * $p < 0.05$ (Student's t-test).

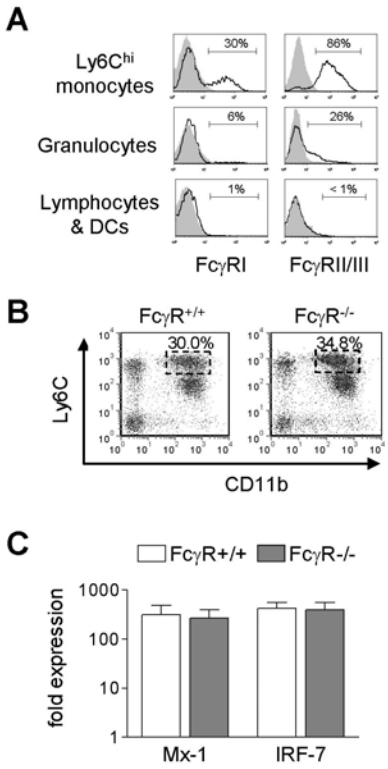

Figure 4-4. Dispensable role of FcγRI and FcγRIII in TMPD-induced IFN-I production. A) Flow cytometry analysis of FcγRI (CD64) and FcγRII/III (CD32/CD16) in PEC populations in TMPD-treated wild-type mice. B) Peritoneal cell influx and C) ISG expression in wild-type mice and FcγRI/III$^{-/-}$ (γ-chain deficient) mice two weeks after TPMD treatment. Each bar represents the mean (n = 3) and error bars indicate SE.

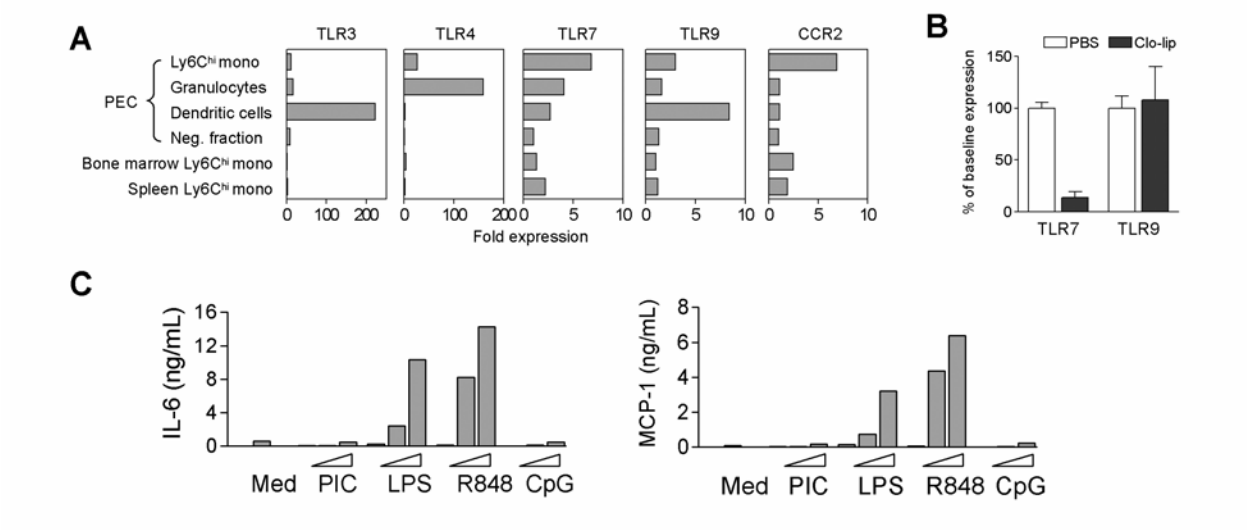

Figure 4-5. Immature Ly6C^{hi} monocytes express high levels of TLR7. A) RT-PCR analysis of TLR expression in sorted PEC populations, splenic Ly6C^{hi} monocytes and bone marrow monocyte precursors from wild-type TMPD-treated mice. B) RT-PCR analysis of TLR7 and TLR9 expression in PECs from TMPD-treated mice 48 hrs after i.p. injection of PBS or clodronate-liposomes. C) ELISA for MCP-1 and IL-6 produced by sorted peritoneal Ly6C^{hi} monocytes (5 X 10^4 cells/well) 24 h after TLR ligand stimulation. Wedge denotes increasing concentrations of LPS, R848, CpG DNA (100 ng/mL, 1 µg/mL, and 10 µg/mL) and poly I:C (200 ng/mL, 2 µg/mL, and 20 µg/mL). All mice were treated with TMPD for two weeks. Data are representative of two independent experiments.

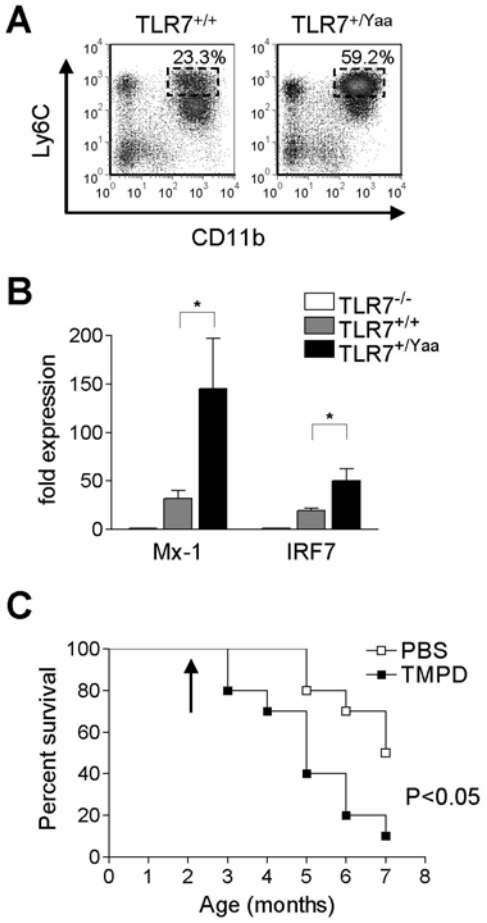

Figure 4-6. Amplification of the response to TMPD by the Yaa locus. A) Flow cytometry of peritoneal cell and B) RT-PCR analysis of ISG expression in BXSB X B6 female ($TLR7^{+/+}$) and male mice ($TLR7^{+}/^{Yaa}$) two weeks after TMPD treatment. * denotes $p<0.05$ (Student's t-test). C) Survival curve for male BXSB mice after PBS or TMPD treatment (arrow denotes treatment at 8-10 weeks of age).

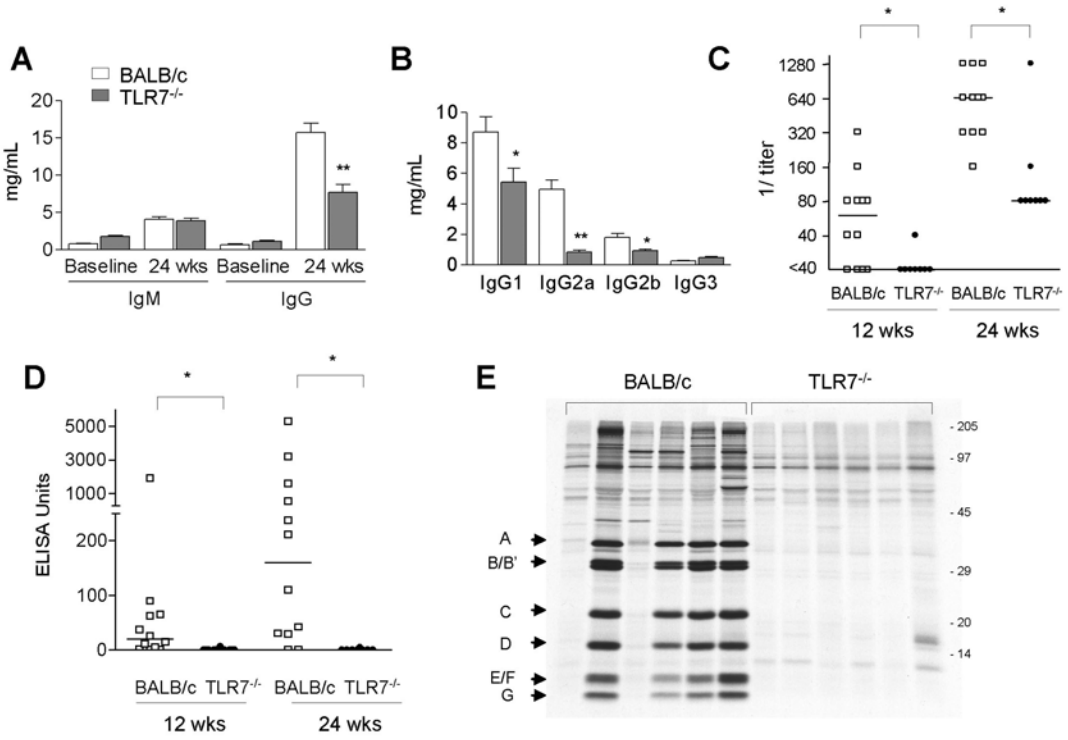

Figure 4-7. Essential role of TLR7 in autoantibody production. A) Total IgM, IgG and B) IgG subclass levels in BALB/c.TLR7$^{-/-}$ (n = 8) and wild-type BALB/c mice (n = 12) before and 24 weeks after TMPD treatment. Bars represent the mean and error bars indicate SE. * $p<0.05$, ** $p<0.001$ (unpaired t-test). C) Fluorescent ANA titers (titration emulation) and D) anti-nRNP/Sm IgG levels (antigen-capture ELISA) at 12 weeks and 24 weeks post-TMPD treatment. Line indicates median and * denotes $p<0.05$ (Mann-Whitney U test). E) Immunoprecipitation of serum autoantibodies (n = 6 per group) using nuclear extracts from ^{35}S-labeled K562 cells (12.5% polyacrylamide gel). Arrows indicate components of nRNP/Sm and numerical values denote the molecular weight (kD).

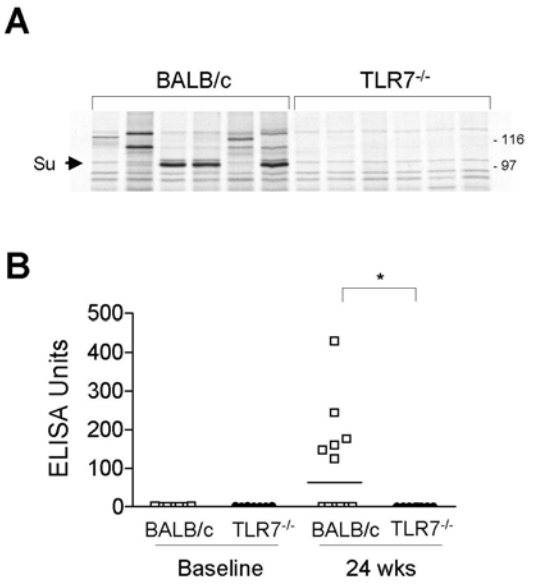

Figure 4-8. Development of anti-Su/ago2 autoantibodies is TLR7-dependent. A) Immunoprecipitation of serum autoantibodies 24 wks after TMPD treatment (n = 6 per group; 8% polyacrylamide gel). Arrows indicate the 100 kD Su antigen and numerical values denote the molecular weight (kD). B) Anti-Su/ago levels at baseline and 24 wks post-TMPD treatment measured by ELISA using recombinant ago2 protein. * indicates $p<0.05$ (Mann-Whitney U test).

CHAPTER 5
TYPE-I INTERFERON-DEPENDENT RECRUITMENT OF INFLAMMATORY MONOCYTES IN TMPD-INDUCED LUPUS

Introduction

Chronic inflammation is a pathological condition characterized by unremitting production of cytokines and other mediators in response to persistent microbial infection or chemical agents (150). In chronic autoimmune disorders such as systemic lupus erythematosus (SLE), endogenous antigens also may play an important role in perpetuating the chronic inflammatory state (26). Regardless of the cause, a common feature of chronic inflammation is the persistent homing of circulating monocytes to the site of injury (150).

Two major subsets of blood monocytes have been identified in mice. Inflammatory monocytes (also called $Ly6C^{hi}$ monocytes), characterized by surface expression of Ly6C and the chemokine receptor CCR2, are newly released from the bone marrow and actively recruited to inflamed tissue (108). On the other hand, residential monocytes (also called $Ly6C^{-}$ monocytes) in the circulation express CX_3CR1 and infiltrate non-inflamed tissues where they differentiate into residential tissue macrophages (MΦ) (105, 108). Under steady-state conditions, inflammatory monocytes spontaneously mature into the residential subset in the circulation. (105, 108). Upon their recruitment to sites of injury, inflammatory monocytes also can differentiate into MΦ, which exhibit enhanced phagocytic activity, or dendritic cells that help capture antigens for presentation to lymphocytes (116, 151). Tissue monocyte/ MΦ also can amplify the immune response by secreting inflammatory cytokines and chemokines, which recruit other immune cells. In chronic inflammation, however, persistent production of these inflammatory mediators often leads to tissue damage, resulting in cycles of tissue destruction and

repair. The mechanism underlying the continuous recruitment of monocytes in chronic inflammation is not well defined.

Intraperitoneal administration of 2,6,10,14 tetramethylpentadecane (TMPD; also known as pristane) potently induces chronic inflammation in mice. The influx of mononuclear and polymorphonuclear leukocytes to the peritoneal cavity persists for months after injection of this hydrocarbon oil (152). The chronic inflammatory state also promotes tumorigenesis, as TMPD was found to induce plasmacytomas more than three decades ago (94). Subsequently, TMPD was used to enhance monoclonal antibody production by hybridoma cells implanted in the peritoneal cavity (95). TMPD treatment stimulates the development of highly organized ectopic lymphoid structures ("lipogranulomas"), a feature often associated with chronic inflammatory disorders (152). The ectopic lymphoid tissue may play a key role in the induction of lupus-like autoimmune disease (autoantibodies, glomerulonephritis, arthritis, pulmonary vasculitis) in TMPD treated mice (103).

How TMPD causes chronic inflammation is not well understood, but a pathological role of several cytokines has been suggested. IL-6 is essential for the generation of plasmacytomas (153), whereas IL-12 is required for the development of TMPD-induced glomerulonephritis (24). Recently, it was found that type I interferons (IFN-I; including IFN-α and IFN-β) and type II interferon (IFN-γ) both contribute to autoantibody production in TMPD-treated mice (23, 103). Using TMPD-induced chronic peritonitis as a model, we examined the mechanism(s) underlying the chronic recruitment of monocytes and granulocytes to sites of inflammation.

Methods

Mice

These studies were approved by the Institutional Animal Care and Use Committee. Wild-type C57BL/6, IL-6$^{-/-}$, TNF$\alpha^{-/-}$, CCR2$^{-/-}$ and IL-1R$^{-/-}$ mice (all on a C57BL/6 background),

C3H/HeJ, C3H/HeOuJ, BALB/c, and BALB/c.IFN-$\gamma^{-/-}$ were from Jackson Laboratories (Bar Harbor, ME). 129Sv/Ev Type I interferon receptor α-chain deficient (IFNAR$^{-/-}$) mice and wild type controls (129Sv/Ev), originally from B&K Universal Limited (Grimston, Aldbrough, England), were bred in our facility. All mice were maintained a specific pathogen free facility at the University of Florida. Mice (8- to 10-weeks old) received TMPD (0.5 ml i.p., from Sigma-Aldrich, St. Louis, MO), 4% thioglycollate (BD Bioscience, San Jose, CA) or PBS. Peritoneal exudate cells were isolated as described (100, 103). For morphological analysis, 5 x 104 sorted cells were cytospun onto glass slides (Fisher Scientific, Pittsburg, PA) and stained using the Hema3 kit (Fisher).

Real-Time PCR

RT-PCR was performed as described (103). Briefly, total RNA was extracted from 106 peritoneal cells using Trizol reagent (Invitrogen, Carlsbad, CA) and cDNA was synthesized using Superscript II First-Strand Synthesis Kit (Invitrogen). RT-PCR was performed using the SYBR Green Core Reagent Kit (Applied Biosystems, Foster City, CA) with an Opticon II thermocycler (MJ Research, Waltham, MA). Amplification conditions were: 95°C for 10 min, followed by 45 cycles of 94°C for 15 s, 60°C for 25 s, and 72°C for 25 s. After the final extension (72°C for 10 min), a melting-curve analysis was performed to ensure specificity of the products. Primers used in this study are included in Table 2-1.

Flow Cytometry

All antibodies were purchased from BD Bioscience with the exceptions of anti-Ly6C-FITC, anti-Ly6C-biotin, avidin-APC (eBioscience, San Diego, CA), anti-F4/80-FITC, and anti-CD11b-Pacific blue (Caltag Laboratories, Burlingame, CA). Cell staining was performed as described (103). Fifty thousand events per sample were acquired using a CYAN ADP flow

cytometer (Dako, Fort Collins, CO) and analyzed with FCS Express 3 (De Novo Software, Ontario, Canada).

Monocyte Labeling

Clodronate (a gift from Roche Diagnostics) liposomes (Clo-lip) and 1,1'-dioctadecyl-3,3,3',3'-tetramethylindodicarbocyanine perchlorate (DiD)-liposomes were produced as described (105, 106). To label Ly6C$^-$ monocytes, 150 μL of DiD-liposomes were injected i.v. into TMPD-treated mice. Clo-lip (200 μl) was delivered i.v. 24 hr prior to the injection of DiD-liposomes for the labeling of Ly6C^{hi} monocytes (105). Cells were analyzed 24 or 72 h after labeling. To test phagocytic activity of peritoneal monocyte/MΦ in vivo, 50 μL of DiD-liposomes were injected i.p. and peritoneal cells were analyzed by flow cytometry 1 h later.

In Vitro Stimulation

PECs resuspended in complete DMEM (containing 10% FCS, 10 mmol/L HEPES, glutamine, and penicillin/streptomycin plus 10 U/ml heparin) were seeded on 96 well cell-culture plates (105 cells/well). Cells were stimulated with the indicated doses of peptidoglycan, R848 (Invivogen, San Diego, CA), or LPS (from Salmonella typhimurium; Sigma) and incubated at 37 °C in a 5% CO2 atmosphere for 24 h before collecting the supernatant. IL-12, TNF-α , MCP-1 and IL-6 ELISAs (BD Biosciences) were performed following the manufacturer's instructions. Optical density was converted to concentration using standard curves based on recombinant cytokines analyzed by a four-parameter logistic equation (Softmax Pro 3.1).

Results

Peritoneal Recruitment of Ly6C^{hi} Monocytes after TMPD Treatment

We analyzed the peritoneal cell infiltrate at various time points after i.p. injection of TMPD. In untreated mice, peritoneal lavage yielded mainly B220$^+$CD11b$^+$ B1 lymphocytes

(Figure 5-1A, circle) and $B220^{-}CD11b^{+}$ myeloid cells (Figure 5-1A, box) that included mostly granulocytes and monocyte/MΦ. Granulocytes, characterized by the expression of Ly6G, comprised only a small portion of the myeloid population ($CD11b^{+}B220^{-}$ gate; Figure 5-1A, right). Thus, the $Ly6G^{-}$ cells were predominantly monocyte/MΦ. Consistent with other studies (105, 107), residential peritoneal macrophages did not exhibit surface expression of Ly6C ($CD11b^{+}B220^{-}Ly6G^{-}$ gate; Figure 5-1A right), a marker highly expressed on inflammatory monocytes.

Using the same method of analysis, a strikingly different pattern was observed 18 hrs after TMPD treatment (Figure 5-1B). A dramatic expansion of $CD11b^{+}B220^{-}$ peritoneal exudate cells (PEC) and a reduction in both B1 lymphocytes and conventional B cells were observed (Figure 5-1B left). Granulocytes were the predominant population at this time point, outnumbering monocyte/MΦ by ~2 to 1. Unlike residential peritoneal MΦ, the majority of monocytes elicited by TMPD expressed high levels of Ly6C, suggestive of an inflammatory phenotype. The chronic nature of the response to TMPD was confirmed by the presence of granulocytes and $Ly6C^{hi}$ monocytes in the peritoneal cavity two weeks, and even two months after the initial injection (Figure 5-1B).

An early influx of granulocytes and $Ly6C^{hi}$ monocytes was also detected in the sterile peritonitis induced by thioglycollate (Figure 5-1C). However, the response was transient by comparison with TMPD. Monocytes elicited by thioglycollate gradually developed a mature $Ly6C^{-}$ phenotype whereas granulocytes were absent by 72 h (Figure 5-1C). The depletion of B lymphocytes was also not a feature of thioglycollate-induced inflammation (the reduced percentage of these cells was due to expansion of the myeloid populations).

Chronic Recruitment of Ly6C^{hi} Monocytes is Dependent on IFN-I signaling

Proinflammatory cytokines including IL-6, TNFα, IFN-γ and IFN-I are produced in the peritoneum of TMPD-treated mice (103, 146, 154). We asked whether these cytokines play a role in the persistent inflammatory cell influx in response to TMPD. Compared to wild-type C57BL/6 controls, mice deficient of IL-6 or TNFα showed a similar influx of granulocytes and Ly6C^{hi} monocytes to the peritoneal cavity two weeks after TMPD treatment (Figure 5-2A, Table 1). The persistent inflammatory response also was not explained by the presence of endotoxin as a similar pattern was seen in C3H/HeJ mice, which carry a mutation in Toll-like receptor (TLR)-4. Moreover, the absence of IFN-γ also did not affect the pattern of inflammatory cell recruitment, although the BALB/c background itself was associated with a greater number of granulocytes (Figure 5-2B, Table 5-1). Interestingly, while a sustained accumulation of granulocytes was found in TMPD-treated IFNAR$^{-/-}$ mice, the majority of monocyte/MΦ in the peritoneal cavity exhibited a mature, Ly6C^{-} phenotype (Figure 5-2B, Table 5-1). This observation was not caused by genetic background differences as wild-type 129Sv and B6 mice demonstrated comparable responses to TMPD (Table 5-1). Consistent with our analysis by flow cytometry, visual examination of PECs showed numerous polymorphonuclear cells in wild-type and IFNAR$^{-/-}$ mice (Figure 5-2B). Whereas cells with monocytic morphology were found in the peritoneal cavity of wild-type mice, PECs from IFNAR$^{-/-}$ mice consisted mainly of revealed the presence of larger, vacuolated cells consistent with a mature, MΦ-like morphology (Figure 5-2C). These findings were specific for TMPD as the inflammatory response to thioglycollate was similar in wild-type and IFNAR$^{-/-}$ mice (Figure 5-2C and not shown).

Under steady state conditions, both residential (Ly6C^{-}) and inflammatory monocytes (Ly6C^{hi}) are present in the circulation (105, 108). The accumulation of Ly6C^{-} monocyte/MΦ in

TMPD-treated IFNAR$^{-/-}$ mice suggests that either this subset is preferentially recruited to the peritoneal cavity, or the infiltrating Ly6C^{hi} monocytes rapidly attains a mature phenotype at the site of inflammation. To address these possibilities, we monitored the influx of monocytes to the peritoneal cavity *in vivo* using fluorescently labeled liposomes. Neither Ly6C^{-} nor Ly6C^{hi} circulating monocytes displayed fluorescence prior to labeling (CD11b^{+}Ly6G^{-} gate; Figure 5-3A). As described previously (105), i.v. injection of liposomes containing the fluorescent dye DiD (DiD-lip) selectively labeled Ly6C- monocytes (Figure 5-3B,C). After 24 h, > 40% of circulating Ly6C^{-} monocytes were DiD^{+} in TMPD-treated wild-type and IFNAR$^{-/-}$ mice, but few DiD^{+} cells had migrated into the peritoneal cavity in either strain. Thus, the absence of IFN-I signaling does not result in the preferential recruitment of Ly6C^{-} monocytes from the bone marrow.

To track the migration of circulating Ly6C^{hi} monocytes, clodronate-liposomes (clo-lip) were first given to deplete the Ly6C^{-} subset. Twenty-four hours after the administration of DiD-lip, ~50% of peripheral blood Ly6C^{hi} monocytes were fluorescently labeled in TMPD-treated wild-type and IFNAR$^{-/-}$ mice (Figure 5-3D,E). Importantly, a similar percentage of Ly6C^{hi} monocytes in the peritoneal cavity of wild-type mice were DiD^{+}, indicating that the majority of cells in this subset entered the peritoneal cavity within the past 24 h. Although fewer peritoneal Ly6C^{hi} monocytes were found in the absence of IFN-I signaling, a milder influx of DiD^{+} Ly6C^{hi} monocytes were seen in IFNAR$^{-/-}$ mice (Figure 5-3D,E).

We extended the analysis to 72 h after i.v. injection of DiD-lip. Based on preliminary studies, few DiD^{+} monocytes remained in the circulation at this time and further influx of labeled cells to the peritoneal cavity was negligible (not shown). This allowed us to trace the fate of DiD^{+}Ly6C^{hi} monocytes that had migrated into the peritoneal cavity during the previous 48 h. In

contrast to the earlier time point, few peritoneal Ly6C^{hi} monocytes were DiD^{+} in wild-type mice at this time, suggestive of a high turnover rate of the infiltrating monocytes (Figure 5-3F). Curiously, the number of DiD^{+} monocytes in IFNAR$^{-/-}$ remained similar compared to 24 h post-labeling. A maturation continuum was also evident in IFNAR-/- mice, as the majority of DiD^{+} monocytes at this time-point showed reduced or no expression of Ly6C (Figure 5-3F). Hence, maturation of Ly6C^{hi} monocytes, rather than recruitment of the Ly6C^{-} subset, is responsible for the accumulation of Ly6C^{-} monocytes/MΦ in IFNAR$^{-/-}$ mice. Taken together, these data illustrate the essential role of IFN-I in promoting the continuous recruitment of Ly6C^{hi} monocytes to the peritoneal cavity following TMPD treatment and are consistent with an IFN-induced monocyte maturation deficit.

Monocyte Recruitment Induced by TMPD Requires CCR2

Since IFN-I are not known to possess direct chemotactic properties, we reasoned that the production of chemokines induced by IFN-I signaling may be responsible for the influx of Ly6C^{hi} monocytes. Previous studies have shown that several monocyte chemoattractants including CCL2, CCL7, and CCL12 are IFN-inducible genes (127, 155). Indeed, these chemokines were highly expressed in PECs from TMPD-treated wild-type mice, but not IFNAR$^{-/-}$ mice (Figure 5-4A). Reduced levels of CCL2 protein also were observed in the peritoneal lavage fluid of IFNAR$^{-/-}$ mice (Figure 5-4B). Conversely, the expression of CX3CL1, which mediates the migration of Ly6C- monocytes (108), and the neutrophil attractants CXCL1 and CXCL5, was affected modestly at best by the absence of IFN-signaling (Figure 5-4A). These data supported the observation that IFN-I is essential for the influx of inflammatory monocytes, but not Ly6C^{-} monocytes or granulocytes.

To further examine the role of monocyte chemoattractants, we administered TMPD to mice deficient of CCR2, the major receptor for CCL2, CCL7 and CCL12. Supporting the role of these chemokines, PECs from $CCR2^{-/-}$ mice were comprised of primarily of granulocytes two weeks post-treatment (Figure 5-4C, D). Both $Ly6C^{hi}$ and $Ly6C^{-}$ monocyte subsets were largely absent in $CCR2^{-/-}$ animals whereas the number of granulocytes increased slightly compared to controls (Figure 5-4D). Thus, the chronic influx of $Ly6C^{hi}$ monocytes induced by TMPD requires the interaction between IFN-inducible chemokines and CCR2.

Functions of Monocyte Subsets in TMPD-Treated Mice

To evaluate the functional significance of the preferential recruitment of $Ly6C^{hi}$ monocytes induced by IFN-I, we stimulated peritoneal monocyte/MΦ from wild-type and $IFNAR^{-/-}$ mice with the TLR ligands peptidoglycan, lipopolysaccharide, and R848. Strikingly, the production of IL-6, TNF-α, and MCP-1 in response to TLR-ligands were dramatically reduced in the absence of IFN-I signaling (Figure 5-5A). Monocytes/MΦ from TMPD-treated $IFNAR^{-/-}$ mice showed minimal production of TNF-α and MCP-1, even at the highest dose of TLR ligands tested.

The lack of inflammatory cytokine production in monocyte/MΦ from TMPD-treated $IFNAR^{-/-}$ mice raised the question whether these cells differentiated towards the alternatively activated M2 phenotype. Downregulation of inducible nitric oxide synthase (iNOS) and upregulation of arginase-1 (arg-1) and TGF-β expression are characteristic features of M2 macrophages (156, 157). RT-PCR analysis of these genes in peritoneal monocytes/MΦ did not reveal any differences between wild-type and $IFNAR^{-/-}$ mice (Figure 5-5B), suggesting that alternative activation of monocyte/MΦ in the absence of IFN-I signaling is unlikely to explain the discrepancy in cytokine production.

We assessed phagocytic function of peritoneal monocyte/MΦ *in vivo* by direct i.p. injection of DiD-labeled liposomes. In contrast to cytokine production, phagocytosis was greatly enhanced in monocyte/MΦ from IFNAR$^{-/-}$ mice compared with wild-type controls (Figure 5-5C). Both the percentage of cells engulfing liposomes and the amount of uptake per cell (measured by mean fluorescence intensity) were increased in the absence of IFN-I signaling (Figure 5-5C). Further analysis revealed that the discrepancy was largely due to the predominance of Ly6C^{-} monocyte/MΦ in IFNAR$^{-/-}$ mice, which were more highly phagocytic than the Ly6C^{hi} monocytes (Figure 5-5D). It is noteworthy that although present in smaller numbers, the Ly6C^{-} subset in wild-type mice was also highly phagocytic. IFN-I treatment of bone-marrow derived MΦ *in vitro* did not inhibit phagocytosis (not shown), indicating that the difference seen in wild-type and IFNAR$^{-/-}$ mice was probably due to the difference in monocyte/MΦ subsets rather than a direct effect of IFN-I. Therefore, IFN-I directs the recruitment of Ly6C^{hi} monocytes that are highly responsive to pathogenic stimuli but only weakly phagocytic.

Chronic Recruitment of Granulocytes Requires IL-1 Signaling

Finally, we investigated the mechanism of chronic granulocyte recruitment in TMPD-treated mice. In contrast to Ly6C^{hi} monocytes, the influx of granulocytes was independent of IFN-I signaling and CCR2 interactions (Figures 5-2B, 5-4D). Deficiency of IL-6, TNF-α, IFN-γ, or functional TLR4 also did not affect granulocyte recruitment. A recent study found that IL-1 signaling plays a role in granulocyte influx in urate crystal-induced peritonitis (158). To examine the contribution of IL-1 signaling, we tested the effect of TMPD on IL-1 receptor-deficient (IL-1R$^{-/-}$) mice. The number of granulocytes in the peritoneal cavity was greatly reduced in IL-1R$^{-/-}$ mice, whereas the accumulation of Ly6C^{hi} monocytes was unaffected (Figure 5-6A, B). PECs from IL-1R$^{-/-}$ mice showed significantly reduced expression of the granulocyte

attractant CXCL5 and a slight reduction in CXCL1 (Figure 5-6C). Consistent with the normal recruitment of Ly6C^{hi} monocytes, expression of the IFN-inducible monocyte chemoattractants CCL2, CCL7 and CCL12 as well as CX3CL1 was not affected.

We further analyzed whether components of the recently described inflammasome complex act upstream of IL-1R. Upon detecting certain foreign stimuli [i.e. asbestos, silica (159)] or endogenous molecules released by damaged cells [i.e. ATP, urate crystals (158)], activation of the inflammasome results in the release of proinflammatory cytokines including IL-1β (160), which mediates the recruitment of granulocytes . However, the deficiency of the major inflammasome components NALP3 (cryopyrin), ASC (apoptosis-associated speck-like protein containing a caspase recruitment domain), or caspase-1 did not impact the influx of granulocytes or monocytes in TMPD-treated mice (Figure 5-6D and not shown). These findings suggest that granulocyte influx in the chronic inflammatory response to TMPD is specifically mediated by an IL-1R-dependent pathway, independent of inflammasome signaling or the mechanisms utilized in monocyte recruitment.

Discussion

Chronic inflammation can be caused by persistent immune responses to microbes, chemicals, or autoantigens (150). Despite the heterogeneity of etiologic factors, continuous infiltration of monocytes is a common feature of many types of chronic inflammation . Using TMPD to induce chronic peritonitis, we show in this study that the persistent recruitment of inflammatory Ly6C^{hi} monocytes was mediated specifically by IFN-I. These antiviral cytokines activate the production of monocyte chemoattractants and recruit Ly6C^{hi} monocytes in a CCR2-dependent manner. Curiously, the rapid turnover of recruited monocytes in the peritoneum of

TMPD-treated mice was associated with a lack of differentiation into phagocytic Ly6C$^-$ monocyte/MΦ, consistent with previous observations that the uptake of carbon particles is reduced substantially following TMPD injection (161). These findings define an important role of IFN-I in maintaining the chronic inflammatory state.

IFN-I are primarily known for their antiviral and anti-proliferative properties and a prominent role in chronic inflammation has not been established previously (36). Studies on acute murine cytomegalovirus infection illustrated that early antiviral defense is orchestrated by IFN-I and the downstream production of IFN-inducible chemokines. Recruitment of NK cells and macrophages to the site of infection is mediated by the production of CXCL3 and CCL2, respectively (162, 163). Our results suggest that a similar mechanism is involved in the chronic inflammation induced by TMPD, as IFN-I (but not other inflammatory mediators such as TNFα, IL-6 and IFNγ) is required to maintain the chronic recruitment of inflammatory monocytes to the peritoneum. PECs from wild-type mice treated with TMPD displayed elevated expression of the IFN-inducible monocyte chemoattractants CCL2, CCL7, and CCL12, promoting the migration of monocytes to the site of inflammation through interactions with CCR2. Due to shared receptor utilization, the relative contribution of each of these chemokines is unclear, although recent studies suggest a synergy of CCL2 and CCL7 in recruiting monocytes (164, 165).

Interestingly, the chronic influx and rapid turnover of Ly6C^{hi} monocytes was accompanied by a concomitant reduction of Ly6C$^-$ monocyte/MΦ in the peritoneal cavity of TMPD-treated mice. While Ly6C^{hi} monocytes were also initially recruited following thioglycollate treatment, few were found in the peritoneal cavity after 72 h as the majority of PECs were F4/80$^+$Ly6C$^-$ residential monocytes/MΦ. Unexpectedly, the pattern induced by TMPD was almost completely dependent on IFN-I signaling. Labeling studies suggested that the accumulation of Ly6C$^-$

monocyte/MΦ in IFNAR$^{-/-}$ mice was not due to direct recruitment of circulating Ly6C- monocytes. Instead, the small number of Ly6C^{hi} monocytes recruited to the peritoneal cavity later differentiated into the Ly6C^{-} subset. This view is supported by the deficiency of both Ly6C^{hi} and Ly6C^{-} subsets in the absence of CCR2, which mediates the migration of Ly6C^{hi} but not Ly6C^{-} monocytes (108, 119). How IFN-I interfere with differentiation or maturation of Ly6C^{hi} monocytes into the Ly6C^{-} subset remains unclear.

The predominance of Ly6C^{hi} monocytes is likely to amplify the inflammatory cascade as these cells produced large amounts of inflammatory mediators in response to stimulation with TLR2, 4, or 7 ligands. Ly6C^{hi} monocytes may establish a vicious cycle of monocyte recruitment and cytokine/chemokine production as they constitute a major source of IFN-I and CCL2 in TMPD-treated mice (see Chapter 3). In contrast, Ly6C^{-} monocyte/MΦ exhibited much greater phagocytic capacity, but produced only small amounts of IFN-I, CCL2, IL-12, or TNFα. Enhanced phagocytic function of Ly6C^{-} monocytes *in vivo* also is illustrated by the preferential labeling of this subset upon administration of DiD-liposomes alone, whereas depletion by clo-liposomes was required in order to effectively label the Ly6C^{hi} subset. We conclude that the relative deficiency of Ly6C^{-} monocyte/MΦ in the presence of IFN-I impairs phagocytic capacity at the site of inflammation, leading to defective clearance of the triggering stimuli and perpetuation of the inflammatory response. This possibility also is supported by the defective clearance of carbon particles following i.p. TMPD injection (161).

Our findings suggest a potential role of IFN-I in clinical conditions associated with chronic inflammation. In SLE, a chronic autoimmune condition characterized by the production of antibodies to numerous self-antigens, serum levels of IFN-I correlate with disease severity, kidney inflammation, and the presence of autoantibodies (31, 32). Numerous IFN-inducible

genes, including CCL2 and CCL7, are also coordinately overexpressed in lupus patients (127). Interestingly, defective phagocyte function is well-established in SLE (26). Aberrant clearance of apoptotic debris is thought to provide the autoantigens that initiate the autoimmune response (166). Whether the dysregulation of IFN-I production in human SLE disrupts the balance of inflammatory vs. residential monocyte subsets and/or contributes to the phagocytosis defect warrants detailed investigation.

In addition, IFN-I may contribute to chronic inflammation in atherosclerosis. Circulating $Ly6C^{hi}$ monocytes are chronically elevated in mice with atherosclerotic heart disease and these inflammatory monocytes infiltrate the atheromatous lesion in apoE-deficient mice (119, 151). Recombinant IFN-I administration accelerates plaque development in mice and human plaque tissue exhibits elevated expression of IFN-α as well as CCL2 (167, 168). In view of our findings, it will be interesting to determine whether a similar IFN-I-chemokine feedback loop contributes to the chronic monocytosis in atherogenesis or the accelerated atherosclerosis of SLE patients (169).

We have also partially elucidated the mechanism for chronic granulocytes recruitment in the TMPD model. Because of shared utilization of IL-1R, whether IL-1α and/or IL-1β are essential for this process remains to be determined. We have ruled out the involvement of major components of the inflammasome complex, which activates caspase-1 and stimulates the release of IL-1β in response to exogenous and endogenous danger signals (158-160). However, other mechanisms of IL-1β production remains possible (170) and recruitment of granulocytes to the peritoneal cavity can also be mediated by IL-1α (171). Futures studies are needed to further define the pathway(s) responsible for granulocyte recruitment.

In conclusion, our study defines an essential role of IFN-I in the recruitment of monocytes in the TMPD-induced model of chronic inflammation. These findings suggest that novel therapies aimed at neutralizing IFN-I and/or downstream chemokines may be effective treating lupus and other chronic inflammatory conditions.

Table 5-1. Peritoneal exudate cell subsets two weeks following TMPD treatment

Strain	n	$Ly6C^{hi}$ monocytes ($CD11b^{+}Ly6C^{hi}$)	Granulocytes ($CD11b^{+}Ly6G^{+}$)	$Ly6C^{-}$ mono/MΦ ($CD11b^{+}Ly6C^{-}$)	Dendritic cells ($CD11c^{+}IA^{+}$)	B lymphocytes ($B220^{+}$)
C57BL/6	6	6.32 ± 1.44	5.04 ± 1.25	2.01 ± 0.33	0.68 ± 0.11	0.88 ± 0.15
B6.TNFα$^{-/-}$	3	4.80 ± 0.50	4.75 ± 0.77	0.95 ± 0.20	0.80 ± 0.21	1.10 ± 0.39
B6.IL-6$^{-/-}$	3	4.81 ± 0.62	6.13 ± 0.78	1.47 ± 0.29	0.43 ± 0.07	0.40 ± 0.25
C3H/HeJ	4	4.5 ± 1.58	4.24 ± 1.10	1.31 ± 0.37	0.53 ± 0.11	1.35 ± 0.39
BALB/cJ	2	2.61 ± 0.09	9.7 ±1.93	0.23 ± 0.05	0.24 ± 0.01	1.15 ± 0.25
c.IFN-γ$^{-/-}$	2	2.86 ± 0.34	12.53 ± 0.47	0.66 ± 0.06	0.28 ± 0.01	1.42 ± 0.02
129Sv	7	4.85 ± 0.48	3.23 ± 0.54	0.35 ± 0.16	0.33 ± 0.11	0.95 ± 0.22
129.IFNAR$^{-/-}$	7	0.63 ± 0.11	7.00 ± 0.65	2.98 ± 0.76	0.25 ± 0.02	1.05 ± 0.29

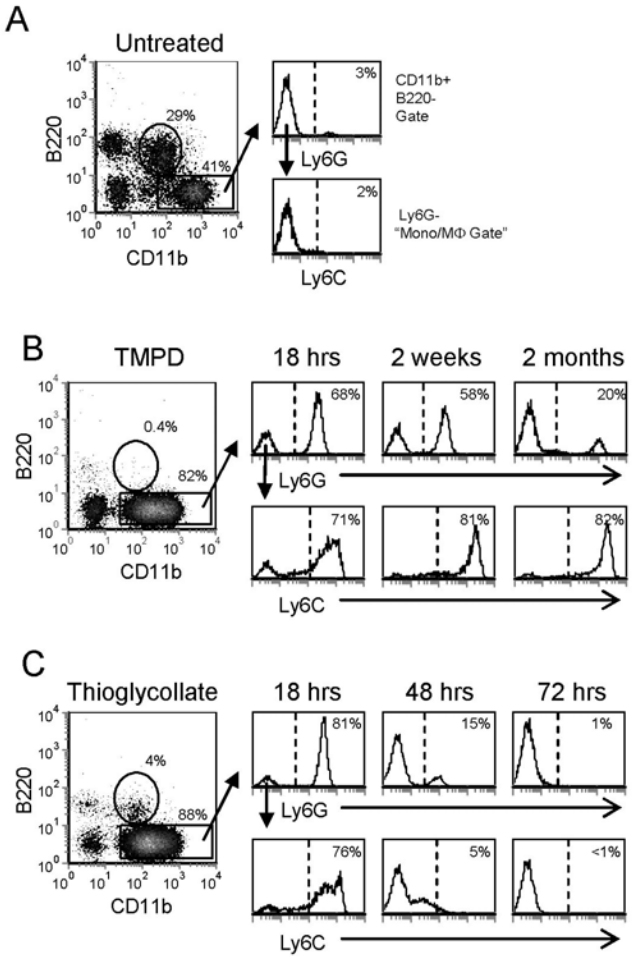

Figure 5-1. Chronic recruitment of Ly6C^{hi} monocytes in TMPD-treated mice. A) Cell subset analysis of peritoneal cells from untreated C57BL/6 mice by flow cytometry. Left: two-dimensional dot plot (left) shows the presence of CD11b^{+} B220^{+} B1 lymphocytes (circle) and CD11b^{+}B220^{-} myeloid cells (box). Right: (upper) histogram analysis of the percentage of Ly6G^{+} granulocytes and Ly6G- monocyte/MΦ in the myeloid cell gate (CD11b^{+}B220^{-}); (lower) histogram analysis of Ly6C expression on monocyte/MΦ (CD11b^{+} B220^{-} Ly6G^{-} gate). Flow cytometry analysis of peritoneal exudate cells (PECs) from B) TMPD-treated or C) thioglycollate-treated mice. Left: two-dimensional dot plot of PECs 18 h after treatment; Right: histogram analysis of Ly6G and Ly6C expression (as described above) at the indicated time points after treatment.

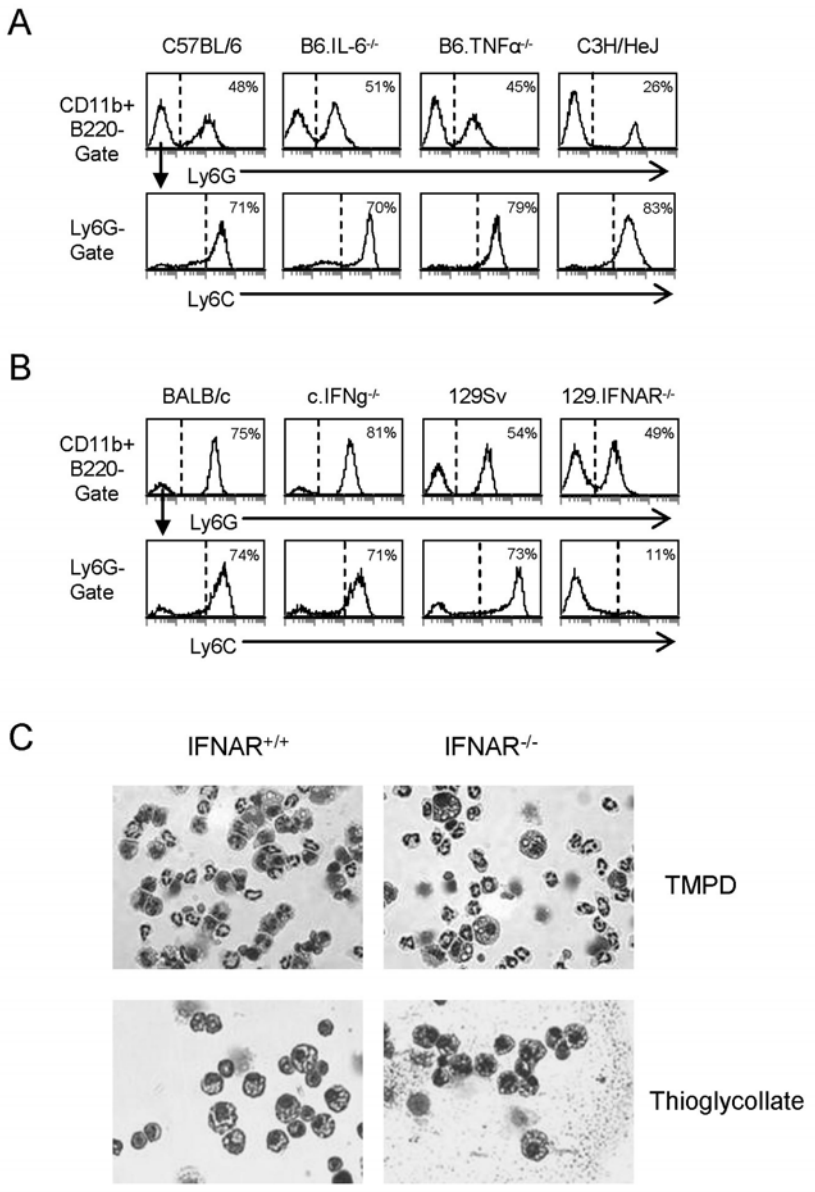

Figure 5-2. The recruitment of Ly6C^{hi} monocytes induced by TMPD requires IFN-I signaling. Flow cytometry analysis of PECs from A) wild-type C57BL6, IL-6$^{-/-}$, TNF-α$^{-/-}$, C3H/HeJ and B) BALB/c, IFN-γ$^{-/-}$, 129Sv, and IFNAR$^{-/-}$ mice two weeks after TMPD-treatment. Upper panels: histogram analysis of the percentage of Ly6G^{+} granulocytes and Ly6G^{-} monocyte/MΦ in the myeloid cell gate (CD11b^{+}B220^{-}); lower panels: histogram analysis of Ly6C expression on monocyte/MΦ (CD11b^{+} B220^{-} Ly6G^{-} gate). C) Morphologic analysis of PECs from 129Sv and IFNAR$^{-/-}$ mice after TMPD (2 weeks) or thioglycollate treatment (3 days).

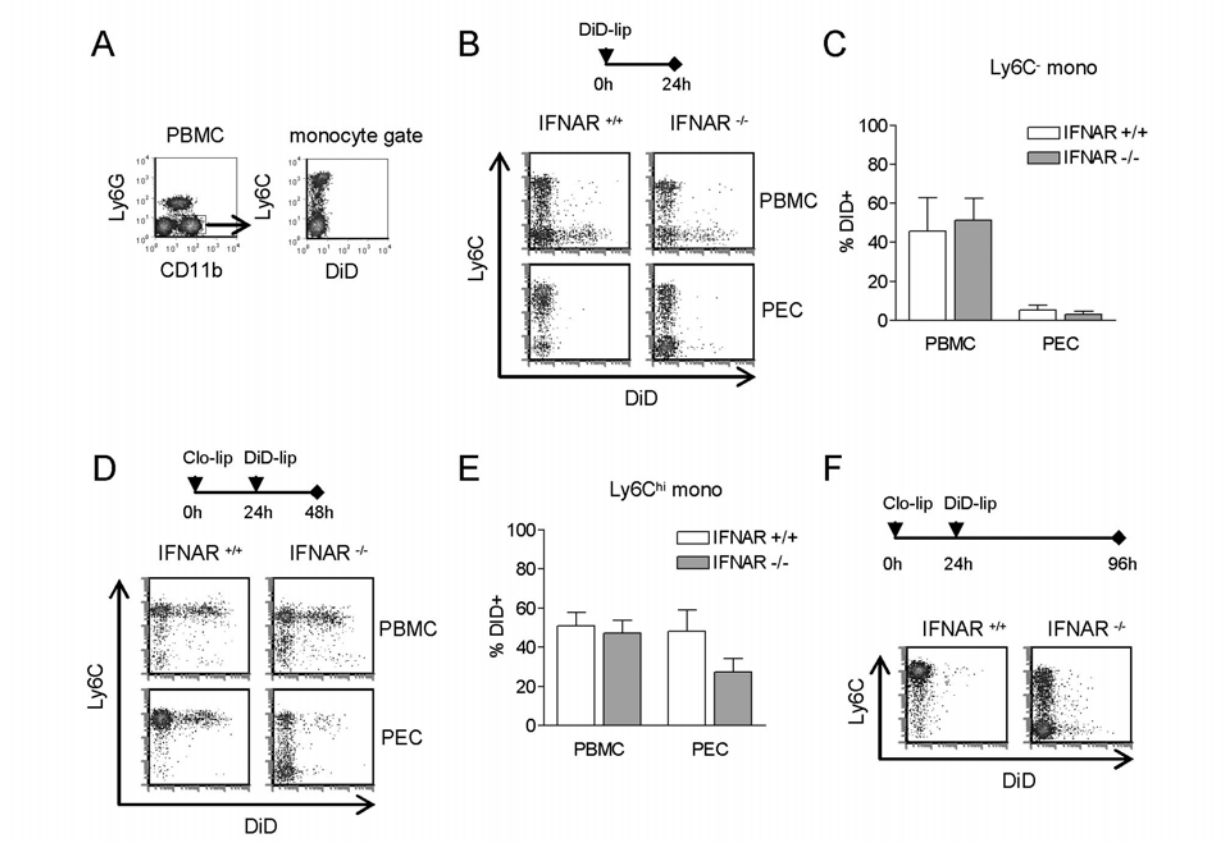

Figure 5-3. Rapid turnover and decreased maturation of Ly6C^{hi} monocytes is the presence of IFN-I signaling. A) Gating strategy for the analysis of peripheral blood monocytes (CD11b^{+} Ly6G^{-}) used for subsequent labeling experiments. B) Flow cytometry analysis and C) quantification of DiD^{+} Ly6C^{-} monocytes in the peripheral blood and peritoneum in TMPD-treated mice IFNAR$^{+/+}$ (129Sv) or IFNAR$^{-/-}$ mice 24 hr after administration of DiD-liposomes. D) Flow cytometry analysis and E) quantification of DiD^{+} Ly6C^{hi} monocytes 48 h or F) 96 h after pretreatment with clodronate-liposomes followed by subsequent labeling with DiD-liposomes. All mice were treated with TMPD two weeks before liposome injection. Bars represent the average of 3 or more mice.

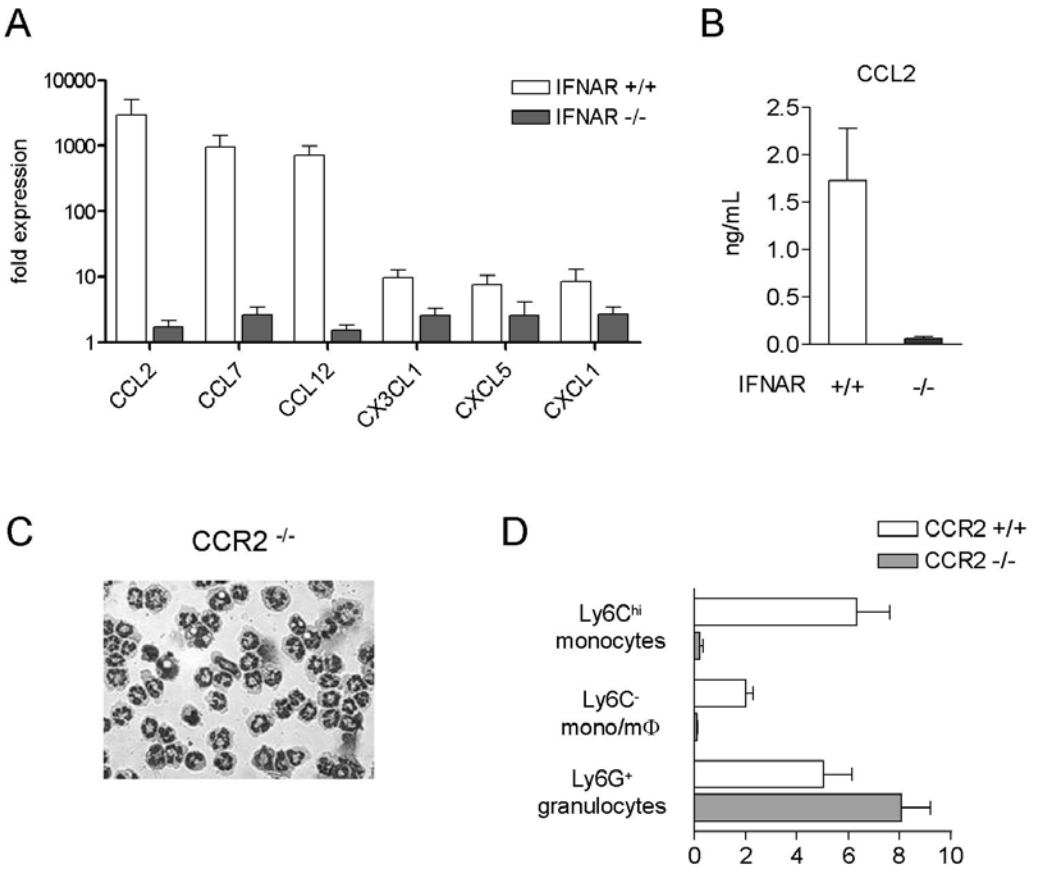

Figure 5-4. Monocyte recruitment induced by TMPD is dependent on CCR2. A) RT-PCR of chemokine expression in PECs and B) ELISA analysis of CCL2 in peritoneal lavage from IFNAR$^{+/+}$ (129Sv) or IFNAR$^{-/-}$ mice 2 weeks after TMPD treatment. C) Morphologic analysis and D) quantification of granulocytes and monocyte/MΦ in wild-type and CCR2$^{-/-}$ mice.

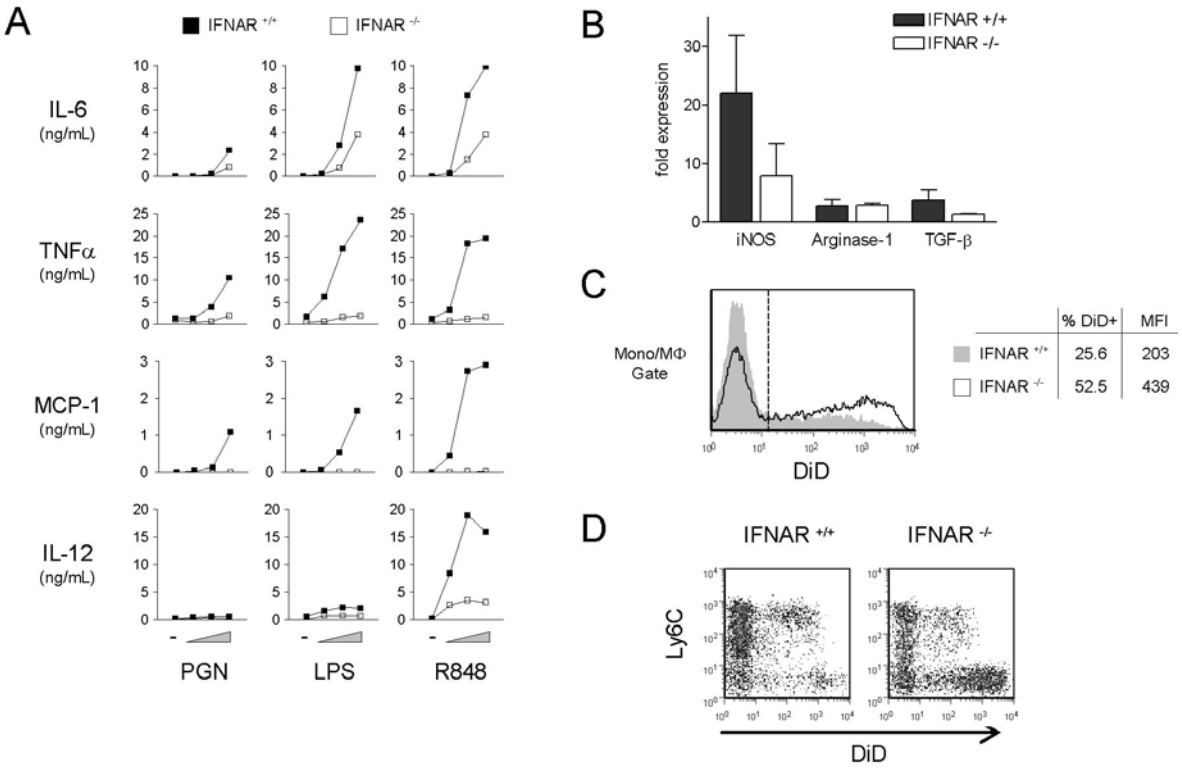

Figure 5-5. Functions of monocyte subsets in TMPD-treated mice. A) ELISA quantification of cytokine and chemokine production in adherent PECs from TMPD-treated IFNAR$^{+/+}$ (129Sv) or IFNAR$^{-/-}$ mice cocultured with peptidoglycan (2 μg/mL), LPS (1 μg/mL) or R848 (μg/mL) for 20 h. B) RT-PCR analysis of iNOS, Arginase-1, and TGF-β expression in PECs. Flow cytometry analysis of DiD-liposome phagocytosis in C) total PECs or D) monocyte/MΦ (CD11b^{+}B220^{-}Ly6G^{-} gate) in IFNAR$^{+/+}$ or IFNAR$^{-/-}$ mice two weeks after TMPD treatement.

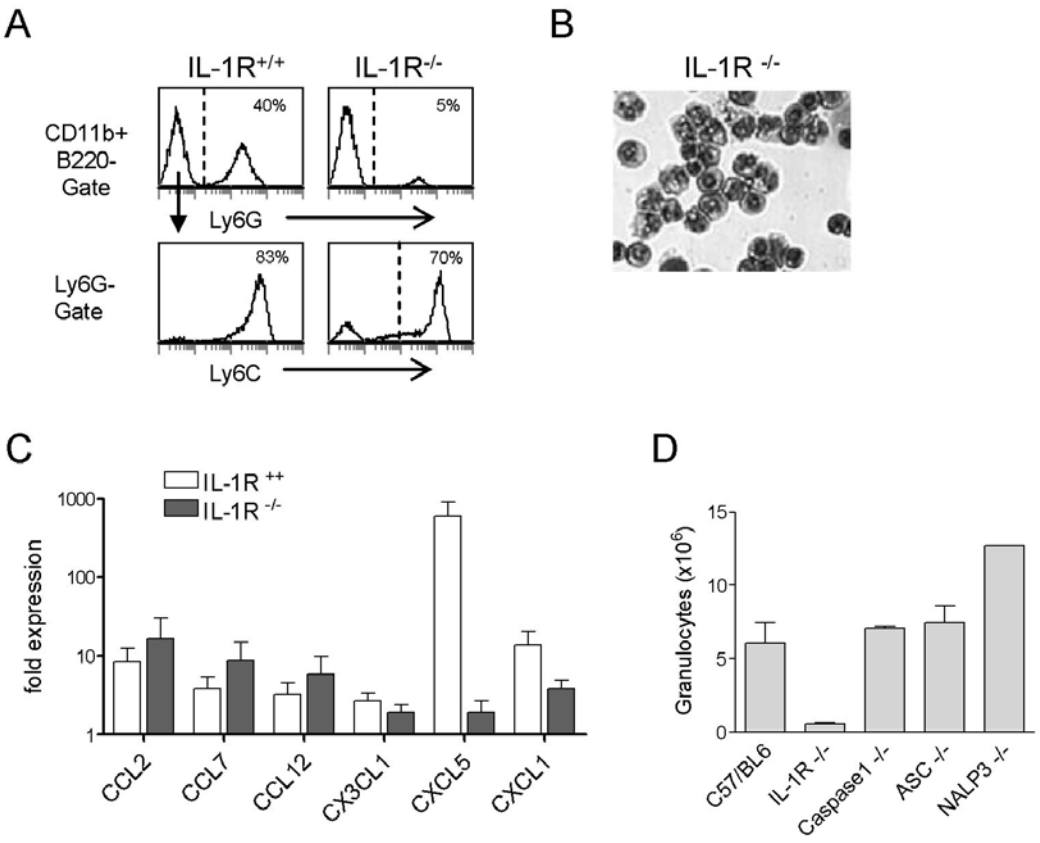

Figure 5-6. Granulocyte influx following TMPD treatment requires IL-1 receptor. A) Flow cytometry analysis of PECs from wild-type C57BL/6 and IL-1R$^{-/-}$mice two weeks after TMPD-treatment. Upper panel: histogram analysis of the percentage of Ly6G^{+} granulocytes and Ly6G- monocyte/MΦ in the myeloid cell gate (CD11b^{+}B220^{-}); lower panel: histogram analysis of Ly6C expression on monocyte/MΦ (CD11b^{+} B220^{-} Ly6G^{-} gate). B) Morphologic analysis of PECs from IL-1R$^{-/-}$mice. C) RT-PCR of chemokine expression in PECs from wild-type C57BL/6 and IL-1R$^{-/-}$ mice 2 weeks after TMPD treatment. Each bar represents the average from 5 mice. C) Quantification of granulocyte influx in mice deficient in IL-1R$^{-/-}$ or various components of the inflammasome complex (2 weeks after TMPD treatment).

CHAPTER 6
DISCUSSION AND FUTURE DIRECTIONS

Although the etiology of SLE remains unknown, early studies focused on the adaptive immune system as abnormalities of B and T lymphocytes were thought to be the basis of the autoimmune condition. This paradigm has undergone a dramatic change with recent advances in the field of innate immunity. It is now increasingly recognized that components of the innate immune system, normally function to recognize invasion by microbial pathogens, play an essential role in the recognition of self-antigens and subsequent initiation of the adaptive immune response. The involvement of TLRs and IFN-I in SLE are among the best examples illustrating the link between aberrant activation of innate immune system and the induction of autoimmunity.

The work presented in previous chapters highlights the importance of innate immunity in experimental SLE induced by TMPD. Supporting a pathogenic role of IFN-I, overproduction of the anti-viral cytokines was responsible for many manifestations of lupus in TMPD-treated mice including the development of autoantibodies and glomerulonephritis (93). We found that a population of immature, inflammatory monocytes characterized by high levels of Ly6C expression was a major source of IFN-I in TMPD-treated mice. Further investigation revealed that activation of TLR7, an innate sensor of ssRNA in endosomes, was responsible for the production of IFN-I and the recruitment of $Ly6C^{hi}$ monocytes, where as the CpG-DNA sensor TLR9 and other pathways of IFN-I induction were not required. We also uncovered a new role of IFN-I in mediating the chronic influx of $Ly6C^{hi}$ monocytes, establishing a vicious cycle of monocyte recruitment and IFN-I production. In spite of these novel findings, many questions regarding the TMPD model of SLE remain to be addressed.

Suitability of the TMPD-Model for the Study of SLE

Since its initial discovery more than 14 yrs ago, the TMPD model has often been criticized for the lack of relevance to human SLE. The use of an exogenous hydrocarbon and the inducible nature in non-autoimmune prone mice are incompatible with the human disease, which is heavily influenced by genetic factors. However, because the etiology of lupus is unknown and likely to be multi-factorial, no current animal models fully resemble the human syndrome, which itself is heterogeneous as symptoms vary widely among lupus patients (1).

While the inducible nature of the model is not suitable for genetic studies of lupus, many of the autoimmune features in mice treated with TMPD recapitulate the human disease. The combination of lupus-specific antibodies (anti-Sm and anti-dsDNA), glomerulonephritis, and female predisposition in TMPD-induced lupus is only paralleled by the MRl-lpr model (91). Importantly, the TMPD model is currently the only model that exhibits the "interferon signature" seen in more than half of lupus patients (32, 103). As the role of innate immunity is increasingly recognized, our findings presented in previous chapters illustrate that innate components such as TLRs and IFN-I are essential for disease development in this model. The inducible nature of TMPD-induced lupus, in fact, offers an advantage over the genetic models as it allows temporal assessment of upstream and downstream effects. This model further provides the opportunity to test the efficacy of anti-IFN and anti-TLR7 therapeutic approaches. Therefore, the TMPD model can yield valuable insights into the pathogenesis of SLE.

Complexity of the TMPD Model

The previous chapters have individually described novel features pertinent to the involvement of IFN-I in the TMPD model. The observation of IFN-I production by Ly6C^{hi} monocytes (Chapter 3), the involvement of TLR7 activation (Chapter 4), and the role of IFN-I in maintaining monocyte recruitment (Chapter 5) together illustrate that activation of specific

pathways involved in innate immunity, rather than "non-specific inflammation", is responsible for the early effects of TMPD. Creating a model for how TMPD causes lupus based on our current understanding uncovers a complex network of feedback interactions between the recruitment of Ly6C^{hi} monocytes, the production of IFN-I, and the expression of TLR7. While Ly6C^{hi} monocytes constitute a major subset of IFN-I producing cells, IFN-I and IFN-inducible chemokines mediate further recruitment of monocytes from the peripheral blood and bone marrow (Figure 6-1). This process is amplified by IFN-I signaling, which is subject to autocrine feedback that enhances production of IFN-I. The expression of TLR7, which mediates the production of IFN-I in this model, is also IFN-inducible. High levels of TLR7 expression in Ly6C^{hi} monocytes may further contribute to their ability to produce IFN-I. Finally, the chronic presence of high levels of IFN-I may induce the activation of lymphocytes and dendritic cells and initiate the immune response to autoantigens.

An important unanswered question is how TMPD initiates this cycle of monocyte recruitment and IFN-I production. Since Ly6C^{hi} monocytes are not normally present in the peritoneal cavity and their recruitment is largely dependent on CCR2, another cell type likely initiates the inflammatory response by producing the first wave of IFN-I and monocyte chemoattractants (Figure 6-1). This hypothesis is supported by the presence of IFN-I production (albeit at reduced levels) in CCR2$^{-/-}$ mice despite the absence of Ly6C^{hi} monocytes (unpublished observation). Because most of our previous studies have focused on the peritoneal inflammatory infiltrates, further studies are needed to determine whether cells lining the peritoneal cavity (i.e. mesothelial cells and stromal cells) contribute to the inflammatory response to TMPD.

We recognize that the *in vivo* effect of TMPD may be more complex as at least one other pathway (MyD88- and IL-1R dependent but TLR7- and IFNAR-independent) is activated for the

recruitment of granulocytes. Nevertheless, our results argue against the prevailing hypothesis that the interaction between immune complexes and FcγRs is required for TLR7-mediated IFN-I production. FcγRs seem to be dispensable in this model as both short-term IFN-I production and long-term autoantibody development (142) are unaffected in FcγR-deficient mice, although we do not exclude the possibility that immune complex-FcγR interaction may amplify the autoimmune response after the onset of autoantibodies.

Mechanism of TLR7 Activation

The hydrocarbon structure of TMPD does not resemble any synthetic ligands (such as R848, loxoribine, and other guanosine analogues) or natural agonists (ssRNA) for TLR7. Therefore, it remains enigmatic why TMPD preferentially induces TLR7 activation *in vivo*. To further investigate the link between TMPD treatment and TLR7 activation, we studied the effect of TMPD in vitro. Although TMPD has been used for decades, mechanistic studies on its cellular effects have been limited by the hydrocarbon's poor immiscibility in aqueous solutions. We found that this problem could be circumvented by first mixing TMPD with fetal bovine serum prior to the addition of culture medium. Typically TMPD was incorporated at a concentration of 1 μg/mL as determined by gas chromatography-mass spectroscopy (M. Satoh and N. Szabo, UF Toxicology Core; unpublished observation). Unlike stimulation with R848, a TLR7 ligand that elicits IL-6 production and costimulatory molecule upregulation in murine J774 macrophages, the addition of TMPD in vitro did not induce these responses (Figure 6-2A and not shown). TMPD solubilized in non-physiological solvents such as ethanol, DMSO, mannide monooleate, or β-cyclodextrin were also ineffective in triggering TLR7 activation (Figure 6-2A), suggesting that TMPD itself is not a ligand for TLR7.

However, exposure to TMPD dramatically enhanced the response to subsequent stimulation with TLR7 ligands. R848-induced IL-6 production and costimulatory molecule upregulation were augmented in J774 cells pretreated overnight with TMPD (Figure 6-2B) and similar enhancement of chemokine and cytokine production was found in bone-marrow derived macrophages (Figure 6-2C). Importantly, these observations were specific to TMPD as treatment with other hydrocarbon oils that do not induce lupus, such as medicinal mineral oil and squalene, did not enhance stimulation by R848 (Figure 6-2D).

We further examined whether TMPD augments the response to TLR7 ligands by altering the expression or location of TLR7. TLR7 remained exclusively intracellular regardless of TMPD treatment and its expression levels were not affected at the protein or mRNA level (Figure 6-2E). Moreover, TMPD treatment did not enhance endocytosis of FITC-dextran or phagocytosis of latex beads (Figure 6-3), suggesting that accelerated uptake of ligands is also unlikely to explain our findings. Taken together, these data indicate that TMPD is not a direct ligand for TLR7 but instead acts to enhance the response to TLR7 stimulation. Although the underlying mechanisms are distinct, the pathologic consequences of excess TLR7 activation are shared by TMPD-induced lupus and the Yaa (BXSB male) lupus model. An important unanswered question that encompasses both models is the nature of the exogenous or endogenous ligands responsible for activating the TLR7 pathway. Future studies are also needed to better understand the cellular targets of TMPD responsible for the enhancement of TLR responses.

Role of TLR7 in Autoantibody Production

We have shown in TLR7$^{-/-}$ mice that in addition to mediating IFN-I production, TLR7 is required for the development of anti-nRNP/Sm autoantibodies. The latter was also reported in a previous study in the MRL-lpr model (136), which does not exhibit IFN-I dysregulation,

suggesting that TLR7 may mediate the generation these autoantibody specificities even in the absence of excess IFN-I. However, anti-nRNP/Sm autoantibodies were also absent in TMPD-treated IFNAR$^{-/-}$ mice (93) and multiple groups have reported a strong association between the "interferon signature" and the presence of these autoantibodies in human SLE (32, 33, 76). Therefore, it was unclear whether TLR7 simply provides the IFN-I necessary to promote class-switch of anti-nRNP/Sm autoantibodies, or act upstream to generate these autoantibodies.

This question was addressed by analyzing IgM autoantibodies to nRNP/Sm. If TLR7 was only required for IFN-I production, normal or higher levels of IgM anti-nRNP/Sm would be expected in TLR7$^{-/-}$ mice due to the lack of isotype class-switch, whereas a complete absence of IgM anti-nRNP/Sm would be expected if TLR7 acts upstream in generating these autoantibodies. Results were consistent with the latter possibility as IgM anti-nRNP/Sm also was reduced significantly in TLR7$^{-/-}$ mice (Figure 6-4A). The mechanism linking activation of TLR7 to the production of autoantibodies against RNA-associated antigens remains to be elucidated, although the proposed synergism of TLR7 and the B-cell receptor may play a role in this model (144).

Furthermore, we extended our analysis to the production of autoantibodies to DNA and chromatin. Studies in the MRL-lpr model showed that TLR9 is required to generate these autoantibodies (136). Consistent with previous observations, TMPD-treated BALB/c mice produced moderate levels of autoantibodies against dsDNA, ssDNA, and chromatin by 24 weeks post-treatment. Curiously, IgG autoantibodies to these antigens were largely absent in TLR7$^{-/-}$ mice whereas IgM levels were comparable to the control group (Figure 6-4B-D). This suggests that although TLR7 is not directly required to generate the immune response to DNA and DNA-associated antigens, IFN-I production downstream of TLR7 activation promotes the IgG class-switch of these autoantibody specificities.

For unclear reasons, a single animal in the TLR7$^{-/-}$ group produced high levels of autoantibodies to DNA and ssDNA. The same animal also displayed a high titer of ANA (1:1280) in an earlier analysis (Figure 4-7C). The TLR7$^{-/-}$ genotype was confirmed by PCR (not shown) and also supported by the absence of anti-nRNP/Sm autoantibodies, suggesting that the presence of other factors, such as a viral infection, may bypass the requirement of IFN-I production (downstream of TLR7 activation) and drive the class-switch of anti-DNA autoantibodies. A similar pattern was previously found in IFN-γ-deficient mice (23). Despite a reduction in the overall frequency of IgG anti-nRNP/Sm autoantibodies (22% vs. ~70% in wild type), a few IFN-γ$^{-/-}$ mice produced them at high levels comparable to wild-type controls. The explanation for this observation will require study of larger numbers of mice.

The role of TLR9 in TMPD model has not been assessed fully. While TLR9 does not contribute significantly to IFN-I production, it is probably required to initiate autoantibody production against DNA and DNA-association antigens as in other models (136). The autoantibody profile in TLR9$^{-/-}$ mice will need to be determined in future studies. Whether TLR9 also exerts protective effects, as shown in MRL-lpr mice (136), also warrants further evaluation.

Sequential Generation of Autoantibody Specificities in TMPD-Induced Lupus

Another intriguing aspect of TMPD-lupus is the sequential appearance of autoantibody specificities. Those targeting RNA-associated antigens (IgG anti-RNP/Sm and anti-Su/ago2) tend to appear by 3 months post-treatment whereas IgG anti-ssDNA and anti-dsDNA autoantibodies typically do not appear until 5-6 months (96). If TLR9 indeed mediates anti-DNA autoantibody production in this model, it raises the question of why TLR7-dependent autoantibody specificities are consistently generated two months before the onset of TLR9-

dependent specificities. Preferential enhancement of TLR7, but not TLR9 activation *in vitro* by TMPD may have implications in this issue.

The timing of autoantibody production is also interesting in view of our finding that IFN-I production appears within days of TMPD treatment. Additional cofactors are required to break tolerance and initiate the autoimmune response between the onset of IFN-I upregulation to the appearance of the first wave of autoantibodies after ~3 months. Supporting this view, administration of exogenous IFN-α alone was not sufficient to trigger autoantibody production in BALB/c mice (88). A potentially important cofactor in the TMPD-model is the development of ectopic lymphoid tissue known as lipogranulomas (94). These lymphoid structures typically appear in the peritoneal cavity within 2-3 months of TMPD treatment, coinciding with the onset of autoantibody production. This ectopic tissue morphologically resembles secondary lymphoid structures and contains B lymphocytes, T lymphocytes, DCs, as well as monocytes/MΦ (103). Lipogranulomas are functional lymphoid structures as demonstrated by their ability generate antigen-specific B and T lymphocytes (J. Weinstein et. al. manuscript in press). Importantly, anti-Sm/RNP autoantibody-producing cells also are observed within the ectopic tissue. In view the similar timing between lipogranuloma formation and autoantibody development, it is possible that these lipogranulomas serve as a location permissive to the breach of tolerance and the generation of autoreactive lymphocytes. Interestingly, as the inflammatory response to TMPD began to resolve in the peritoneal cavity by 6 months post-treatment, the expression of IFN-I (103) and the influx of $Ly6C^{hi}$ monocytes seemed to be maintained within the lipogranulomas (Figure 6-5).

The contribution of lymphoid neogenesis to the development of autoimmunity is a subject of ongoing investigation in our laboratory. Although medicinal mineral oil and squalene

treatment also induce the formation of lipogranulomas, mice treated with these hydrocarbons do not develop the "interferon signature" or lupus autoantibodies [anti-nRNP/Sm, anti-dsDNA (114)]. Thus, the presence of ectopic lymphoid structures and excess production of IFN-I may be co-requisites driving the onset of autoimmunity in the TMPD model. This possibility can be further evaluated by 1) introducing exogenous IFN-I to mice treated with mineral oil or squalene; and by 2) inhibiting lymphoid neogenesis by targeting lymphotoxin α/β.

An additional variable that that affects autoantibody production is the genetic variation among mouse strains. The frequency of anti-nRNP/Sm following TMPD treatment, for example, ranges from ~70% in BALB/c mice to ~35% in the C57/BL6 background (172). On the other hand, the production of anti-ribosomal P autoantibodies was common in SJL but rare in BALB/c mice (173). Even within the same strain, the female gender is more susceptible to autoantibody production and kidney disease development following TMPD treatment (141). We found that these discrepancies are not explained by differences in TLR7 activation and IFN-I production. Among the wild-type mice tested in our studies (BALB/c, C57/BL6, 129Sv, C3H), the expression of ISGs two weeks after treatment was similar regardless of strain or sex. Further studies will be required to examine the contribution of genetics and sex in this model.

Therapeutic Implications

With accumulating evidence on the pathogenic role of IFN-I in SLE, monoclonal antibodies to IFN-α as well as IFNAR are already being tested in phase I clinical trials. However, efficacy of these antibodies has not been shown in murine lupus, probably due to the absence of IFN-I dysregulation in most spontaneous models (C Szeto, et al., Manuscript in Preparation). A possible unwanted effect of global IFN-I blockade is an increased risk for viral infection, a problem that may be reduced by selectively inhibiting TLR7 while leaving other pathways of IFN-I induction intact. In fact, oligodeoxynucleotides capable of antagonizing

TLR7 and/or TLR9 have also been recently described (80). These compounds have ameliorated disease features in MRL-lpr (174), but effects on IFN-I were not reported . Based on our findings, the TMPD model offers the unique opportunity to assess therapeutic approaches targeting IFN-I as well as TLR7. The appearance of the "interferon signature" and accumulation of $Ly6C^{hi}$ monocytes within two weeks of TMPD treatment allow rapid assessment of the efficacy of IFN-I inhibition by various therapeutic approaches. In addition, the sequential generation of lupus autoantibodies and the development of glomerulonephritis (as well as arthritis and pulmonary vasculitis) in the TMPD model further allow the evaluation of clinical efficacy in long-term studies.

Conclusion

The work presented here illustrates the important contribution of innate immunity to the development of autoimmunity in the TMPD model of SLE. Our findings define for the first time a pathway responsible for chronic overproduction of IFN-I, a feature seen in more than half of SLE patients. In addition, we have identified a novel subset of IFN-producing cells and uncovered novel actions of IFN-I. These studies enhance our understanding of the TMPD model and argue against current paradigms for the pathogenesis of SLE, which are based largely on *in vitro* findings. Although the complexity of the TMPD-induced lupus has just begun to unravel, our findings may provide novel insight into the pathogenesis of human SLE as well.

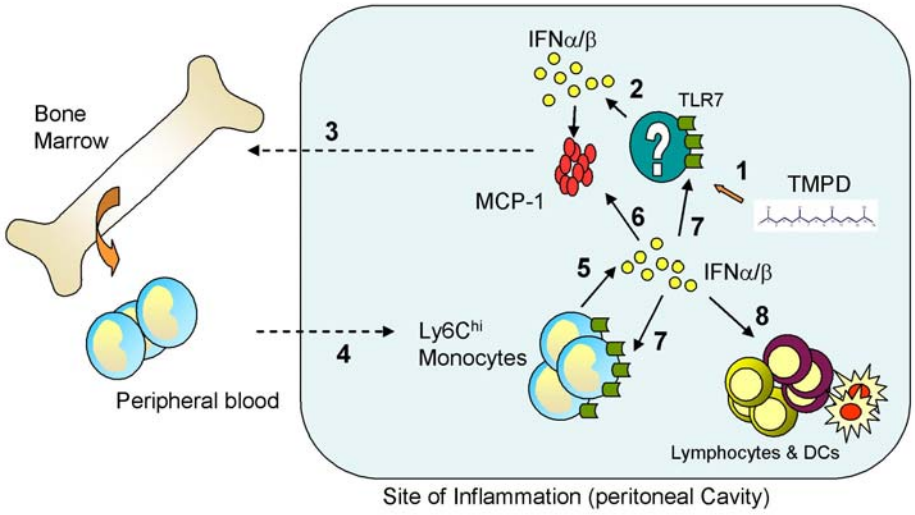

Figure 6-1. Proposed model of TMPD-induced inflammation. Upon i.p. administration of TMPD (1), TLR7-dependent production of IFN-I by cells in the peritoneal cavity (2) induces the production of MCP-1 (3), which elicits release of immature inflammatory monocytes from the bone marrow and induces the expression of TLR7 on Ly6C^{hi} monocytes. Ly6C^{hi} monocytes recruited to the site of inflammation become a major source of IFN-I and CCL2/MCP-1 (5), establishing a vicious cycle of IFN-I production and monocyte recruitment. IFN-I further perpetuate the inflammatory response by inducing the expression of more TLR7 (7), exacerbating the overproduction of IFN-I. Finally, the chronic presence of high levels of IFN-I induces the activation of lymphocytes and dendritic cells (8), initiating inappropriate immune response to autoantigens.

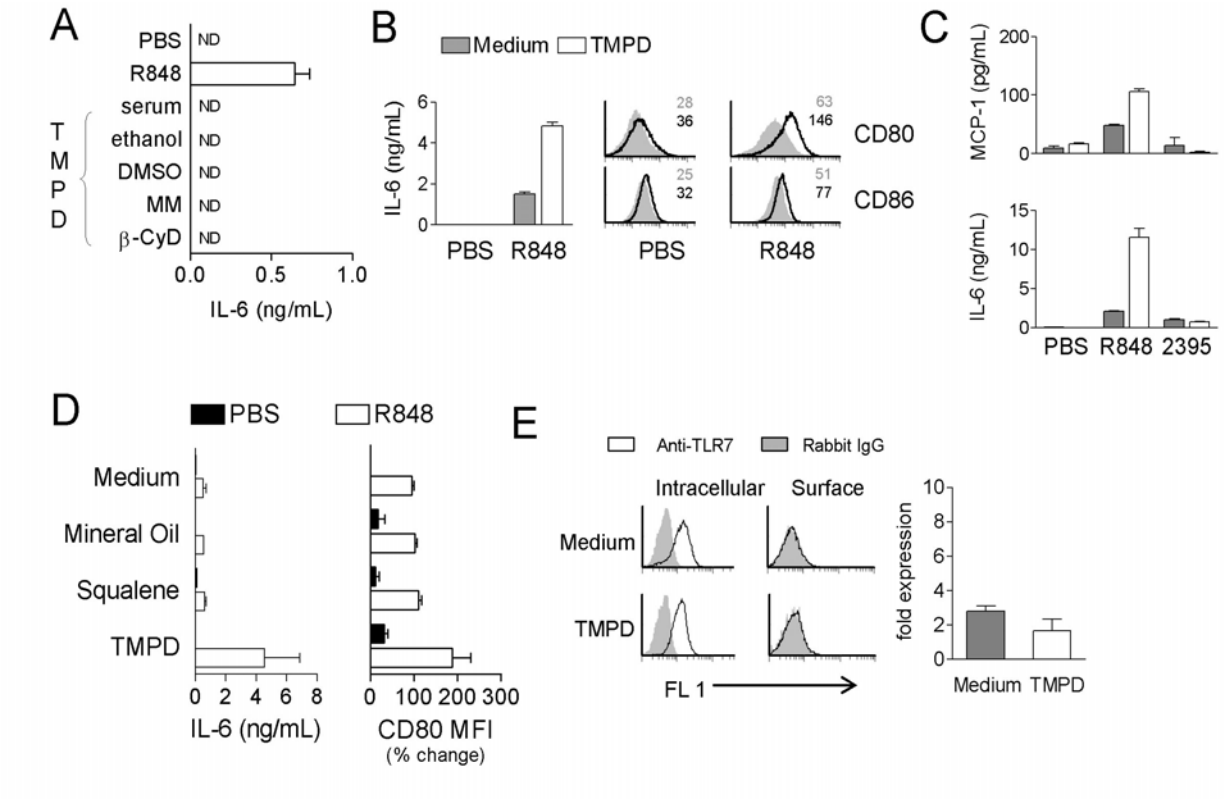

Figure 6-2. Enhancement TLR7 stimulation by TMPD *in vitro*. A) ELISA for IL-6 production in J774 cells cultured in the presence of R848 (1 μg/mL), TMPD incorporated in serum (1 μg/mL), or TMPD (300 μM) solubilized in ethanol, DMSO, mannide monooleate (MM) or β-cyclodextrin (β-CyD). ND, not detectable. B) ELISA (IL-6 , IL-12 and MCP-1) and flow cytometric analysis (CD80 and CD86) in J774 cells or C) bone marrow-derived macrophages cultured for 20 h with or without TMPD and stimulated with PBS, R848 (1 μg/mL) or ODN 2395 (2μg/mL) for 24 h. Mean fluorescent intensity (MFI) values are provided in each histogram. D) Comparison of IL-6 production and CD80 expression (MFI) in J774 cells cultured with various hydrocarbon oils and stimulated with PBS or R848. E) Flow cytometry and RT-PCR analysis of TLR7 expression in J774 cells cultured with or without TMPD for 20 h. Data are representative of three or more independent experiments.

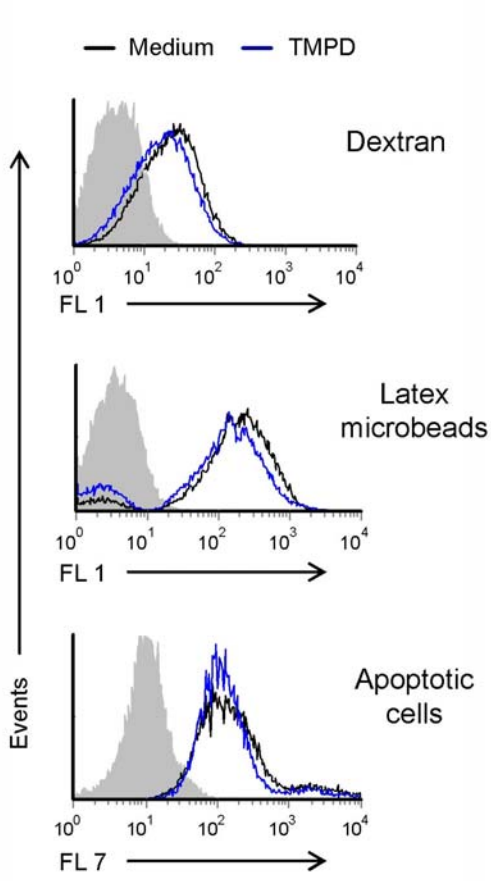

Figure 6-3. Endocytosis and phagocytosis are not affected by TMPD treatment. Quantification of endocytosis (FITC-dextran) and phagocytosis (FITC-microbeads and DiD-labeled apoptotic cells) in J774 cells treated with or without TMPD. Shaded curve represents the staining of cells prior to the addition of fluorescent substrates.

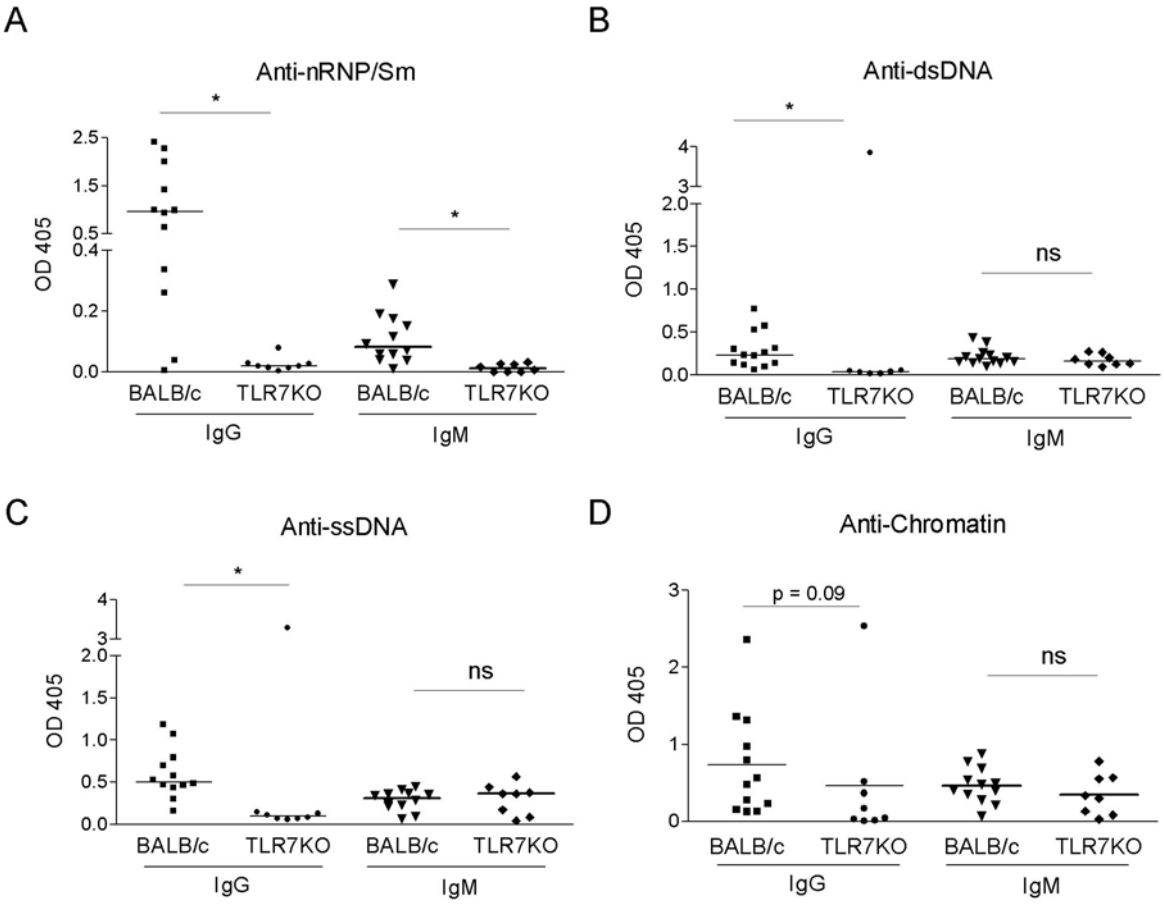

Figure 6-4. Profile of autoantibody production in TLR7$^{-/-}$ mice. ELISA measurement of serum IgM and IgG autoantibodies against A) nRNP/Sm, B) dsDNA, C) ssDNA, and D) chromatin in wild-type BALB/c (n = 12) and TLR7$^{-/-}$ mice (n = 8) 24 weeks after TMPD treatment. * $p<0.05$; ns: not significant (Mann-Whitney U test).

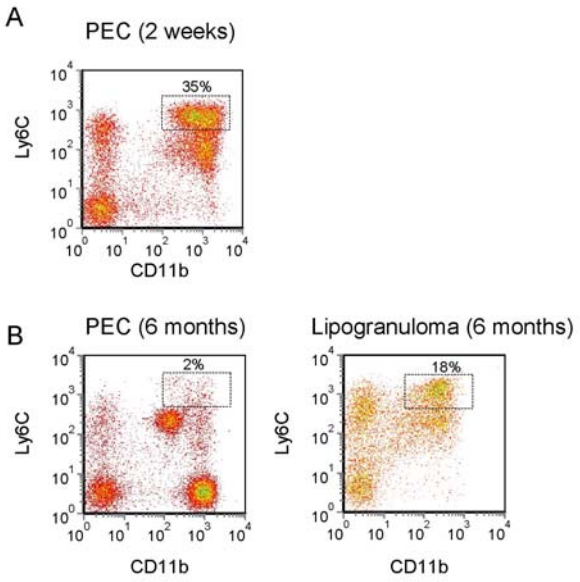

Figure 6-5. Accumulation of Ly6C^{hi} monocytes in lipogranulomas. Flow cytometry analysis comparing the presence of Ly6C^{hi} monocytes A) in the peritoneal cavity two weeks after TMPD treatment and B) in the peritoneal cavity as well as lipogranulomas 6 months after treatment.

LIST OF REFERENCES

1. Reeves, W.H., Narain,S., and Satoh,M. 2004. Autoantibodies in systemic lupus erythematosus. *In* Arthritis and Allied Conditions. L.W. W.J.Koopman and Moreland, editor. Lippincott Williams & Wilkins, Philadelphia, PA. 1497-1521.

2. Hanh, B.H. 2005. Systemic Lupus Erythematosus. *In* Harrison's Principles of Internal Medicine. D.L.e.a. Kasper, editor. McGraw-Hill Medical, New York City. 1956-1967.

3. Deapen, D., A. Escalante, L. Weinrib, D. Horwitz, B. Bachman, P. Roy-Burman, A. Walker, and T.M. Mack. 1992. A revised estimate of twin concordance in systemic lupus erythematosus. *Arthritis Rheum* 35:311-318.

4. Tsao, B.P., and H. Wu. 2006. Genetics of Human Lupus. *In* Dubois' Lupus Erythematosus. D.J.e.a. Wallace, editor. Lippincott Williams & Wilkins. 54-80.

5. Alarcon-Segovia, D., M.E. Alarcon-Riquelme, M.H. Cardiel, F. Caeiro, L. Massardo, A.R. Villa, and B.A. Pons-Estel. 2005. Familial aggregation of systemic lupus erythematosus, rheumatoid arthritis, and other autoimmune diseases in 1,177 lupus patients from the GLADEL cohort. *Arthritis Rheum* 52:1138-1147.

6. Tan, E.M., A.S. Cohen, J.F. Fries, A.T. Masi, D.J. McShane, N.F. Rothfield, J.G. Schaller, N. Talal, and R.J. Winchester. 1982. The 1982 revised criteria for the classification of systemic lupus erythematosus. *Arthritis Rheum* 25:1271-1277.

7. Hochberg, M.C. 1997. Updating the American College of Rheumatology revised criteria for the classification of systemic lupus erythematosus. *Arthritis & Rheumatism* 40:1725.

8. Arbuckle, M.R., M.T. McClain, M.V. Rubertone, R.H. Scofield, G.J. Dennis, J.A. James, and J.B. Harley. 2003. Development of autoantibodies before the clinical onset of systemic lupus erythematosus. *N Engl J Med* 349:1526-1533.

9. Urowitz, M.B., A.A. Bookman, B.E. Koehler, D.A. Gordon, H.A. Smythe, and M.A. Ogryzlo. 1976. The bimodal mortality pattern of systemic lupus erythematosus. *Am J Med* 60:221-225.

10. Klinman, D.M., A. Shirai, Y. Ishigatsubo, J. Conover, and A.D. Steinberg. 1991. Quantitation of IgM- and IgG-secreting B cells in the peripheral blood of patients with systemic lupus erythematosus. *Arthritis Rheum* 34:1404-1410.

11. Liossis, S.N., B. Kovacs, G. Dennis, G.M. Kammer, and G.C. Tsokos. 1996. B cells from patients with systemic lupus erythematosus display abnormal antigen receptor-mediated early signal transduction events. *J Clin Invest* 98:2549-2557.

12. Odendahl, M., A. Jacobi, A. Hansen, E. Feist, F. Hiepe, G.R. Burmester, P.E. Lipsky, A. Radbruch, and T. Dorner. 2000. Disturbed peripheral B lymphocyte homeostasis in systemic lupus erythematosus. *J Immunol* 165:5970-5979.

13. Liossis, S.N., X.Z. Ding, G.J. Dennis, and G.C. Tsokos. 1998. Altered pattern of TCR/CD3-mediated protein-tyrosyl phosphorylation in T cells from patients with systemic lupus erythematosus. Deficient expression of the T cell receptor zeta chain. *J Clin Invest* 101:1448-1457.

14. Desai-Mehta, A., L. Lu, R. Ramsey-Goldman, and S.K. Datta. 1996. Hyperexpression of CD40 ligand by B and T cells in human lupus and its role in pathogenic autoantibody production. *J Clin Invest* 97:2063-2073.

15. Goldman, J.A., A. Litwin, L.E. Adams, R.C. Krueger, and E.V. Hess. 1972. Cellular immunity to nuclear antigens in systemic lupus erythematosus. *J Clin Invest* 51:2669-2677.

16. Gottlieb, A.B., R.G. Lahita, N. Chiorazzi, and H.G. Kunkel. 1979. Immune function in systemic lupus erythematosus. Impairment of in vitro T-cell proliferation and in vivo antibody response to exogenous antigen. *J Clin Invest* 63:885-892.

17. Linker-Israeli, M., R.J. Deans, D.J. Wallace, J. Prehn, T. Ozeri-Chen, and J.R. Klinenberg. 1991. Elevated levels of endogenous IL-6 in systemic lupus erythematosus. A putative role in pathogenesis. *J Immunol* 147:117-123.

18. Llorente, L., W. Zou, Y. Levy, Y. Richaud-Patin, J. Wijdenes, J. Alcocer-Varela, B. Morel-Fourrier, J.C. Brouet, D. Alarcon-Segovia, P. Galanaud, and D. Emilie. 1995. Role of interleukin 10 in the B lymphocyte hyperactivity and autoantibody production of human systemic lupus erythematosus. *J Exp Med* 181:839-844.

19. Pers, J.O., C. Daridon, V. Devauchelle, S. Jousse, A. Saraux, C. Jamin, and P. Youinou. 2005. BAFF overexpression is associated with autoantibody production in autoimmune diseases. *Ann N Y Acad Sci* 1050:34-39.

20. Kurt-Jones, E.A., S. Hamberg, J. Ohara, W.E. Paul, and A.K. Abbas. 1987. Heterogeneity of helper/inducer T lymphocytes. I. Lymphokine production and lymphokine responsiveness. *J Exp Med* 166:1774-1787.

21. Haas, C., B. Ryffel, and M. Le Hir. 1997. IFN-gamma is essential for the development of autoimmune glomerulonephritis in MRL/Ipr mice. *J Immunol* 158:5484-5491.

22. Haas, C., B. Ryffel, and M. Le Hir. 1998. IFN-gamma receptor deletion prevents autoantibody production and glomerulonephritis in lupus-prone (NZB x NZW)F1 mice. *J Immunol* 160:3713-3718.

23. Richards, H.B., M. Satoh, J.C. Jennette, B.P. Croker, H. Yoshida, and W.H. Reeves. 2001. Interferon-gamma is required for lupus nephritis in mice treated with the hydrocarbon oil pristane. *Kidney Int* 60:2173-2180.

24. Calvani, N., M. Satoh, B.P. Croker, W.H. Reeves, and H.B. Richards. 2003. Nephritogenic autoantibodies but absence of nephritis in Il-12p35-deficient mice with pristane-induced lupus. *Kidney Int* 64:897-905.

25. Pittoni, V., and G. Valesini. 2002. The clearance of apoptotic cells: implications for autoimmunity. *Autoimmun Rev* 1:154-161.

26. Herrmann, M., R.E. Voll, O.M. Zoller, M. Hagenhofer, B.B. Ponner, and J.R. Kalden. 1998. Impaired phagocytosis of apoptotic cell material by monocyte-derived macrophages from patients with systemic lupus erythematosus. *Arthritis Rheum* 41:1241-1250.

27. Kelly, K.M., H. Zhuang, D.C. Nacionales, P.O. Scumpia, R. Lyons, J. Akaogi, P. Lee, B. Williams, M. Yamamoto, S. Akira, M. Satoh, and W.H. Reeves. 2006. "Endogenous adjuvant" activity of the RNA components of lupus autoantigens Sm/RNP and Ro 60. *Arthritis Rheum* 54:1557-1567.

28. Vallin, H., A. Perers, G.V. Alm, and L. Ronnblom. 1999. Anti-double-stranded DNA antibodies and immunostimulatory plasmid DNA in combination mimic the endogenous IFN-alpha inducer in systemic lupus erythematosus. *J Immunol* 163:6306-6313.

29. Tew, M.B., R.W. Johnson, J.D. Reveille, and F.K. Tan. 2001. A molecular analysis of the low serum deoxyribonuclease activity in lupus patients. *Arthritis Rheum* 44:2446-2447.

30. Hooks, J.J., H.M. Moutsopoulos, S.A. Geis, N.I. Stahl, J.L. Decker, and A.L. Notkins. 1979. Immune interferon in the circulation of patients with autoimmune disease. *N Engl J Med* 301:5-8.

31. Baechler, E.C., F.M. Batliwalla, G. Karypis, P.M. Gaffney, W.A. Ortmann, K.J. Espe, K.B. Shark, W.J. Grande, K.M. Hughes, V. Kapur, P.K. Gregersen, and T.W. Behrens. 2003. Interferon-inducible gene expression signature in peripheral blood cells of patients with severe lupus. *Proc Natl Acad Sci U S A* 100:2610-2615.

32. Bennett, L., A.K. Palucka, E. Arce, V. Cantrell, J. Borvak, J. Banchereau, and V. Pascual. 2003. Interferon and granulopoiesis signatures in systemic lupus erythematosus blood. *J Exp Med* 197:711-723.

33. Zhuang, H., S. Narain, E. Sobel, P.Y. Lee, D.C. Nacionales, K.M. Kelly, H.B. Richards, M. Segal, C. Stewart, M. Satoh, and W.H. Reeves. 2005. Association of anti-nucleoprotein autoantibodies with upregulation of Type I interferon-inducible gene transcripts and dendritic cell maturation in systemic lupus erythematosus. *Clin Immunol*.

34. Diaz, M.O., H.M. Pomykala, S.K. Bohlander, E. Maltepe, K. Malik, B. Brownstein, and O.I. Olopade. 1994. Structure of the human type-I interferon gene cluster determined from a YAC clone contig. *Genomics* 22:540-552.

35. Fountain, J.W., M. Karayiorgou, D. Taruscio, S.L. Graw, A.J. Buckler, D.C. Ward, N.C. Dracopoli, and D.E. Housman. 1992. Genetic and physical map of the interferon region on chromosome 9p. *Genomics* 14:105-112.

36. Pestka, S., C.D. Krause, and M.R. Walter. 2004. Interferons, interferon-like cytokines, and their receptors. *Immunol Rev* 202:8-32.

37. Darnell, J.E., Jr., I.M. Kerr, and G.R. Stark. 1994. Jak-STAT pathways and transcriptional activation in response to IFNs and other extracellular signaling proteins. *Science* 264:1415-1421.

38. Schindler, C., X.Y. Fu, T. Improta, R. Aebersold, and J.E. Darnell, Jr. 1992. Proteins of transcription factor ISGF-3: one gene encodes the 91-and 84-kDa ISGF-3 proteins that are activated by interferon alpha. *Proc Natl Acad Sci U S A* 89:7836-7839.

39. Fu, X.Y., C. Schindler, T. Improta, R. Aebersold, and J.E. Darnell, Jr. 1992. The proteins of ISGF-3, the interferon alpha-induced transcriptional activator, define a gene family involved in signal transduction. *Proc Natl Acad Sci U S A* 89:7840-7843.

40. Goh, K.C., S.J. Haque, and B.R. Williams. 1999. p38 MAP kinase is required for STAT1 serine phosphorylation and transcriptional activation induced by interferons. *Embo J* 18:5601-5608.

41. Li, Y., A. Sassano, B. Majchrzak, D.K. Deb, D.E. Levy, M. Gaestel, A.R. Nebreda, E.N. Fish, and L.C. Platanias. 2004. Role of p38alpha Map kinase in Type I interferon signaling. *J Biol Chem* 279:970-979.

42. Uddin, S., B. Majchrzak, J. Woodson, P. Arunkumar, Y. Alsayed, R. Pine, P.R. Young, E.N. Fish, and L.C. Platanias. 1999. Activation of the p38 mitogen-activated protein kinase by type I interferons. *J Biol Chem* 274:30127-30131.

43. Theofilopoulos, A.N., R. Baccala, B. Beutler, and D.H. Kono. 2005. Type I interferons (alpha/beta) in immunity and autoimmunity. *Annu Rev Immunol* 23:307-336.

44. Dalod, M., T. Hamilton, R. Salomon, T.P. Salazar-Mather, S.C. Henry, J.D. Hamilton, and C.A. Biron. 2003. Dendritic cell responses to early murine cytomegalovirus infection: subset functional specialization and differential regulation by interferon alpha/beta. *J Exp Med* 197:885-898.

45. Doyle, S., S. Vaidya, R. O'Connell, H. Dadgostar, P. Dempsey, T. Wu, G. Rao, R. Sun, M. Haberland, R. Modlin, and G. Cheng. 2002. IRF3 mediates a TLR3/TLR4-specific antiviral gene program. *Immunity* 17:251-263.

46. Sen, G.C., and R.M. Ransohoff. 1993. Interferon-induced antiviral actions and their regulation. *Adv Virus Res* 42:57-102.

47. Marrack, P., J. Kappler, and T. Mitchell. 1999. Type I interferons keep activated T cells alive. *J Exp Med* 189:521-530.

48. Finkelman, F.D., A. Svetic, I. Gresser, C. Snapper, J. Holmes, P.P. Trotta, I.M. Katona, and W.C. Gause. 1991. Regulation by interferon alpha of immunoglobulin isotype selection and lymphokine production in mice. *J Exp Med* 174:1179-1188.

49. Le Bon, A., G. Schiavoni, G. D'Agostino, I. Gresser, F. Belardelli, and D.F. Tough. 2001. Type i interferons potently enhance humoral immunity and can promote isotype switching by stimulating dendritic cells in vivo. *Immunity* 14:461-470.

50. Sharif, M.N., I. Tassiulas, Y. Hu, I. Mecklenbrauker, A. Tarakhovsky, and L.B. Ivashkiv. 2004. IFN-alpha priming results in a gain of proinflammatory function by IL-10: implications for systemic lupus erythematosus pathogenesis. *J Immunol* 172:6476-6481.

51. Takeda, K., T. Kaisho, and S. Akira. 2003. Toll-like receptors. *Annu Rev Immunol* 21:335-376.

52. Yamamoto, M., S. Sato, H. Hemmi, K. Hoshino, T. Kaisho, H. Sanjo, O. Takeuchi, M. Sugiyama, M. Okabe, K. Takeda, and S. Akira. 2003. Role of adaptor TRIF in the MyD88-independent toll-like receptor signaling pathway. *Science* 301:640-643.

53. Kagan, J.C., T. Su, T. Horng, A. Chow, S. Akira, and R. Medzhitov. 2008. TRAM couples endocytosis of Toll-like receptor 4 to the induction of interferon-beta. *Nat Immunol* 9:361-368.

54. Hemmi, H., T. Kaisho, O. Takeuchi, S. Sato, H. Sanjo, K. Hoshino, T. Horiuchi, H. Tomizawa, K. Takeda, and S. Akira. 2002. Small anti-viral compounds activate immune cells via the TLR7 MyD88-dependent signaling pathway. *Nat Immunol* 3:196-200.

55. Diebold, S.S., T. Kaisho, H. Hemmi, S. Akira, and C. Reis e Sousa. 2004. Innate antiviral responses by means of TLR7-mediated recognition of single-stranded RNA. *Science* 303:1529-1531.

56. Hemmi, H., O. Takeuchi, T. Kawai, T. Kaisho, S. Sato, H. Sanjo, M. Matsumoto, K. Hoshino, H. Wagner, K. Takeda, and S. Akira. 2000. A Toll-like receptor recognizes bacterial DNA. *Nature* 408:740-745.

57. Levy, D.E., I. Marie, E. Smith, and A. Prakash. 2002. Enhancement and diversification of IFN induction by IRF-7-mediated positive feedback. *J Interferon Cytokine Res* 22:87-93.

58. Sato, M., N. Hata, M. Asagiri, T. Nakaya, T. Taniguchi, and N. Tanaka. 1998. Positive feedback regulation of type I IFN genes by the IFN-inducible transcription factor IRF-7. *FEBS Lett* 441:106-110.

59. Kato, H., O. Takeuchi, S. Sato, M. Yoneyama, M. Yamamoto, K. Matsui, S. Uematsu, A. Jung, T. Kawai, K.J. Ishii, O. Yamaguchi, K. Otsu, T. Tsujimura, C.S. Koh, C. Reis e Sousa, Y. Matsuura, T. Fujita, and S. Akira. 2006. Differential roles of MDA5 and RIG-I helicases in the recognition of RNA viruses. *Nature* 441:101-105.

60. Yoneyama, M., M. Kikuchi, T. Natsukawa, N. Shinobu, T. Imaizumi, M. Miyagishi, K. Taira, S. Akira, and T. Fujita. 2004. The RNA helicase RIG-I has an essential function in double-stranded RNA-induced innate antiviral responses. *Nat Immunol* 5:730-737.

61. Kawai, T., K. Takahashi, S. Sato, C. Coban, H. Kumar, H. Kato, K.J. Ishii, O. Takeuchi, and S. Akira. 2005. IPS-1, an adaptor triggering RIG-I- and Mda5-mediated type I interferon induction. *Nat Immunol* 6:981-988.

62. Stetson, D.B., and R. Medzhitov. 2006. Recognition of cytosolic DNA activates an IRF3-dependent innate immune response. *Immunity* 24:93-103.

63. Ishii, K.J., C. Coban, H. Kato, K. Takahashi, Y. Torii, F. Takeshita, H. Ludwig, G. Sutter, K. Suzuki, H. Hemmi, S. Sato, M. Yamamoto, S. Uematsu, T. Kawai, O. Takeuchi, and S. Akira. 2006. A Toll-like receptor-independent antiviral response induced by double-stranded B-form DNA. *Nat Immunol* 7:40-48.

64. Cella, M., D. Jarrossay, F. Facchetti, O. Alebardi, H. Nakajima, A. Lanzavecchia, and M. Colonna. 1999. Plasmacytoid monocytes migrate to inflamed lymph nodes and produce large amounts of type I interferon. *Nat Med* 5:919-923.

65. Coccia, E.M., M. Severa, E. Giacomini, D. Monneron, M.E. Remoli, I. Julkunen, M. Cella, R. Lande, and G. Uze. 2004. Viral infection and Toll-like receptor agonists induce a differential expression of type I and lambda interferons in human plasmacytoid and monocyte-derived dendritic cells. *Eur J Immunol* 34:796-805.

66. Dzionek, A., Y. Sohma, J. Nagafune, M. Cella, M. Colonna, F. Facchetti, G. Gunther, I. Johnston, A. Lanzavecchia, T. Nagasaka, T. Okada, W. Vermi, G. Winkels, T. Yamamoto, M. Zysk, Y. Yamaguchi, and J. Schmitz. 2001. BDCA-2, a novel plasmacytoid dendritic cell-specific type II C-type lectin, mediates antigen capture and is a potent inhibitor of interferon alpha/beta induction. *J Exp Med* 194:1823-1834.

67. Izaguirre, A., B.J. Barnes, S. Amrute, W.S. Yeow, N. Megjugorac, J. Dai, D. Feng, E. Chung, P.M. Pitha, and P. Fitzgerald-Bocarsly. 2003. Comparative analysis of IRF and IFN-alpha expression in human plasmacytoid and monocyte-derived dendritic cells. *J Leukoc Biol* 74:1125-1138.

68. Diebold, S.S., M. Montoya, H. Unger, L. Alexopoulou, P. Roy, L.E. Haswell, A. Al-Shamkhani, R. Flavell, P. Borrow, and C. Reis e Sousa. 2003. Viral infection switches non-plasmacytoid dendritic cells into high interferon producers. *Nature* 424:324-328.

69. Matsui, K., Y. Kumagai, H. Kato, S. Sato, T. Kawagoe, S. Uematsu, O. Takeuchi, and S. Akira. 2006. Cutting edge: Role of TANK-binding kinase 1 and inducible IkappaB kinase in IFN responses against viruses in innate immune cells. *J Immunol* 177:5785-5789.

70. Kalkner, K.M., L. Ronnblom, A.K. Karlsson Parra, M. Bengtsson, Y. Olsson, and K. Oberg. 1998. Antibodies against double-stranded DNA and development of polymyositis during treatment with interferon. *Qjm* 91:393-399.

71. Ioannou, Y., and D.A. Isenberg. 2000. Current evidence for the induction of autoimmune rheumatic manifestations by cytokine therapy. *Arthritis Rheum* 43:1431-1442.

72. Ronnblom, L.E., G.V. Alm, and K.E. Oberg. 1991. Autoimmunity after alpha-interferon therapy for malignant carcinoid tumors. *Ann Intern Med* 115:178-183.

73. Wilson, L.E., D. Widman, S.H. Dikman, and P.D. Gorevic. 2002. Autoimmune disease complicating antiviral therapy for hepatitis C virus infection. *Semin Arthritis Rheum* 32:163-173.

74. Blanco, P., A.K. Palucka, M. Gill, V. Pascual, and J. Banchereau. 2001. Induction of dendritic cell differentiation by IFN-alpha in systemic lupus erythematosus. *Science* 294:1540-1543.

75. Kirou, K.A., C. Lee, S. George, K. Louca, I.G. Papagiannis, M.G. Peterson, N. Ly, R.N. Woodward, K.E. Fry, A.Y. Lau, J.G. Prentice, J.G. Wohlgemuth, and M.K. Crow. 2004. Coordinate overexpression of interferon-alpha-induced genes in systemic lupus erythematosus. *Arthritis Rheum* 50:3958-3967.

76. Kirou, K.A., C. Lee, S. George, K. Louca, M.G. Peterson, and M.K. Crow. 2005. Activation of the interferon-alpha pathway identifies a subgroup of systemic lupus erythematosus patients with distinct serologic features and active disease. *Arthritis Rheum* 52:1491-1503.

77. Vallin, H., S. Blomberg, G.V. Alm, B. Cederblad, and L. Ronnblom. 1999. Patients with systemic lupus erythematosus (SLE) have a circulating inducer of interferon-alpha (IFN-alpha) production acting on leucocytes resembling immature dendritic cells. *Clin Exp Immunol* 115:196-202.

78. Barton, G.M., J.C. Kagan, and R. Medzhitov. 2006. Intracellular localization of Toll-like receptor 9 prevents recognition of self DNA but facilitates access to viral DNA. *Nat Immunol* 7:49-56.

79. Means, T.K., E. Latz, F. Hayashi, M.R. Murali, D.T. Golenbock, and A.D. Luster. 2005. Human lupus autoantibody-DNA complexes activate DCs through cooperation of CD32 and TLR9. *J Clin Invest* 115:407-417.

80. Barrat, F.J., T. Meeker, J. Gregorio, J.H. Chan, S. Uematsu, S. Akira, B. Chang, O. Duramad, and R.L. Coffman. 2005. Nucleic acids of mammalian origin can act as endogenous ligands for Toll-like receptors and may promote systemic lupus erythematosus. *J Exp Med* 202:1131-1139.

81. Savarese, E., O.W. Chae, S. Trowitzsch, G. Weber, B. Kastner, S. Akira, H. Wagner, R.M. Schmid, S. Bauer, and A. Krug. 2006. U1 small nuclear ribonucleoprotein immune complexes induce type I interferon in plasmacytoid dendritic cells through TLR7. *Blood* 107:3229-3234.

82. Bave, U., M. Magnusson, M.L. Eloranta, A. Perers, G.V. Alm, and L. Ronnblom. 2003. Fc gamma RIIa is expressed on natural IFN-alpha-producing cells (plasmacytoid dendritic cells) and is required for the IFN-alpha production induced by apoptotic cells combined with lupus IgG. *J Immunol* 171:3296-3302.

83. Marshak-Rothstein, A. 2006. Toll-like receptors in systemic autoimmune disease. *Nat Rev Immunol* 6:823-835.

84. Ronnblom, L., M.L. Eloranta, and G.V. Alm. 2006. The type I interferon system in systemic lupus erythematosus. *Arthritis Rheum* 54:408-420.

85. Hornung, V., S. Rothenfusser, S. Britsch, A. Krug, B. Jahrsdorfer, T. Giese, S. Endres, and G. Hartmann. 2002. Quantitative expression of toll-like receptor 1-10 mRNA in cellular subsets of human peripheral blood mononuclear cells and sensitivity to CpG oligodeoxynucleotides. *J Immunol* 168:4531-4537.

86. Farkas, L., K. Beiske, F. Lund-Johansen, P. Brandtzaeg, and F.L. Jahnsen. 2001. Plasmacytoid dendritic cells (natural interferon- alpha/beta-producing cells) accumulate in cutaneous lupus erythematosus lesions. *Am J Pathol* 159:237-243.

87. Burnet, F.M., and M.C. Holmes. 1965. The natural history of the NZB/NZW F1 hybrid mouse: a laboratory model of systemic lupus erythematosus. *Australas Ann Med* 14:185-191.

88. Mathian, A., A. Weinberg, M. Gallegos, J. Banchereau, and S. Koutouzov. 2005. IFN-alpha induces early lethal lupus in preautoimmune (New Zealand Black x New Zealand White) F1 but not in BALB/c mice. *J Immunol* 174:2499-2506.

89. Santiago-Raber, M.L., R. Baccala, K.M. Haraldsson, D. Choubey, T.A. Stewart, D.H. Kono, and A.N. Theofilopoulos. 2003. Type-I interferon receptor deficiency reduces lupus-like disease in NZB mice. *J Exp Med* 197:777-788.

90. Jorgensen, T.N., E. Roper, J.M. Thurman, P. Marrack, and B.L. Kotzin. 2007. Type I interferon signaling is involved in the spontaneous development of lupus-like disease in B6.Nba2 and (B6.Nba2 x NZW)F(1) mice. *Genes Immun* 8:653-662.

91. Pisetsky, D.S., G.A. McCarty, and D.V. Peters. 1980. Mechanisms of autoantibody production in autoimmune MRL mice. *J Exp Med* 152:1302-1310.

92. Hron, J.D., and S.L. Peng. 2004. Type I IFN protects against murine lupus. *J Immunol* 173:2134-2142.

93. Nacionales, D.C., K.M. Kelly-Scumpia, P.Y. Lee, J.S. Weinstein, R. Lyons, E. Sobel, M. Satoh, and W.H. Reeves. 2007. Deficiency of the type I interferon receptor protects mice from experimental lupus. *Arthritis Rheum* 56:3770-3783.

94. Anderson, P.N., and M. Potter. 1969. Induction of plasma cell tumours in BALB-c mice with 2,6,10,14-tetramethylpentadecane (pristane). *Nature* 222:994-995.

95. Hoogenraad, N., T. Helman, and J. Hoogenraad. 1983. The effect of pre-injection of mice with pristane on ascites tumour formation and monoclonal antibody production. *J Immunol Methods* 61:317-320.

96. Satoh, M., and W.H. Reeves. 1994. Induction of lupus-associated autoantibodies in BALB/c mice by intraperitoneal injection of pristane. *J Exp Med* 180:2341-2346.

97. Satoh, M., A. Kumar, Y.S. Kanwar, and W.H. Reeves. 1995. Anti-nuclear antibody production and immune-complex glomerulonephritis in BALB/c mice treated with pristane. *Proc Natl Acad Sci U S A* 92:10934-10938.

98. Yoshida, H., M. Satoh, K.M. Behney, C.G. Lee, H.B. Richards, V.M. Shaheen, J.Q. Yang, R.R. Singh, and W.H. Reeves. 2002. Effect of an exogenous trigger on the pathogenesis of lupus in (NZB x NZW)F1 mice. *Arthritis Rheum* 46:2235-2244.

99. Jung, S., D. Unutmaz, P. Wong, G. Sano, K. De los Santos, T. Sparwasser, S. Wu, S. Vuthoori, K. Ko, F. Zavala, E.G. Pamer, D.R. Littman, and R.A. Lang. 2002. In vivo depletion of CD11c(+) dendritic cells abrogates priming of CD8(+) T cells by exogenous cell-associated antigens. *Immunity* 17:211-220.

100. Scumpia, P.O., P.F. McAuliffe, K.A. O'Malley, R. Ungaro, T. Uchida, T. Matsumoto, D.G. Remick, M.J. Clare-Salzler, L.L. Moldawer, and P.A. Efron. 2005. CD11c+ dendritic cells are required for survival in murine polymicrobial sepsis. *J Immunol* 175:3282-3286.

101. Kumar, H., T. Kawai, H. Kato, S. Sato, K. Takahashi, C. Coban, M. Yamamoto, S. Uematsu, K.J. Ishii, O. Takeuchi, and S. Akira. 2006. Essential role of IPS-1 in innate immune responses against RNA viruses. *J Exp Med* 203:1795-1803.

102. Adachi, O., T. Kawai, K. Takeda, M. Matsumoto, H. Tsutsui, M. Sakagami, K. Nakanishi, and S. Akira. 1998. Targeted disruption of the MyD88 gene results in loss of IL-1- and IL-18-mediated function. *Immunity* 9:143-150.

103. Nacionales, D.C., K.M. Kelly, P.Y. Lee, H. Zhuang, Y. Li, J.S. Weinstein, E. Sobel, Y. Kuroda, J. Akaogi, M. Satoh, and W.H. Reeves. 2006. Type I interferon production by tertiary lymphoid tissue developing in response to 2,6,10,14-tetramethyl-pentadecane (pristane). *Am J Pathol* 168:1227-1240.

104. Janz, S., and E. Shacter. 1991. A new method for delivering alkanes to mammalian cells: preparation and preliminary characterization of an inclusion complex between beta-cyclodextrin and pristane (2,6,10,14-tetramethylpentadecane). *Toxicology* 69:301-315.

105. Sunderkotter, C., T. Nikolic, M.J. Dillon, N. Van Rooijen, M. Stehling, D.A. Drevets, and P.J. Leenen. 2004. Subpopulations of mouse blood monocytes differ in maturation stage and inflammatory response. *J Immunol* 172:4410-4417.

106. Van Rooijen, N., and A. Sanders. 1994. Liposome mediated depletion of macrophages: mechanism of action, preparation of liposomes and applications. *J Immunol Methods* 174:83-93.

107. Cook, A.D., E.L. Braine, and J.A. Hamilton. 2003. The phenotype of inflammatory macrophages is stimulus dependent: implications for the nature of the inflammatory response. *J Immunol* 171:4816-4823.

108. Geissmann, F., S. Jung, and D.R. Littman. 2003. Blood monocytes consist of two principal subsets with distinct migratory properties. *Immunity* 19:71-82.

109. Asselin-Paturel, C., A. Boonstra, M. Dalod, I. Durand, N. Yessaad, C. Dezutter-Dambuyant, A. Vicari, A. O'Garra, C. Biron, F. Briere, and G. Trinchieri. 2001. Mouse type I IFN-producing cells are immature APCs with plasmacytoid morphology. *Nat Immunol* 2:1144-1150.

110. Spangrude, G.J., Y. Aihara, I.L. Weissman, and J. Klein. 1988. The stem cell antigens Sca-1 and Sca-2 subdivide thymic and peripheral T lymphocytes into unique subsets. *J Immunol* 141:3697-3707.

111. Kassim, S.H., N.K. Rajasagi, X. Zhao, R. Chervenak, and S.R. Jennings. 2006. In vivo ablation of CD11c-positive dendritic cells increases susceptibility to herpes simplex virus type 1 infection and diminishes NK and T-cell responses. *J Virol* 80:3985-3993.

112. Asselin-Paturel, C., G. Brizard, J.J. Pin, F. Briere, and G. Trinchieri. 2003. Mouse strain differences in plasmacytoid dendritic cell frequency and function revealed by a novel monoclonal antibody. *J Immunol* 171:6466-6477.

113. Blasius, A.L., E. Giurisato, M. Cella, R.D. Schreiber, A.S. Shaw, and M. Colonna. 2006. Bone marrow stromal cell antigen 2 is a specific marker of type I IFN-producing cells in the naive mouse, but a promiscuous cell surface antigen following IFN stimulation. *J Immunol* 177:3260-3265.

114. Kuroda, Y., J. Akaogi, D.C. Nacionales, S.C. Wasdo, N.J. Szabo, W.H. Reeves, and M. Satoh. 2004. Distinctive patterns of autoimmune response induced by different types of mineral oil. *Toxicol Sci* 78:222-228.

115. Dumont, F.J., and L.Z. Coker. 1986. Interferon-alpha/beta enhances the expression of Ly-6 antigens on T cells in vivo and in vitro. *Eur J Immunol* 16:735-740.

116. Serbina, N.V., and E.G. Pamer. 2006. Monocyte emigration from bone marrow during bacterial infection requires signals mediated by chemokine receptor CCR2. *Nat Immunol* 7:311-317.

117. Kadowaki, N., S. Antonenko, J.Y. Lau, and Y.J. Liu. 2000. Natural interferon alpha/beta-producing cells link innate and adaptive immunity. *J Exp Med* 192:219-226.

118. Scheinecker, C., B. Zwolfer, M. Koller, G. Manner, and J.S. Smolen. 2001. Alterations of dendritic cells in systemic lupus erythematosus: phenotypic and functional deficiencies. *Arthritis Rheum* 44:856-865.

119. Tacke, F., D. Alvarez, T.J. Kaplan, C. Jakubzick, R. Spanbroek, J. Llodra, A. Garin, J. Liu, M. Mack, N. van Rooijen, S.A. Lira, A.J. Habenicht, and G.J. Randolph. 2007. Monocyte subsets differentially employ CCR2, CCR5, and CX3CR1 to accumulate within atherosclerotic plaques. *J Clin Invest* 117:185-194.

120. Hemmi, H., T. Kaisho, K. Takeda, and S. Akira. 2003. The roles of Toll-like receptor 9, MyD88, and DNA-dependent protein kinase catalytic subunit in the effects of two distinct CpG DNAs on dendritic cell subsets. *J Immunol* 170:3059-3064.

121. Hornung, V., J. Ellegast, S. Kim, K. Brzozka, A. Jung, H. Kato, H. Poeck, S. Akira, K.K. Conzelmann, M. Schlee, S. Endres, and G. Hartmann. 2006. 5'-Triphosphate RNA is the ligand for RIG-I. *Science* 314:994-997.

122. Stockinger, S., B. Reutterer, B. Schaljo, C. Schellack, S. Brunner, T. Materna, M. Yamamoto, S. Akira, T. Taniguchi, P.J. Murray, M. Muller, and T. Decker. 2004. IFN regulatory factor 3-dependent induction of type I IFNs by intracellular bacteria is mediated by a TLR- and Nod2-independent mechanism. *J Immunol* 173:7416-7425.

123. Pawar, R.D., P.S. Patole, D. Zecher, S. Segerer, M. Kretzler, D. Schlondorff, and H.J. Anders. 2006. Toll-like receptor-7 modulates immune complex glomerulonephritis. *J Am Soc Nephrol* 17:141-149.

124. Richards, H.B., M. Satoh, M. Shaw, C. Libert, V. Poli, and W.H. Reeves. 1998. Interleukin 6 dependence of anti-DNA antibody production: evidence for two pathways of autoantibody formation in pristane-induced lupus. *J Exp Med* 188:985-990.

125. Ikeda, K., M. Satoh, K.M. Pauley, M.J. Fritzler, W.H. Reeves, and E.K. Chan. 2006. Detection of the argonaute protein Ago2 and microRNAs in the RNA induced silencing complex (RISC) using a monoclonal antibody. *J Immunol Methods* 317:38-44.

126. Takaoka, A., Z. Wang, M.K. Choi, H. Yanai, H. Negishi, T. Ban, Y. Lu, M. Miyagishi, T. Kodama, K. Honda, Y. Ohba, and T. Taniguchi. 2007. DAI (DLM-1/ZBP1) is a cytosolic DNA sensor and an activator of innate immune response. *Nature* 448:501-505.

127. Bauer, J.W., E.C. Baechler, M. Petri, F.M. Batliwalla, D. Crawford, W.A. Ortmann, K.J. Espe, W. Li, D.D. Patel, P.K. Gregersen, and T.W. Behrens. 2006. Elevated serum levels of interferon-regulated chemokines are biomarkers for active human systemic lupus erythematosus. *PLoS Med* 3:e491.

128. Batteux, F., P. Palmer, M. Daeron, B. Weill, and P. Lebon. 1999. FCgammaRII (CD32)-dependent induction of interferon-alpha by serum from patients with lupus erythematosus. *Eur Cytokine Netw* 10:509-514.

129. Yasuda, K., C. Richez, J.W. Maciaszek, N. Agrawal, S. Akira, A. Marshak-Rothstein, and I.R. Rifkin. 2007. Murine dendritic cell type I IFN production induced by human IgG-RNA immune complexes is IFN regulatory factor (IRF)5 and IRF7 dependent and is required for IL-6 production. *J Immunol* 178:6876-6885.

130. Murphy, E.D., and J.B. Roths. 1979. A Y chromosome associated factor in strain BXSB producing accelerated autoimmunity and lymphoproliferation. *Arthritis Rheum* 22:1188-1194.

131. Izui, S., M. Higaki, D. Morrow, and R. Merino. 1988. The Y chromosome from autoimmune BXSB/MpJ mice induces a lupus-like syndrome in (NZW x C57BL/6)F1 male mice, but not in C57BL/6 male mice. *Eur J Immunol* 18:911-915.

132. Bolland, S., Y.S. Yim, K. Tus, E.K. Wakeland, and J.V. Ravetch. 2002. Genetic modifiers of systemic lupus erythematosus in FcgammaRIIB(-/-) mice. *J Exp Med* 195:1167-1174.

133. Subramanian, S., K. Tus, Q.Z. Li, A. Wang, X.H. Tian, J. Zhou, C. Liang, G. Bartov, L.D. McDaniel, X.J. Zhou, R.A. Schultz, and E.K. Wakeland. 2006. A Tlr7 translocation accelerates systemic autoimmunity in murine lupus. *Proc Natl Acad Sci U S A* 103:9970-9975.

134. Pisitkun, P., J.A. Deane, M.J. Difilippantonio, T. Tarasenko, A.B. Satterthwaite, and S. Bolland. 2006. Autoreactive B cell responses to RNA-related antigens due to TLR7 gene duplication. *Science* 312:1669-1672.

135. Deane, J.A., P. Pisitkun, R.S. Barrett, L. Feigenbaum, T. Town, J.M. Ward, R.A. Flavell, and S. Bolland. 2007. Control of toll-like receptor 7 expression is essential to restrict autoimmunity and dendritic cell proliferation. *Immunity* 27:801-810.

136. Christensen, S.R., J. Shupe, K. Nickerson, M. Kashgarian, R.A. Flavell, and M.J. Shlomchik. 2006. Toll-like receptor 7 and TLR9 dictate autoantibody specificity and have opposing inflammatory and regulatory roles in a murine model of lupus. *Immunity* 25:417-428.

137. Hamilton, K.J., M. Satoh, J. Swartz, H.B. Richards, and W.H. Reeves. 1998. Influence of microbial stimulation on hypergammaglobulinemia and autoantibody production in pristane-induced lupus. *Clin Immunol Immunopathol* 86:271-279.

138. Satoh, M., J.J. Langdon, C.H. Chou, D.P. McCauliffe, E.L. Treadwell, T. Ogasawara, M. Hirakata, A. Suwa, P.L. Cohen, R.A. Eisenberg, and et al. 1994. Characterization of the Su antigen, a macromolecular complex of 100/102 and 200-kDa proteins recognized by autoantibodies in systemic rheumatic diseases. *Clin Immunol Immunopathol* 73:132-141.

139. Jakymiw, A., K. Ikeda, M.J. Fritzler, W.H. Reeves, M. Satoh, and E.K. Chan. 2006. Autoimmune targeting of key components of RNA interference. *Arthritis Res Ther* 8:R87.

140. Lee, P.Y., Y. Li, H.B. Richards, F.S. Chan, H. Zhuang, S. Narain, E.J. Butfiloski, E.S. Sobel, W.H. Reeves, and M.S. Segal. 2007. Type I interferon as a novel risk factor for endothelial progenitor cell depletion and endothelial dysfunction in systemic lupus erythematosus. *Arthritis Rheum* 56:3759-3769.

141. Smith, D.L., X. Dong, S. Du, M. Oh, R.R. Singh, and R.R. Voskuhl. 2007. A female preponderance for chemically induced lupus in SJL/J mice. *Clin Immunol* 122:101-107.

142. Clynes, R., N. Calvani, B.P. Croker, and H.B. Richards. 2005. Modulation of the immune response in pristane-induced lupus by expression of activation and inhibitory Fc receptors. *Clin Exp Immunol* 141:230-237.

143. Satoh, M., J.P. Weintraub, H. Yoshida, V.M. Shaheen, H.B. Richards, M. Shaw, and W.H. Reeves. 2000. Fas and Fas ligand mutations inhibit autoantibody production in pristane-induced lupus. *J Immunol* 165:1036-1043.

144. Lau, C.M., C. Broughton, A.S. Tabor, S. Akira, R.A. Flavell, M.J. Mamula, S.R. Christensen, M.J. Shlomchik, G.A. Viglianti, I.R. Rifkin, and A. Marshak-Rothstein. 2005. RNA-associated autoantigens activate B cells by combined B cell antigen receptor/Toll-like receptor 7 engagement. *J Exp Med* 202:1171-1177.

145. Berland, R., L. Fernandez, E. Kari, J.H. Han, I. Lomakin, S. Akira, H.H. Wortis, J.F. Kearney, A.A. Ucci, and T. Imanishi-Kari. 2006. Toll-like receptor 7-dependent loss of B cell tolerance in pathogenic autoantibody knockin mice. *Immunity* 25:429-440.

146. Kuroda, Y., D.C. Nacionales, J. Akaogi, W.H. Reeves, and M. Satoh. 2004. Autoimmunity induced by adjuvant hydrocarbon oil components of vaccine. *Biomed Pharmacother* 58:325-337.

147. Vollmer, J., S. Tluk, C. Schmitz, S. Hamm, M. Jurk, A. Forsbach, S. Akira, K.M. Kelly, W.H. Reeves, S. Bauer, and A.M. Krieg. 2005. Immune stimulation mediated by autoantigen binding sites within small nuclear RNAs involves Toll-like receptors 7 and 8. *J Exp Med* 202:1575-1585.

148. Bly, J.E., L.R. Garrett, and M.A. Cuchens. 1990. Pristane induced changes in rat lymphocyte membrane fluidity. *Cancer Biochem Biophys* 11:145-154.

149. Jego, G., A.K. Palucka, J.P. Blanck, C. Chalouni, V. Pascual, and J. Banchereau. 2003. Plasmacytoid dendritic cells induce plasma cell differentiation through type I interferon and interleukin 6. *Immunity* 19:225-234.

150. Kumar, V., A. Abbas, and N. Fausto. 2004. Robbins & Cotran Pathologic Basis of Disease. Elsevier Health Sciences, Philadephia, PA. 1552 pp.

151. Swirski, F.K., P. Libby, E. Aikawa, P. Alcaide, F.W. Luscinskas, R. Weissleder, and M.J. Pittet. 2007. Ly-6Chi monocytes dominate hypercholesterolemia-associated monocytosis and give rise to macrophages in atheromata. *J Clin Invest* 117:195-205.

152. Cancro, M., and M. Potter. 1976. The requirement of an adherent cell substratum for the growth of developing plasmacytoma cells in vivo. *J Exp Med* 144:1554-1567.

153. Richards, H.B., M. Satoh, V.M. Shaheen, H. Yoshida, and W.H. Reeves. 1999. Induction of B cell autoimmunity by pristane. *Curr Top Microbiol Immunol* 246:387-392; discussion 393.

154. Lee, P.Y., J.S. Weinstein, D.C. Nacionales, P.O. Scumpia, Y. Li, E. Butfiloski, N. van Rooijen, L. Moldawer, M. Satoh, and W.H. Reeves. 2008. A novel Type I IFN-producing cell subset in murine lupus. *J Immunol* 180:5101-5108.

155. Toshchakov, V., B.W. Jones, P.Y. Perera, K. Thomas, M.J. Cody, S. Zhang, B.R. Williams, J. Major, T.A. Hamilton, M.J. Fenton, and S.N. Vogel. 2002. TLR4, but not TLR2, mediates IFN-beta-induced STAT1alpha/beta-dependent gene expression in macrophages. *Nat Immunol* 3:392-398.

156. Mills, C.D., K. Kincaid, J.M. Alt, M.J. Heilman, and A.M. Hill. 2000. M-1/M-2 macrophages and the Th1/Th2 paradigm. *J Immunol* 164:6166-6173.

157. Munder, M., M. Mallo, K. Eichmann, and M. Modolell. 1998. Murine macrophages secrete interferon gamma upon combined stimulation with interleukin (IL)-12 and IL-18: A novel pathway of autocrine macrophage activation. *J Exp Med* 187:2103-2108.

158. Martinon, F., V. Petrilli, A. Mayor, A. Tardivel, and J. Tschopp. 2006. Gout-associated uric acid crystals activate the NALP3 inflammasome. *Nature* 440:237-241.

159. Dostert, C., V. Petrilli, R. Van Bruggen, C. Steele, B.T. Mossman, and J. Tschopp. 2008. Innate immune activation through Nalp3 inflammasome sensing of asbestos and silica. *Science* 320:674-677.

160. Martinon, F., K. Burns, and J. Tschopp. 2002. The inflammasome: a molecular platform triggering activation of inflammatory caspases and processing of proIL-beta. *Mol Cell* 10:417-426.

161. Moore, J.M., and T.V. Rajan. 1994. Pristane retards clearance of particulate materials from the peritoneal cavity of laboratory mice. *J Immunol Methods* 173:273-278.

162. Salazar-Mather, T.P., T.A. Hamilton, and C.A. Biron. 2000. A chemokine-to-cytokine-to-chemokine cascade critical in antiviral defense. *J Clin Invest* 105:985-993.

163. Salazar-Mather, T.P., C.A. Lewis, and C.A. Biron. 2002. Type I interferons regulate inflammatory cell trafficking and macrophage inflammatory protein 1alpha delivery to the liver. *J Clin Invest* 110:321-330.

164. Tsou, C.L., W. Peters, Y. Si, S. Slaymaker, A.M. Aslanian, S.P. Weisberg, M. Mack, and I.F. Charo. 2007. Critical roles for CCR2 and MCP-3 in monocyte mobilization from bone marrow and recruitment to inflammatory sites. *J Clin Invest* 117:902-909.

165. Jia, T., N.V. Serbina, K. Brandl, M.X. Zhong, I.M. Leiner, I.F. Charo, and E.G. Pamer. 2008. Additive roles for MCP-1 and MCP-3 in CCR2-mediated recruitment of

inflammatory monocytes during Listeria monocytogenes infection. *J Immunol* 180:6846-6853.

166. Kalden, J.R. 1997. Defective phagocytosis of apoptotic cells: possible explanation for the induction of autoantibodies in SLE. *Lupus* 6:326-327.

167. Niessner, A., M.S. Shin, O. Pryshchep, J.J. Goronzy, E.L. Chaikof, and C.M. Weyand. 2007. Synergistic proinflammatory effects of the antiviral cytokine interferon-alpha and Toll-like receptor 4 ligands in the atherosclerotic plaque. *Circulation* 116:2043-2052.

168. Yla-Herttuala, S., B.A. Lipton, M.E. Rosenfeld, T. Sarkioja, T. Yoshimura, E.J. Leonard, J.L. Witztum, and D. Steinberg. 1991. Expression of monocyte chemoattractant protein 1 in macrophage-rich areas of human and rabbit atherosclerotic lesions. *Proc Natl Acad Sci U S A* 88:5252-5256.

169. Roman, M.J., B.A. Shanker, A. Davis, M.D. Lockshin, L. Sammaritano, R. Simantov, M.K. Crow, J.E. Schwartz, S.A. Paget, R.B. Devereux, and J.E. Salmon. 2003. Prevalence and correlates of accelerated atherosclerosis in systemic lupus erythematosus. *N Engl J Med* 349:2399-2406.

170. Mehta, V.B., J. Hart, and M.D. Wewers. 2001. ATP-stimulated release of interleukin (IL)-1beta and IL-18 requires priming by lipopolysaccharide and is independent of caspase-1 cleavage. *J Biol Chem* 276:3820-3826.

171. Chen, C.J., H. Kono, D. Golenbock, G. Reed, S. Akira, and K.L. Rock. 2007. Identification of a key pathway required for the sterile inflammatory response triggered by dying cells. *Nat Med* 13:851-856.

172. Akaogi, J., D.C. Nacionales, Y. Kuroda, W.H. Reeves, and M. Satoh. 2003. Ecotropic murine leukemia viruses and exogenous mouse mammary tumor viruses are not essential for pristane-induced lupus. *Arthritis Rheum* 48:2990-2992.

173. Satoh, M., K.J. Hamilton, A.K. Ajmani, X. Dong, J. Wang, Y.S. Kanwar, and W.H. Reeves. 1996. Autoantibodies to ribosomal P antigens with immune complex glomerulonephritis in SJL mice treated with pristane. *J Immunol* 157:3200-3206.

174. Pawar, R.D., A. Ramanjaneyulu, O.P. Kulkarni, M. Lech, S. Segerer, and H.J. Anders. 2007. Inhibition of Toll-like receptor-7 (TLR-7) or TLR-7 plus TLR-9 attenuates glomerulonephritis and lung injury in experimental lupus. *J Am Soc Nephrol* 18:1721-1731.

BIOGRAPHICAL SKETCH

Pui Yuen Lee was born in 1981, in Guangzhou, China. He moved to Florida, USA, with his family in 1993 and graduated from Palm Beach Gardens High School in 1999. He then attended the University of Florida, where he graduated with highest honors in 2002 and received Bachelor of Science degrees in molecular biology and medical sciences. Pui was admitted to the University of Florida Junior Honors Medical Program in 2001 and subsequently the MD-PhD program in 2002.

Pui began his research studies in Dr. Mark Segal's laboratory with the University Scholars Program in 2000 and completed his undergraduate thesis there after 2 years. During the summer before medical school, he completed a Clinical Research Center fellowship in Dr. Westley Reeve's laboratory. Following the first year of medical school, Pui was accepted to the NIH/NSF East Asia fellowship program, where he spent the summer working in Dr. Shizuo Akira's laboratory in Osaka University in Japan. In 2004, Pui returned to Dr. Reeve's laboratory to begin his Ph.D. training and studied the role of type-I interferons and Toll-like receptors in a mouse model of lupus. Upon completing the Ph.D. degree, he plans to finish the final two years of medical school and enter residency training in internal medicine.